Activation of endothelial cells and its potential involvement in blood-brain barrier damage in cerebral malaria: an *in vitro* study

Mohd Hamzah MOHD NASIR

Thesis submitted for the degree of Doctor of Philosophy in Life Sciences

Keele University

January 2015

Keele University

SUBMISSION OF THESIS FOR A RESEARCH DEGREE

Part I. DECLARATION by the candidate for a research degree. To be bound in the thesis

Degree for which thesis being submitted   : Doctor of Philosophy in Life Sciences

Title of thesis : Activation of endothelial cells and its potential involvement in blood-brain barrier damage in cerebral malaria: an *in vitro* study

This thesis contains confidential information and is subject to the protocol set down for the submission and examination of such a thesis.

~~YES~~/NO [please delete as appropriate; if YES the box in Part II should be completed]

Date of submission   Original registration date: **21 September 2011**
(Date of submission must comply with Regulation 2D)

Name of candidate   : **Mohd Hamzah MOHD NASIR**

Research Institute   : **Science and Technology in Medicine (ISTM)**

Name of Lead Supervisor   : **Dr. Srabasti J. Chakravorty**

I certify that:

(a)   The thesis being submitted for examination is my own account of my own research

(b)   My research has been conducted ethically. Where relevant a letter from the approving body confirming that ethical approval has been given has been bound in the thesis as an Annex

(c)   The data and results presented are the genuine data and results actually obtained by me during the conduct of the research

(d)   Where I have drawn on the work, ideas and results of others this has been appropriately acknowledged in the thesis

(e)   Where any collaboration has taken place with one or more other researchers, I have included within an 'Acknowledgments' section in the thesis a clear statement of their contributions, in line with the relevant statement in the Code of Practice (see Note overleaf).

(f)   The greater portion of the work described in the thesis has been undertaken subsequent to my registration for the higher degree for which I am submitting for examination

(g)   Where part of the work described in the thesis has previously been incorporated in another thesis submitted by me for a higher degree (if any), this has been identified and acknowledged in the thesis

(h)   The thesis submitted is within the required word limit as specified in the Regulations

Total words in submitted thesis (including text and footnotes, but excluding references and appendices) : **31 775**

Signature of candidate   .... Date   16/01/2015

Note

Extract from Code of Practice: If the research degree is set within a broader programme of work involving a group of investigators – particularly if this programme of work predates the candidate's registration – the candidate should provide an explicit statement (in an 'Acknowledgments' section) of the respective roles of the candidate and these other individuals in relevant aspects of the work reported in the thesis. For example, it should make clear, where relevant, the candidate's role in designing the study, developing data collection instruments, collecting primary data, analysing such data, and formulating conclusions from the analysis. Others involved in these aspects of the research should be named, and their contributions relative to that of the candidate should be specified (*this does not apply to the ordinary supervision, only if the supervisor or supervisory team has had greater than usual involvement*).

Abstract

One of the severe complications of a *Plasmodium falciparum* infection is cerebral malaria (CM). CM is characterised by the accumulation of mature infected red blood cells (RBC) in the brain microvasculature. One of the consistent detrimental effects of sequestration is the breakdown of the blood-brain barrier (BBB), often with a fatal outcome in children in endemic areas. This study investigates the mechanisms underlying BBB breakdown secondary to sequestration, using immortalised human brain microvascular endothelial cells (tHBEC) as an in-vitro model of BBB and ITG-strain *Plasmodium falciparum.*

First, the tHBEC monolayer was co-cultured with *Plasmodium falciparum* infected red blood cell (PRBC) or uninfected red blood cells (uRBC) control for 20 hours and the supernatant was recovered for subsequent analysis. The co-culture supernatants showed upregulation of inflammatory mediators (MCP-1 and IL-8) and a member of metalloproteases (ADAMTS-1, ADAMTS-4, MMP-2 and MMP-9) in the PRBC-tHBEC co-culture supernatants. The PRBC-tHBEC co-culture supernatants induced loss of endothelial cell monolayer integrity, represented by real time reduction in the transendothelial electrical resistance, measured using Electrical Cell-Substrate Impedance Sensing (ECIS™). The same supernatants also increased the permeability of tHBEC monolayer to the fluorescently labelled 40 kDa dextran showing leakage across the tHBEC monolayer. Interestingly, the loss of barrier function of tHBEC monolayer is partially inhibited by the addition of protease inhibitors GM6001 and rhTIMP-3. Prolonged exposure to PRBC-tHBEC co-culture supernatants reduced the level of vinculin.

This study demonstrates that the interactions between PRBC and tHBEC induces activation of tHBEC and the release of proteases that contribute to BBB breakdown in CM, and could be a potential drug target for adjunct therapy in CM.

Table of contents

Table of figures

Table of tables

List of abbreviations

°C	Degree Celcius
Ω	Ohm ; unit of electrical resistance
% (v/v)	Concentration in percentage of volume over volume
% (w/v)	Concentration in percentage of weight over volume
μl	microliter
Ab	Antibody
ADAMTS	A distintegrin and metalloprotease with thrombospondin motif
BSA	Bovine serum albumin
CO_2	Carbon dioxide
DAPI	4',6-diamidino-2-phenylindole
EDTA	Ethylenediaminetetraacetic acid
ELISA	Enzyme linked immunosorbant assay
FBS	Fetal bovine serum
FITC	Fluorescein isothiocyanate
HBEC	Human brain microvascular endothelialcell
HCl	Hydrochloric acid
HCT	Haematocrit
HDMEC	Human dermal microvascular endothelial cell
HRP	Horseradish peroxidase
HUVEC	Human umbilical vein endothelial cell
ICAM-1	Intercellular adhesion molecule-1
IL-1β	Interleukin 1 beta

IL-8	Interleukin-8
kDA	kilo Dalton ($\times 10^3$ Da)
MCP-1	Monocyte chemoattractant protein-1 (Also known as CCL2)
ml	mililiter
MMP	Matrix metalloprotease
N_2	Nitrogen
ng	nanogram
NO	Nitric oxide
O_2	Oxygen
PAGE	Polyacrylamide gel electrophoresis
PBS	Phosphate buffered saline
PBST	Phosphate buffered saline with TWEEN-20
PCV	Packed cell volume
Pf C-medium	*Plasmodium falciparum* complete medium
Pf G-medium	*Plasmodium falciparum* growh medium
PRBC	*Plasmodium falciparum* infected red blood cells
PRBC-tHBEC	Co-culture of *Plasmodium falciparum* infected red blood cells with immortalised human brain microvascular endothelial cell
$Q_{1\%FBS}$-medium	tHBEC depleted medium with 1% (v/v) fetal bovine serum
$Q_{5\%FBS}$-medium	tHBEC depleted medium with 5% (v/v) fetal bovine serum
RBC	Red blood cell
SDS	Sodium dodecyl sulphate
TBS	Tris buffered saline
TEMED	N,N,N',N'-tetramethylethane-1,2-diamine

tHBEC	Immortilised human brain microvascular endothelial cell
TIMP	Tissue inhibitor of metalloprotease
TJ	Tight junction
TJP	Tight junction protein
TNF-α	Tumor necrosis factor-alpha
ug	microgram
uRBC	Uninfected red blood cell
uRBC-tHBEC	Co-culture of uninfected red blood cells with immortalised human brain microvascular endothelial cell
$\Omega.cm^2$	Ohm in a cm^2 area

Acknowledgement

First praise is to Allah (ﷲ), the Almighty, on whom ultimately we depend for sustenance and guidance. Alhamdulillah, all praises to Allah for the strengths and His blessing in completing this thesis. My sincere appreciation goes to my lead supervisor, Dr. Srabasti J. Chakravorty, for her supervision and constant support. Her invaluable help of constructive comments and suggestions throughout the experimental and thesis works have contributed to the success of this thesis. Not forgotten, my appreciation to my co-supervisor, Professor Gwynn William for his support. I would like to express my appreciation to my advisor, Dr. Mirnaa M. Maarabouni for her constructive advices throughout this study.

I also do wish to thank my friends especially those from room 169 who have encouraged me in so many ways throughout my PhD especially Imran Ullah, Sarah Harris, Nawrooz Kareem, Leanne Patrick and Nahla.

This thesis is dedicated to the people closest to my heart, my parents, Mohd Nasir and Zainab. Also to my mother-in-law, Naemah, for their prayers and understanding, not forgets all my family members for their support. I would also like to thank to my sponsors, Ministry of Education Malaysia, International Islamic University Malaysia and Institute for Science and Technology in Medicine, Keele University for investing huge amount of money in this study.

I thank my lovely wife, Noor Hafiza, for all her support and patience, understanding and love, our sons, Muhammad Ali Al-Hakim and Muhammad Al-Amin, and our daughter, Fatimah Az-Zahra, who enrich my life and provide me with opportunities to learn new things every day. Without their help and understanding, I might never have finished this work.

CHAPTER ONE: INTRODUCTION

Chapter 1: Introduction

1.1 General background

1.1.1   Malaria at glance

Malaria is a life threatening infectious disease caused by *Plasmodium* parasite. The disease is transmitted from person to person through the bite of infected *Anopheles* mosquitoes. Malaria not only affects human, but also animal such as birds, monkey and other vertebrates (Perkins, 2009). There are over 100 species of *Plasmodium* but only 5 species-infecting human with the remaining only causing zoonotic malaria (Garnham, 1966, Conlan et al., 2011). These five species are (i) *Plasmodium falciparum,* (ii) *Plasmodium vivax,* (iii) *Plasmodium malariae,* (iv) *Plasmodium ovale* and (v) *Plasmodium knowlesi.* From these, only the first four species were known to cause human to human malaria, while the fifth which was known to infect monkey was recently detected in human (Singh et al., 2004, Cox-Singh et al., 2008, Figtree et al., 2010, Marchand et al., 2011). Among these, *Plasmodium falciparum* is the most virulent and lethal to human and is the focus of this thesis.

Distribution of malaria infection is geographically defined (Figure 1-1). All of the countries with high prevalence in malaria are located near the equatorial line region (World Health Organisation, 2012). Tropical and subtropical climate in these countries serve as a good ecological environment to support the life cycle of the mosquito vector of malaria.

In 2013 alone, nearly 200 million cases were recorded. From this figure, 600 000 people were killed with the majority being children living in Africa (WHO, 2014). It is estimated that each minute, an African children dies due to this deadly disease. All efforts in malaria eradication and patient management have shown some positive results and more than 25% reduction in mortality rate was observed (O'Meara et al., 2008, WHO, 2013). This

however, cannot be a total relief to stop further research to eliminate the disease. Recently, a study showed the increasing trend in the incidence of malaria caused by artemisinin resistant *Plasmodium falciparum* variant especially in Thailand-Cambodia and Thailand-Myanmar border (Jambou et al., 2005, Phyo et al., 2012). Further, Nwane et al. (2011) has found the insecticide resistant *Anopheles* mosquitoes in at least 45 endemic countries.

The negative impact of malaria is not limited to human health alone, but also to the economic growth of the affected country. Coincidentally, nearly all of the malaria endemic country are categorised as low economic income country. This situation limits the maximal efforts in combating malaria including vector control and patient management (Gallup and Sachs, 2001).
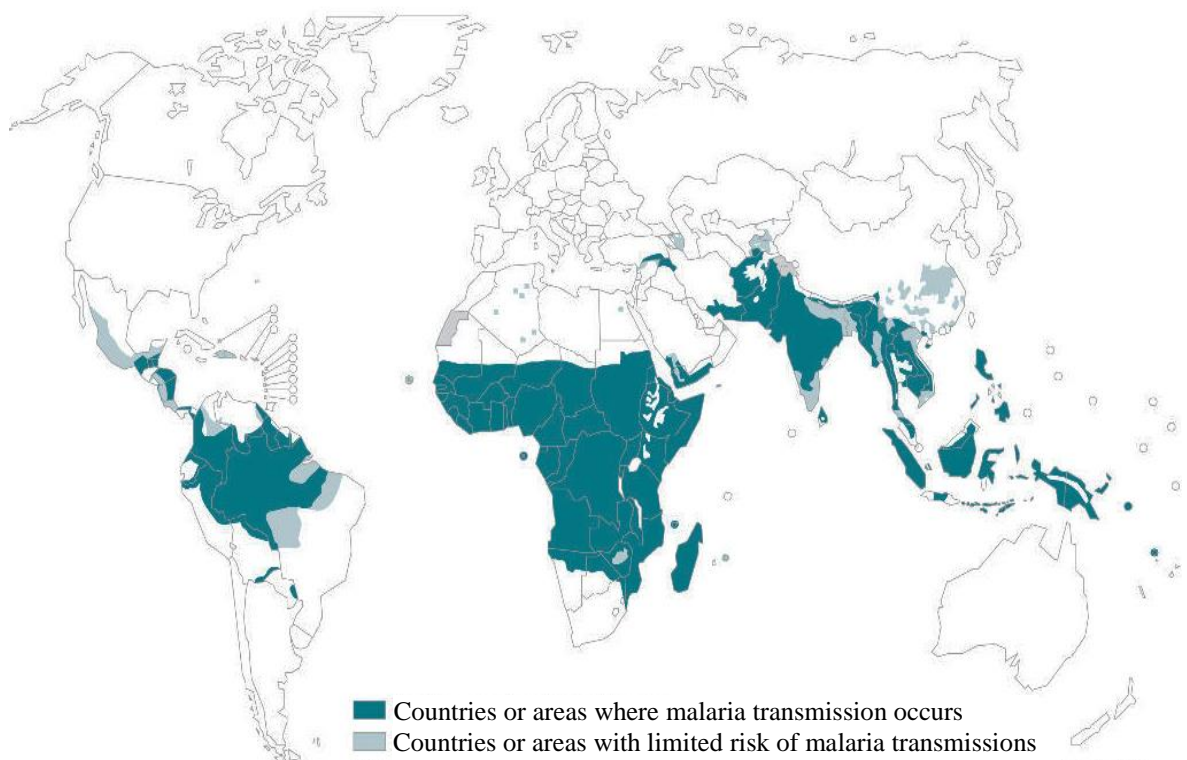
Figure 1-1: The distribution of malaria in 2010 (World Health Organisation, 2012)

1.1.2   The causative agent and vector

Malaria is not a new disease. It is believed that malaria has existed since the ancient era. The earliest records on malaria-like symptoms was revealed in the old Chinese medical treatise, known as *Nei Ching* (2700 B.C) (CDC, 2010). Similar records were also found in Egyptian medical books (1570 B.C) and ancient *Ayurveda* of surgery textbook (500 B.C). These however need an update by utilising the modern science techniques to investigate the more detailed and specific aspect of the disease.

There were many presumptions on the transmitting agent of malaria until Ronald Ross in 1897, discovered mosquitoes carrying the parasite of avian malaria. In 1899, *Anopheles* mosquito was identified to be the transmission agent of human malaria by a group of Italian researchers led by Giovanni Batista Grassi (McGregor, 1992). This genus of mosquito consists of approximately 450 species but only 50 to 60 of them are able to transmit human malaria parasites (reviewed in Cohuet et al. (2010)). In fact, only female *Anopheles* mosquitoes are responsible for malaria transmission to human.

The idea of causative agent for malaria was only proved in the 1880's. Results from the work of Charles Alphonse Laveran demonstrated that malaria is caused by the parasite residing in human red blood cells. The parasites however, were only properly named in the 1880's when Giovanni Batisti and Raimondo Fileti from Italy proposed the name of *Plasmodium vivax* and *Plasmodium malariae.* Laverans's finding has disproved the early assumption of Greek society that the disease was caused by the fetid smell from swamp area hence the name *mala-aria* (bad-air) was given. The discovery has also been a paradigm shift in malaria research with more new findings.

Plasmodium is a member of the phylum apicomplexa. This intracellular obligate protozoon resides in two different hosts, poikilothermic *Anopheles* mosquito vector and homoeothermic human host for its complete life cycle (figure 1-2). It transits in mosquito mid-gut cells while in human it resides in hepatic cells and red blood cells (RBC).
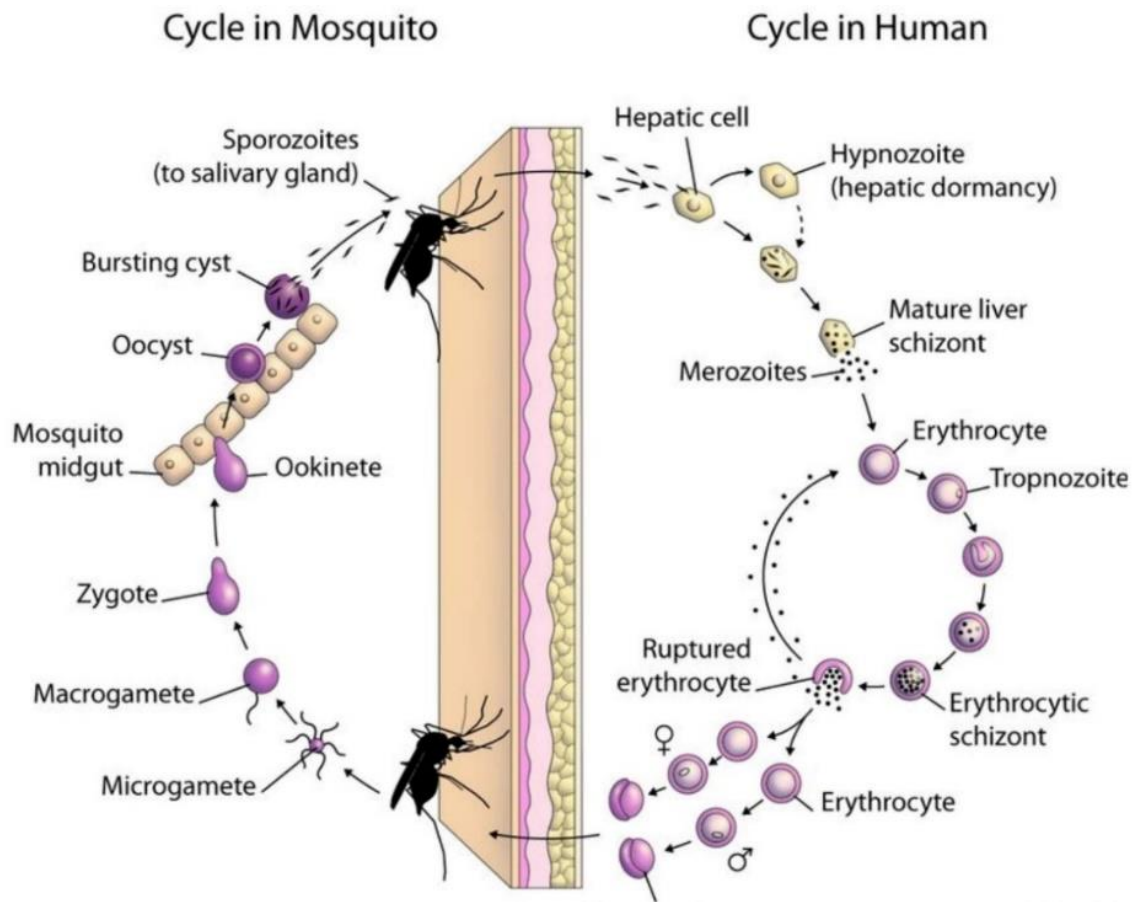
Figure 1-2: The *Plasmodium falciparum* life cycle.

The parasite development in mosquito (left hand side), and in human hepatocyte and erythrocyte (on right hand side). Figure was obtained from John Hopkins University (2012) last accessed on 22nd July 2013.

1.1.2.1 *Plasmodium falciparum* life cycle

In mosquito, the sporogony cycle starts after a female *Anopheles* mosquito takes a blood meal containing gametocytes from an infected human. Both male and female gametocytes start the mating process and form a zygote before entering the midgut cells. The zygote then matures to form an ookinete before turning into oocyst. Matured oocysts then burst and release sporozoites. Later, these sporozoites migrate into the salivary gland ready to be transferred into human blood stream upon the next blood meal.

The sporozoites travel within the blood circulation, quickly infecting hepatocytes through the Kupffer cells (reviewed in Prudêncio et al. (2006)). This series of events involves a complex molecular interaction between the sporozoite and host cells. Circumsporozoite protein (CSP) and thrombospondin-related adhesive protein (TRAP) on the sporozoites are the molecules that mediate the binding to heparan sulphate proteoglycans of host cell (Frevert et al., 1993, Robson et al., 1995, Kappe et al., 2003). This binding has been characterised to be blocked by serine protease which induce the shedding of TRAP on the sporozoite (Silvie et al., 2004). Once in the hepatocyte, the sporozoites undergo differentiation and mitotic replication to form merozoites (liver schizont).

The merozoites then burst out from hepatocytes and start the asexual erythrocytic cycle. The merozoite is expressing the merozoite surface protein (MSP-1) that interacts and binds to the band-3 receptor on red blood cells (RBC) (Goel et al., 2003). Following the successful binding, the merozoite reorients itself to attach its apical end to the RBC *via* apical membrane antigen (AMA-1) (Triglia et al., 2000). This is a very rapid process and helps the parasite to evade the host immune response (as reviewed in Tilley et al. (2011)). The invasion of merozoites into RBC has been extensively reviewed by Cowman and Crabb (2006).

Erythrocytic schizogony of the *Plasmodium falciparum* life cycle is important for the clinical symptoms and diagnosis. In the RBC, the merozoite develops into early trophozoite and appears as a ring shape within RBC under the microscope. The maturation of early trophozoite into late trophozoite involves active ingestion of haemoglobin, which is converted into non-toxic haemozoin (Egan et al., 2002). The parasite also modifies the RBC to help its survival in the RBC, a cell that is lacking in protein synthesis machinery. This forces the parasite to utilise the RBC tubovesicular membrane to import the nucleosides and amino acids (Lauer et al., 1997). The modification of red blood cell by parasite exported protein results in an increase in PRBC rigidity and adhesiveness (Suwanarusk et al., 2004, Maier et al., 2008). Most of these proteins contains PEXEL/VTF motif and are exported *via* *Plasmodium falciparum* translocon of exported protein (PTEX) and Maurer's cleft (de Koning-Ward et al., 2009). The exported proteins also alter the structure and stiffness of PRBC surface with the formation of 'knobs' (figure 1-3) which developed when the parasite turns into late trophozoites (Zhang et al., 2015). One of the best-studied knob proteins is *Plasmodium falciparum* erythrocyte membrane protein 1 (PfEMP-1). PfEMP-1 serves as a ligand and is important for the cytoadherence of PRBC to microvascular endothelial cells (sequestration) and red blood cells (rosetting) (Baruch et al., 1995, Crabb et al., 1997, Hviid and Jensen, 2015). The increase in cytoadherence of the mature parasite to the endothelial cells helps the parasite escape from clearance by the host immune system. This interaction is believed to have significant role in the severity of *Plasmodium falciparum* malaria pathogenesis.

The final stage of *Plasmodium falciparum* life cycle in the RBC is the maturation into schizont. Each schizont can produce between 16 to 32 new merozoites, which then invade more red blood cells. This synchronised event of schizont rupture coincides with the

febrile episodes and is believed to be responsible for the paroxysm in an infected human (As reviewed in Kwiatkowski (1989), Oakley et al. (2011)). Small fraction of merozoites may then undergo differentiation into gametocyte but the majority will continue to the new erythrocytic cycle (Kuehn and Pradel, 2010).
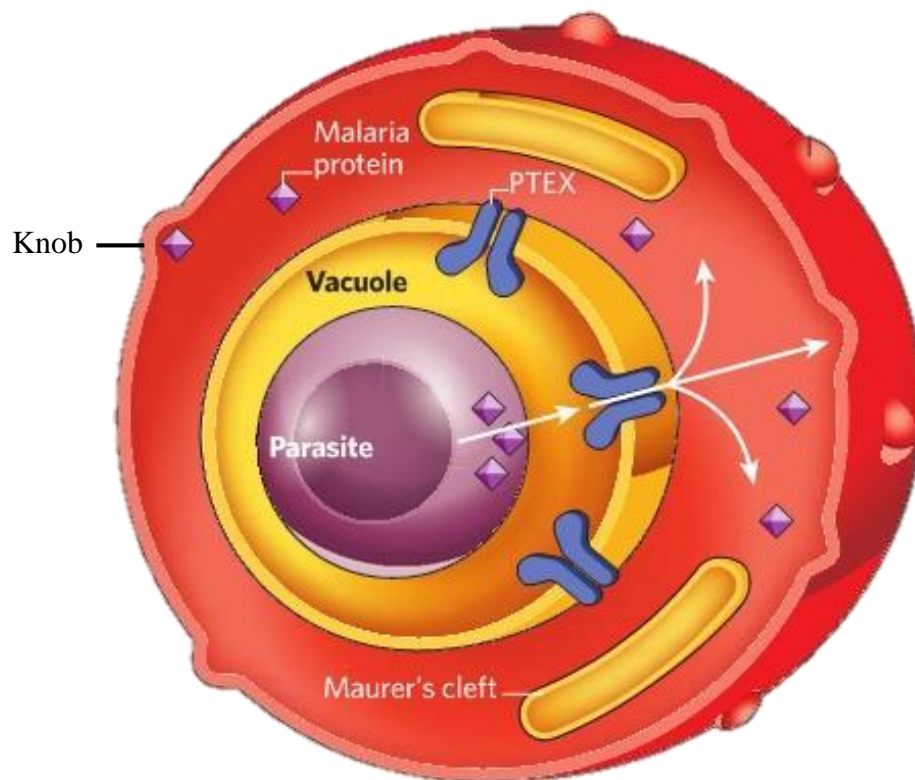
Figure 1-3: *Plasmodium falciparum* modifies the infected RBC.

Once in the red blood cell, the *Plasmodium falciparum* starts its intra-erythrocytic life cycles, which includes the export of parasite protein to the RBC surface, especially the knobs proteins. These modifications increase the adhesiveness and rigidity of RBC (Image was modified from Reiff and Striepen (2009)).

1.1.3 The pathogenesis of malaria

The clinical outcome of malaria is varied. It can be as simple as asymptomatic uncomplicated malaria or a more severe complication leading to death. There are three main factors that can influence the clinical outcome of malaria; parasite factors, host factors and, geographic and social factors (Figure 1-4) (Reyburn et al., 2005). According to the WHO classification, based on the clinical and laboratory investigation, there are two main categories of malaria; mild malaria and severe-malaria. The classical symptom of mild malaria is the cyclical pattern of high fever, which lasts for 6-10 hours every 48 hours (tertian paroxysm). This mild malaria, however, if not properly treated can progress to severe complications which are lethal.
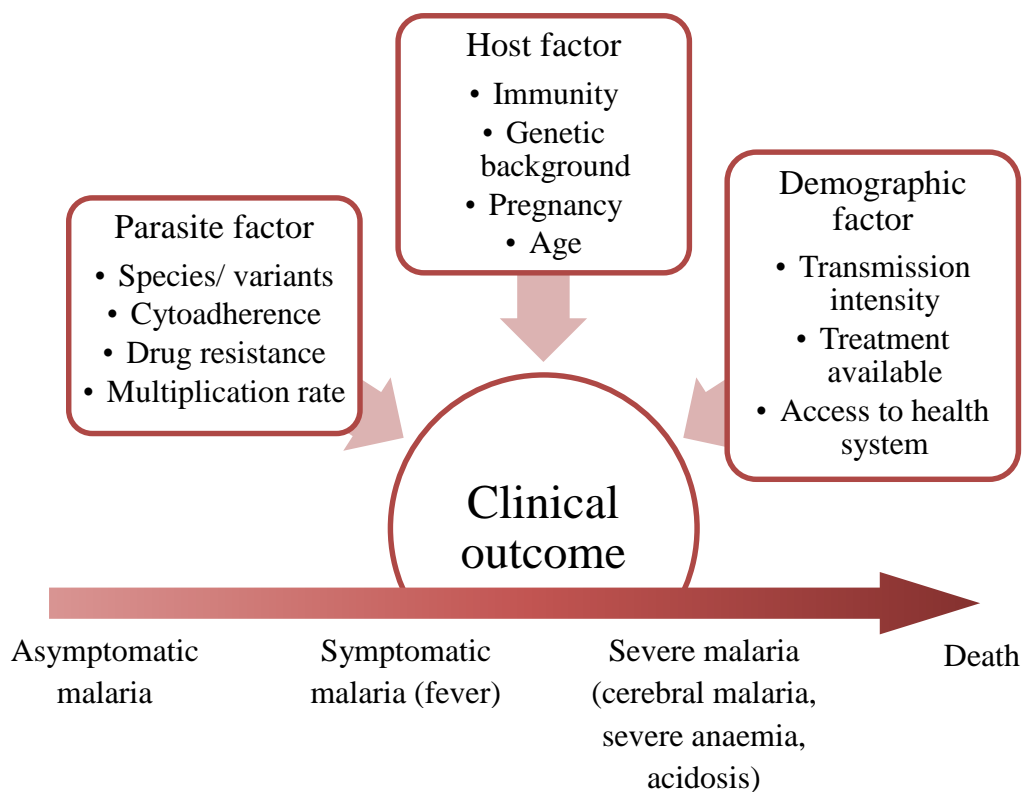
Figure 1-4: The factors that contribute to the variation of clinical outcome of malaria. There are three main group factor that have been outlined; parasite factor, host factor and demographic factor.

1.1.4 Severe complication of malaria

Severe malaria is a complication of malaria infection with organ failure or anomalies in the blood or metabolism. It is characterised by the existence of *Plasmodium falciparum* in the blood stream with the additional symptoms listed in the table 1-1 without any other known cause (World Health Organisation, 2012). Examples of severe complication of malaria are acidosis leading to respiratory distress, placental malaria and cerebral malaria.

Table 1-1: The occurrence of clinical manifestation and laboratory findings in adult and children during severe malaria (data taken from World Health Organisation (2012)).

Clinical manifestations or laboratory findings	Frequency	
	Children	Adult
Prostration	High	High
Impaired consciousness	High	Medium
Multiple convulsion	High	Less
Acidosis	High	Less
Severe anaemia	High	Less
Circulatory collapse	Less	Less
Pulmonary oedema	Rare	Less
Abnormal bleeding	Rare	Less
Jaundice	Less	High
Haemoglobinuria	Rare	Less

Acidosis is one of the manifestation of severe malaria due to the dysfunction in metabolic, circulatory or renal function (Taylor et al., 1993, English et al., 1997a, English et al., 1997b). In children, the acidosis is commonly associated with hyperlactemia (English et al., 1997b) and normally manifested as respiratory distress. In Asia, acidosis increases the risk of death by seven fold among malaria patients compared to malaria without acidosis (Dondorp et al., 2008b).

Another major contributor towards severe malaria mortality is respiratory distress. It is estimated that 20% of death among malaria patients in Asia is due to this complication (Marsh et al., 1995). Respiratory distress is manifested by the high respiratory rate and increased effort for breathing. Post-mortem study on the malaria patients who died due to malaria respiratory distress revealed that there is sequestration of PRBC in the alveolar-capillaries of the lung (as reviewed in Haldar et al. (2007)). Animal models have shown that the acute lung injury in mice is due to the ability of *Plasmodium berghei* ANKA to adhere to the lung endothelial cells CD36 which were protected in $Cd36^{-/-}$ mice (Lovegrove et al., 2008).

1.2 Cerebral malaria

Cerebral malaria (CM) is defined by the manifestation of deep coma with a Blantyre Coma Scale (BCS) less than 5 in children or, 2 or less in adult, positive with PRBC in blood smear, seizures and respiratory distress, which is not caused by any other known reason for encephalopathy (World Health Organisation, 2012). It is estimated that up to 30% of CM patients die with majority of them dying within 24 hours of hospital admission especially in the Sub-Saharan African region where the multiple infection are common (Newton and Krishna, 1998, WHO, 2014). Children and immunocompromised adults are most susceptible to develop this complication than adults from endemic countries (Reyburn et al., 2005). The coma is reversible but it might leave long-term neurological sequelae including cognitive impairment in the survivors (Idro et al., 2005, Boivin et al., 2007). Although several attempts in the adjunct therapy for CM, including the use of albumin and saline (Maitland et al., 2005), there is no specific treatment for cerebral malaria besides the usual anti-malarial drugs

recommended in the region and supportive therapies to control the fever (antipyretics), seizures (anticonvulsants) and anaemia (blood transfusion) (John et al., 2010).

The clinical feature of cerebral malaria varies between children and adults. For instance, the onset of coma starts rapidly after a seizures in African children (Boivin et al., 2007) , while delayed two to three days in adults (Kochar et al., 2002). In addition, coma in children often recovered between 24-48 hours while slightly slower in adults (Idro et al., 2005). Interestingly, the neurological sequelae are more common in children (11%) than adults (less than 5 %) (Newton and Krishna, 1998, Kochar et al., 2002). It is unclear whether these differences are associated with age, immunity or different parasite strain.

It is generally acknowledged that the clinical features of cerebral malaria are complex and are centralised to the outcomes of the dysfunction in the central nervous system. Interestingly, these effects are caused by the parasite that remains within the brain microvascular space. Not only in cerebral malaria, but in almost all of the severe complications of malaria are associated with the sequestration of PRBC in the small vessels of organs including kidney and lung (Pongponratn et al., 1991, Nguansangiam et al., 2007, Ponsford et al., 2011). In cerebral malaria, the sequestration of PRBC in the brain microvasculature may play a central role in causing the complication. Interaction between PRBC and endothelial cells can directly and indirectly modulate the local inflammatory responses of the endothelium as demonstrated in human umbilical vein endothelial cells (HUVEC) (Chakravorty et al., 2007, Chakravorty et al., 2008).

Although the mechanism of pathogenesis is unclear, the characteristic feature of cerebral malaria is that the strictly impermeable endothelial cells of the blood-brain barrier

(BBB) lose their normal function and become leaky as seen in post-mortem studies. Brown et al. (1999) and Dorovini-Zis et al. (2011), through immunohistochemical analysis of the post-mortem brain sections of cerebral malaria patients found positive staining for fibrinogen. Fibrinogen is a large serum protein that is normally maintained in the intact BBB, was found in the perivascular space of brain microvessels containing sequestered PRBC.

The incidence of deep coma among cerebral malaria patients shows a positive relationship with the altered structure and functions of BBB in both animal model studies (de Souza and Riley, 2002) and clinical-pathological data (Brown et al., 2000, Brown et al., 2001). These observations have led to several hypotheses being proposed with clear emphasis on the BBB environment and its components. There are two major models that postulate the pathogenesis of CM: (1) sequestration hypothesis and, (2) inflammation hypothesis. Besides these two main models, there is also a model that combines these hypotheses with the additional involvement of platelets in hemostasis (van der Heyde et al., 2006). Although these three hypotheses may explain some of the events in CM development, none of them can completely describe how the sequestered parasites in brain microvasculature, which do not infiltrate into brain parenchyma can cause the neurological disturbances.

1.2.1   Sequestration hypothesis

The central dogma in cerebral malaria pathogenesis is the interaction of brain microvascular endothelial cells with the *Plasmodium falciparum* infected red blood cells. This assumption was firstly proposed by Marchiafava and Bignami in 1894 (as reviewed in van der Heyde et al. (2006). This idea was then strengthened after several post-mortem observations on cerebral malaria patients showing a consistent appearance of the sequestered

PRBC in the brain vasculature (MacPherson et al., 1985, Pongponratn et al., 1991, Silamut et al., 1999). Sequestration is a term to describe the process of localization of matured PRBC on the endothelial bed of specific organ microvasculature and their disappearance from the peripheral circulation. Sequestration of PRBC can occur in any organ such as heart, lung, intestine and kidney, but is significantly high in the brain vasculature especially in the capillary and post-capillary venules (MacPherson et al., 1985, Pongponratn et al., 1991, Taylor et al., 2004).

The key component of this hypothesis is the vascular obstruction. This event occurs as a result from the modification of PRBC by the parasite proteins. The modification increases the rigidity of the PRBC which may reduce the ability of the PRBC to move along the brain microvessel (Maier et al., 2008). The obstruction of the brain microvessel is also caused by the ability of the PRBC to form rosettes, where the PRBC adhere with two or more uninfected red blood cells (uRBC). *In vitro*, only pigmented trophozoites are able to form rosettes (Hasler et al., 1990) . Interestingly, most of the PRBC isolates from the severe malaria patients in Africa have a high rosetting frequency (Rowe et al., 1995, Rowe et al., 2009, Doumbo et al., 2009). Auto-agglutination of PRBC, the ability of PRBC to adhere to another PRBC is another contributing factor for the microvessel obstruction (Wassmer et al., 2008). Both, rosetting and auto-agglutination of PRBC forms a clump and blocks the blood flow in the microvessel.

Another mechanism for the obstruction of microvessel blood flow is the cytoadhesion of PRBC to the vessel endothelial cells. The cytoadherence of PRBC to endothelial cells in small vessels facilitate the sequestration of mature PRBC. The sequestration of PRBC was first reported by Machiafava in 1894. Since then, several

molecules involved in the interaction between PRBC and endothelial cells have been investigated.

The cytoadherence of PRBC in microvessels is facilitated by the remodelling of the RBC membrane by the exported parasite proteins (Maier et al., 2008). One of the main cytoadhesion molecules on PRBC, which is well characterised is the *Plasmodium falciparum* erythrocyte membrane protein-1 (PfEMP-1). This large protein containing several Duffy-binding like (DBL) domains is encoded by *var* genes. It was hypothesized that, out of 60 *var* genes, only one is transcribed at a time during ring stage giving rise to only one type of PfEMP-1 in the mature stage (Chen et al., 1998, Scherf et al., 1998, Horrocks et al., 2004). This antigenic variation is a known strategy for *Plasmodium falciparum* to avoid the host adaptive immune responses (Kyes et al., 2001). The PRBC surface molecules which are responsible for the cytoadhesion were found to be sensitive to trypsin digestion as the ability of ITG strain *Plasmodium falciparum* to bind to ICAM-1 under flow condition was stopped following trypsin digestion of PRBC (Chakravorty et al., 2007). Although PfEMP-1 is important for cytoadhesion through endothelial ICAM-1, this PRBC surface molecule may not be the key player for the endothelial cells activation where the upregulation of ICAM-1 in HUVEC is not altered when co-cultured with trypsinised PRBC (Chakravorty et al., 2007).

The cytoadhesion of PRBC to the endothelial cells was suggested to be mediated by over 14 adhesion molecules on the endothelial cell. These include the intercellular adhesion molecule-1 (ICAM-1) (Berendt et al., 1989), CD36 (Barnwell et al., 1989), thrombospondin (Roberts et al., 1985), vascular cell adhesion molecule-1 (VCAM-1) (Ockenhouse et al., 1992b), platelet-endothelial cell adhesion molecule-1 (PECAM-1) (Treutiger et al., 1997),

neural cell adhesion molecule-1 (NCAM-1) (CD56) (Pouvelle et al., 2007), P-selectin (Udomsangpetch et al., 1997), E-selectin, (i) integrin alpha (v) beta 3 (Integrin αVβ3) (Siano et al., 1998), (j) gC1qR , (k) HABP1 (Biswas et al., 2007), p32 (Biswas et al., 2007), chondroitin sulphate A (CSA) (Fried and Duffy, 1996) and hyaluronic acid (HA) (Beeson and Brown, 2004). All of these molecules are either expressed constitutively or inducible on endothelial cell, but some may not be expressed by endothelial cells at all locations of the body. Of these endothelial cell adhesion molecules, ICAM-1, has been proposed to play a significant role in sequestration of PRBC and cerebral malaria pathogenesis.

CD36 is one of the well-known adhesion receptor for PRBC, however the involvement of this receptor in the malaria pathogenesis remains debatable (Serghides et al., 2003). *In vitro* study shows that the CIDR1α domain of PfEMP-1 is the ligand for CD36 (Miller et al., 2002). Additionally, field isolate parasites were found to adhere to CD36 (Newbold et al., 1997). There is however, no difference in the ability to adhere to CD36 between the parasites isolated from cerebral malaria and uncomplicated malaria patients in Africa (Newbold et al., 1997, Heddini et al., 2001). Further, CD36 is not expressed by the brain microvascular endothelial cells, thus initially denoted as less important in the mechanism of blood-brain barrier damage in cerebral malaria (MacPherson et al., 1985, Turner et al., 1994, Silamut et al., 1999, Seydel et al., 2006). More recently, a role for CD36 in cytoadhesion in CM has been proposed where platelets as a bridge to present CD36 on the endothelial cell surface (Hollestelle et al., 2006).

The adhesion of PRBC to ICAM-1 (CD54) was firstly seen *in vitro* using ICAM-1 transfected COS cell line (Berendt et al., 1989). Since then, the involvement of ICAM-1 became the main attention in malaria research. The adhesion of PRBC to ICAM-1 not only

seen in the static *in vitro* models, but also in the flow models of cytoadhesion (Chakravorty and Craig, 2005). ICAM-1 is a 70-120 kDa sialylated glycoprotein belonging to the immunoglobulin supergene family (Simmons et al., 1988). The expression of ICAM-1 by endothelial cells was increased upon the activation by the high level of tumour necrosis factor (TNF) cytokines, which was a consistent observation in both post-mortem and *in vitro* studies (Turner et al., 1994, Silamut et al., 1999, Wassmer et al., 2005, Tripathi et al., 2006). In addition, the sequestration of PRBC was found to be higher in the vessel with high level of ICAM-1 (Turner et al., 1994). This however is unclear whether the upregulation of ICAM-1 in the sequestered vessel occurs prior to sequestration of PRBC or as the effect of the sequestration, as the level of ICAM-1 can be upregulated by TNF-α as well as interaction with PRBC, as seen in HUVEC (Viebig et al., 2005, Chakravorty et al., 2007). In contrast to CD36, ICAM-1 is found to be expressed by BBB endothelial cells and this adhesion molecule may have a significant role in cerebral malaria pathogenesis. However, parasite isolates from Africa do not show significant association between ICAM-1 binding and severe malaria (Newbold et al., 1997, Heddini et al., 2001).

P-selectin (CD62P) is expressed by endothelial cells and activated platelets, a glycoprotein of cellular adhesion molecules responsible in priming the binding of leukocytes to endothelial lining (Alón et al., 1995). P-selectin expressed in transfected cells or immobilised on a coverslip can initiate the tethering and rolling of the field isolate of PRBC (Udomsangpetch et al., 1997, Ho and White, 1999). The importance of P-selectin in the pathogenesis of cerebral malaria in human is still unclear, however P-selectin knock-out mice shows protection from the experimental cerebral malaria (Combes et al., 2004).

The involvement of E-selectin (ELAM-1, CD62E) in the PRBC sequestration is considered as minimal, if any, due to the inability of the field isolate PRBC to adhere to the immobilised E-selectin under flow conditions (Udomsangpetch et al., 1997). VCAM-1 (CD106) is an adhesion molecules expressed by the endothelial cells upon activation by cytokines. Under the flow condition, field isolates of PRBC were able to tether and roll on VCAM-1, however no significant binding was recorded (Udomsangpetch et al., 1997).

Sequestration, resulting from the interaction of PRBC with these adhesion molecules was proposed to be the main pathway for the breakdown in the BBB structure and function. The infiltration of serum fibrinogen from vessel lumen to the brain parenchyma is frequently co-localised with the sequestered PRBC (Turner et al., 1994, Brown et al., 1999, Brown et al., 2001, Dorovini-Zis et al., 2011). Although the sequestration of PRBC in the brain microvessels is a common feature of cerebral malaria, the sequestration can also be found in other organ such as kidney, heart, lung and skin (MacPherson et al., 1985, Pongponratn et al., 1991, Seydel et al., 2006). Thus, the sequestration of PRBC may be necessary but not the ultimate cause of cerebral malaria.

In this hypothesis, obstruction of the brain microvessels by PRBC reduces blood flow (Dondorp et al., 2008a), alters the fluid exchange (Brown et al., 1999) and removal of metabolites (as reviewed in Adams et al. (2002)). The obstruction also decreases the number of functional capillaries which potentially leads to localised hypoxia (Dondorp et al., 2000). Another important component in this hypothesis is the increase in lactic acid in the blood due to anaerobic respiration in the tissue has been shown to have significant association with CM pathogenesis (Marsh et al., 1995).

Indirectly, this hypothesis assumes that the vascular obstruction is proportional to the level of parasitaemia but the clinical evidence show only limited low relationship between parasitaemia and mortality (as reviewed in Clark and Cowden (2003)). However, there are some observations that cannot be explained by this hypothesis alone. First, sequestration can be observed in both asymptomatic person (Pongponratn et al., 1991) and non CM patients (Silamut et al., 1999) and there are a few cases of fatal CM in non-sequestering *Plasmodium vivax* (Rogerson and Carter, 2008). Second, there is no clear evidence for irreversible hypoxic damage in fatal CM (Medana et al., 2001). Third, it seems that whilst sequestration occurs in all CM patient, only approximately 30% ended in death and the survivors recover without, or with only limited number of known neurological consequence. Interestingly, the sequestration did not occur in all vessels but the activation of EC has been observed in majority of EC throughout the human body (Turner et al., 1994). Although there are technical explanations on this issue such as the degradation of samples prior to microscopic examination and the sampling was done from a vessel that had PRBC clearance, it is possible that the pathogenesis of CM may be multifactorial induced by local factor as well as generalised systemic factors.

1.2.2 Inflammation model

In contrast to the sequestration model, the inflammation model emphasises the de-regulated humoral responses against *Plasmodium falciparum* infection. The basic idea of this hypothesis was suggested more than 60 years ago by Maegraith with the assumption that the infection will trigger the systemic inflammatory response, which subsequently causes multiple organ failure and death (as reviewed in van der Heyde et al. (2006)).

This series of events start when the erythrocytic schizont ruptures and releases its soluble toxin (most likely glycosylphosphatidylinositol (GPI) or haemazoin) into the human blood stream (Nebl et al., 2005). The toxin then activates both monocytes and neutrophils via toll-like receptors which secrete pro-inflammatory cytokines including tumour necrosis factor-alpha (TNF-α), interferon gamma (IFN-γ), interleukin-1 (IL-1), IL-6, nitric oxide (NO) and lymphotoxin (LT-α) (Gazzinelli and Denkers, 2006). Of these, IL-1β, IL-6 and IL-8 show some degree of relationship with the severity of malaria disease at least among Malian children (Lyke et al., 2004b). TNF-α is proposed to up-regulate the ICAM-1 expression in most endothelial cells by Garcia et al. (1999) and a basal level of TNF-α is required for maintaining optimal levels of ICAM-1 on HBEC to support cytoadhesion *in vitro* (Tripathi et al., 2006). Low concentration of TNF-α is also needed to enhance the upregulation of ICAM-1 on HUVEC by PRBC (Chakravorty et al., 2007).

The involvement of inflammation hypothesis of cerebral malaria can be seen in many cerebral malaria clinical studies. For instance, Malian children suffering cerebral malaria shows increased levels of IL-6 (proinflammatory) and IL-10 (anti-inflammatory) compared to those with non-cerebral malaria (Lyke et al., 2004a). These children however show no significant alteration in the level of IL-1, IL-8, IL-10 and TNF-α. In another study, the levels of serum and cerebrospinal fluid (CSF) IL-8 from Ghanaian children dying of cerebral malaria are markedly increased compared to the children with severe malarial anaemia and non-malaria control (Armah et al., 2007). In contrast, the concentration of TNF-α and TNF-α receptor in Ghanaian and Gambian children with cerebral malaria were higher compared to the uncomplicated malaria (Kwiatkowski et al., 1990). However, the upregulation of IL-6, IL-10 and TNF-α cannot be the best indicator for cerebral malaria as the level of these

cytokines are lower in Vietnamese adult with cerebral malaria only, compared to the patients with multi organ diseases (Day et al., 1999).

Another cytokine that was found to be upregulated in cerebral malaria is the monocyte chemoattactant protein-1 (MCP-1). MCP-1 is involved in the inflammatory responses by attracting monocyte to the inflammation site (Patnaik et al., 1994). In the brain, MCP-1 act as the initiator for leukocyte extravasation across BBB (Stamatovic et al., 2003b), which indirectly increase the BBB permeability. MCP-1 upregulation was also found in the neuroinflammatory diseases such as multiple sclerosis and cerebral ischaemia (Yamagami et al., 1999). Interestingly, increased levels of MCP-1 was reported in the post-mortem serum and CSF of Ghanaian children dying of CM and severe malaria anaemia, compared to non-malaria cases (Armah et al., 2007), even though leukocyte extravasation is not a characteristic feature of CM in human.

Elevated levels of cytokines may also upregulate the inducible nitric oxide synthase (iNOS) which increase the nitric oxide (NO) production. Nitric oxide is important in the maintenance of vascular status, neurotransmission and killing the intracellular organisms. Despite that, NO also inhibits TNF-α synthesis (Iuvone et al., 1996) and ICAM-1 and VCAM-1 receptor expression (Serirom et al., 2003). The increased level of NO may leak into brain tissue and disrupt its normal function (Clark et al., 1992). The importance of NO in the cerebral malaria pathogenesis remains unclear. This hypothesis also cannot be the absolute model for CM pathogenesis as some contradictory issues are raised such as the heterogeneous responses in different individuals and the levels of TNF-α in CM patient is far less than in patients with non-neurological, asymptomatic *Plasmodium vivax* malaria (Karunaweera et al., 1992).

Both models mentioned above failed to show concrete evidence to be an absolute model, but combination of both models, unveils a possible story behind the scene. The unification of both hypotheses including the involvement of haemostasis as proposed by van der Heyde et al. (2006) triggers another stage of understanding on this complex mechanism of disease. Unfortunately, this combination of different possible CM mechanisms is still unable to describe the sequence of events, i.e., which one is the primary event and which one is the secondary event.

1.3 Blood-brain barrier

Both hypotheses on the cerebral malaria pathogenesis clearly focussed on the breakdown of blood-brain barrier (BBB) either functionally or structurally. Blood-brain barrier is a terminology for the anatomical and functional barrier between the blood stream and brain environment. This neurovascular unit is important in maintaining the normal function of the brain.

Blood-brain barrier function was firstly observed by Paul Erlich in 1885. In an experiment, Erlich injected a water-soluble dye, Evan's blue into the peripheral vein of mice. Following the injection, he dissected the mice and found that the dye stained all organs except the brain and spinal cord. He proposed that the finding might be due to the inability of the dye to bind to the nervous tissue.

To prove the hypothesis, Erlich's student, Edwin Goldman in 1913 injecting trypan-blue reagent directly into the CSF. Interestingly in this experiment, the trypan-blue does stain all the cells in the brain, but not the other organs. This experiment shows the existence of a

functional barrier between central nervous system (CNS) and blood stream, which restricts the movements of both dyes from and into the brain environment.

1.3.1 Anatomical structure of BBB

Both experiments described in the section above failed to explain the structure that is responsible for restricting the movement of the dyes between the blood circulation and CNS. It was only in 1941 that Broman identified two types of barrier in the brain; first, the blood-cerebropinal fluid barrier and second, the blood-brain barrier. Blood-cerebrospinal fluid barrier is located at the choroid plexus while blood-brain barrier is the capillaries in the brain. The ultrastructure of BBB was proposed by Reese and Karnovsky in 1967, where he found that the mouse BBB was formed by endothelial cells that restrict the migration of horseradish peroxidase (HRP) to the luminal side of intercellular junction.

The BBB is made up of at least three cellular components, the innermost layer is brain endothelial cells, peripheral to it is the pericytes and the outermost is covered by the astrocyte end feet (Figure 1-5). The restricted permeability of the BBB is mainly due to the specialised brain endothelial cells with its tight junction proteins, which is discussed in section 1.4.

Pericytes are believed to gives structural support and vasodynamic properties to the microvasculature. Pericytes may be actively involved in cerebral autoregulation where receptors to various chemical mediators including catecholamine, angiotensin II (Healy and Wilk, 1993), endothelin-1 and vasopressin (Dehouck et al., 1997) were found.

The importance of astrocytes in the BBB neurovascular unit was demonstrated by the *in-vitro* culture of bovine brain endothelial cells with rat astrocyte which increased the BBB integrity (Neuhaus et al., 1991). The astrocytes were believed to signall between neurons and BBB and also to act as the "house-keeper" in the event of biochemical intrusions *via* BBB (Ballabh et al., 2004).

This thesis focuses on the brain endothelial cells of the BBB whichis the interface for the interaction of the PRBC with the BBB.
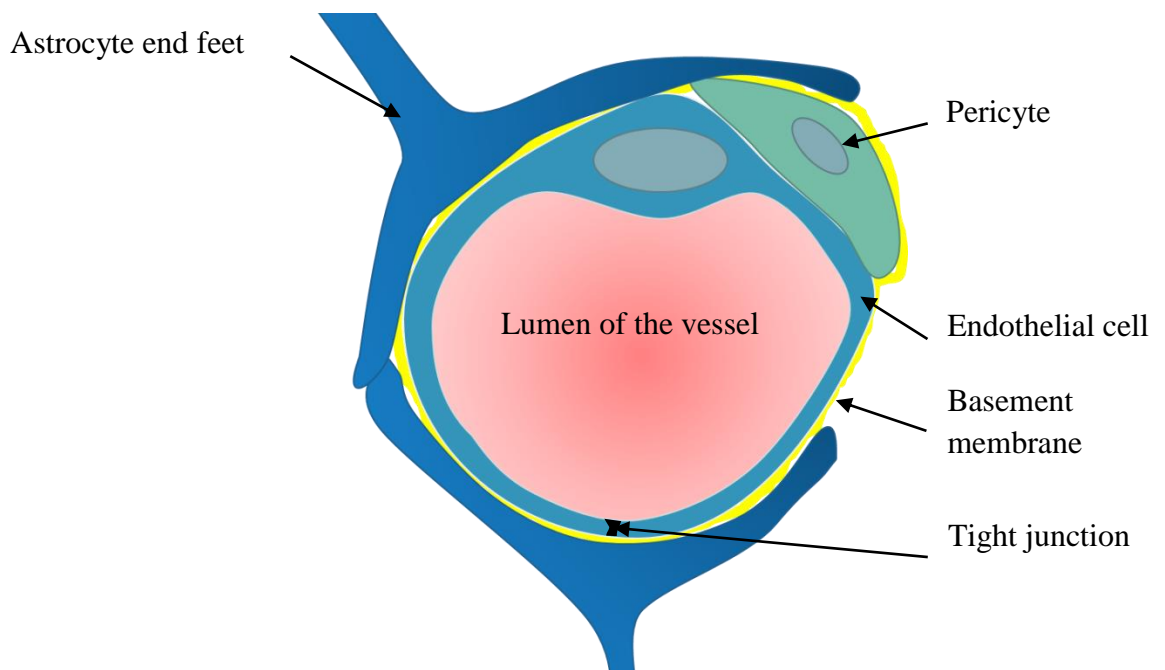
Figure 1-5: A schematic diagram of the components of BBB neurovascular unit.

1.4 Endothelial cells

Although the interior surface of blood vessels in the human body is covered with a single layer of cells called endothelial cells, the brain microvascular endothelial cell is very distinct. Unlike the endothelial cells in the rest of the bodies, brain endothelial cells are a specialised cell that forms a barrier in the brain microvasculature. Brain endothelial cell can be characterised by its glucose transporter (Virgintino et al., 2000), zonula occluden-1 (ZO-1) and occludin (Liebner et al., 2000). The comparison between brain endothelial cells and peripheral vascular endothelial cells has been summarised in table 1-2.

Table 1-2: The differences in selected properties of brain endothelial cells in camparison to the human umbilical vein endothelial cells. The information was gathered from various articles (Kniesel and Wolburg, 2000, Lo et al., 2001, Weksler et al., 2005, Abbott et al., 2006, Nag, 2011).

Properties	Brain endothelial cells	Peripheral vascular endothelial cells
Tight junction	Dense and continuous	Rarely observed
Vesicular transport	Rare	Abundant
Fenestration	Rare	Abundant
Transendothelial electrical resistance	High (>1500 $\Omega.cm^2$)	Low (< 100 $\Omega.cm^2$)
ɣ-Glutamyltranspeptidase	Present	Absent
Glucose transporter	Present	Absent
Light microscopy appearance		 (www.promocell.com)
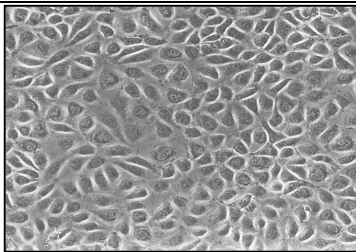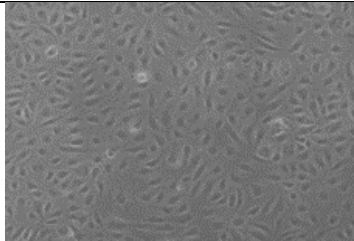
Endothelial cell lining is known as the endothelium. In an adult, it is estimated to be compose of about 1 kg or nearly 1 to 6 x 10^{13} of endothelial cells which covers a surface area of 7 m^2 (as reviewed in Cines et al. (1998)). Endothelial cells are differentiated from the mesoderm. Histologically, the average dimension of an endothelial cell is 3 μm thick, 30 μm long and 10 μm wide. The *in-vitro* culture of endothelial cells has a very characteristic cobblestone appearance when confluent (Figure 1-6).
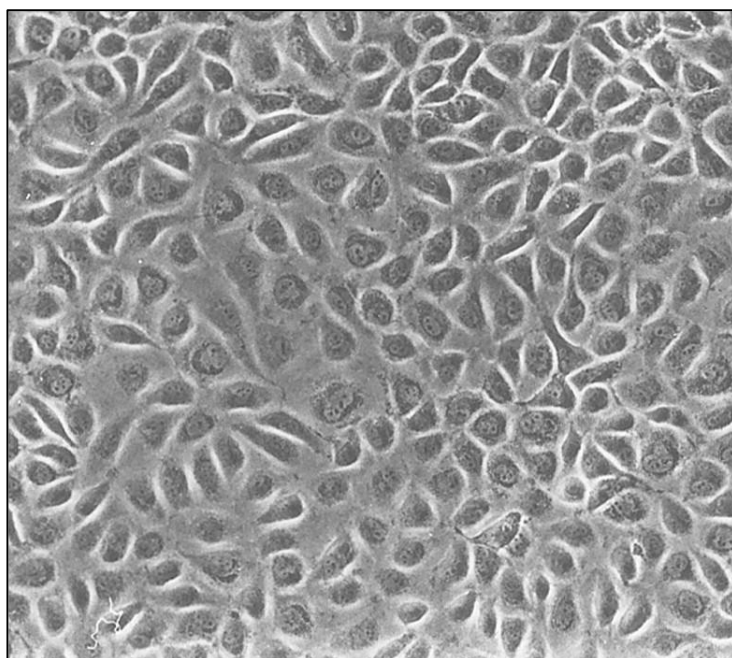
Figure 1-6: The *in-vitro* culture of human brain endothelial cells on a flat surface coated with collagen matrix, in absence of the shear flow, in the confluency state, appears as a 'cobblestone' structure.

Originally, the endothelium was viewed as an inert lining in the vessel. This however changed when Palade in 1953 and Gowan in 1959 showed the dynamicity of the endothelium. Endothelial cells served many functions in health and disease including, forming a barrier, indirect role in blood clotting mechanism and vasoregulation (for review

see Cines et al. (1998)). Several molecules including proteins (e.g.; growth factor, adhesion molecules), lipid transporter (e.g.; low-density lipoprotein), metabolites (e.g.; nitric oxide), and hormones (e.g.; endothelin-1) either on the surface or inside the endothelial cell, contribute to its function.

Besides the specific characteristics of brain endothelial cell as mentioned previously, endothelial cells can generally characterised by their morphology and the expression of specific markers (e.g., von Willerbrand factor (vWF), angiopoietin-1, vascular endothelial growth factor-B (VEGF-B), and platelet-endothelial cell adhesion molecule-1 (PECAM-1)) (Hewett, 2009). However, endothelial cells from different parts of the body have different ultrastructural characteristics. For instance, endothelial cells from brain microvasculature are lacking in fenestrae (Weksler et al., 2005).

One of the main features of the endothelial cell that will be focused on is its barrier capability and its involvement in inflammatory responses. The pericellular migration of solute between the brain endothelial cells is highly regulated by the presence of junction proteins at the intercellular junction between adjacent endothelial cells. There are two major classes of intercellular junction proteins, tight junction proteins (TJP) and adherens junction proteins (AJP). Adherens junction proteins can be found in endothelial cells from various organs while an intense strand of tight junction proteins can only be found in the BBB neurovascular unit. This might reflect the importance of TJP in the normal function of the BBB. It is also well established that loss in occludin, claudin-5, ZO-1 and vinculin are associated with the increase in the BBB permeability which allow serum fibrinogen to infiltrate into brain parenchyma, which consistently seen in many post-mortem study of CM (Turner et al., 1994, Brown et al., 1999, Brown et al., 2001, Dorovini-Zis et al., 2011).

1.4.1 Tight junction proteins (TJPs)

There are four main tight junction proteins that have been identified in the brain endothelial cell intercellular junctions (Kniesel and Wolburg, 2000). It can be divided into two main groups depending on its position in the cell; integral membrane protein and cytoplasmic accessory protein. Occludin, claudins and junctional adhesion molecule (JAM) are categorised as transmembrane tight junction proteins, while zonula occludens (ZO) are the members of cytoplasmic tight junction accessory proteins. Tight junction proteins (TJPs) appear as a continuous fusion site between the adjacent endothelial cells when observed under the electron microscope (Kniesel and Wolburg, 2000). Alterations in these junction proteins are frequently observed in either acute or chronic diseases reflecting its importance in maintaining normal functions of brain endothelial cells (Wolburg, 2007). The molecular arrangement of TJP and AJP of endothelial cells is illustrated as in figure 1-7.

In general, occludin and claudin has four transmembrane domains, two extracellular loop domain and one short N-terminal intracellular domain (see figure 1-8). In addition to the number of domains in occludin, claudin poses a PDZ-binding motif in its C-terminal end. In comparison, junctional adhesion molecule (JAM) has only one transmembrane domain and two loops made of disulphide bond in the extracellular loop region. The extracellular loop domains are important for the homophilic interaction of these TJP at the intercellular junction.
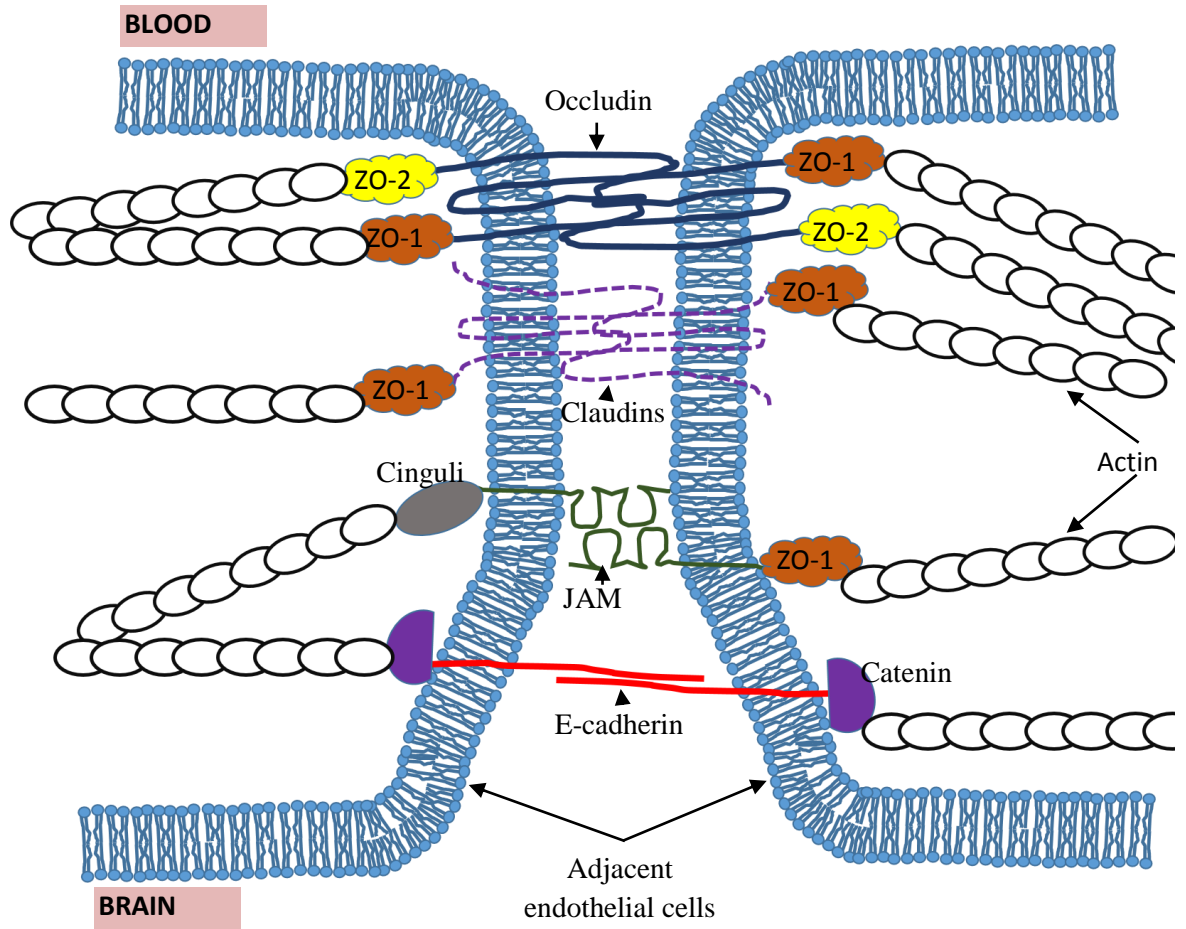
Figure 1-7: Schematic diagram of the arrangement of BBB endothelium intercellular junctions (Modified from Hawkins and Davis (2005))

Occludin

66 a.a	23 a.a	46 a.a	25 a.a	10 a.a	25 a.a	48 a.a	22 a.a	257 a.a
N-terminal (Intracellular strand)	TM1	EL1	TM2	IL	TM3	EL2	TM4	C-terminal (intracellular strand)

Claudin

7 a.a		52 a.a				16-33 a.a		21-36 a.a	
N-terminal (Intracellular strand)	TM1	EL1	TM2	IL	TM3	EL2	TM4	C-terminal (intracellular strand)	

PDZ-binding motif

JAM

N-terminal (Intracellular strand)	TM				S S			S S	
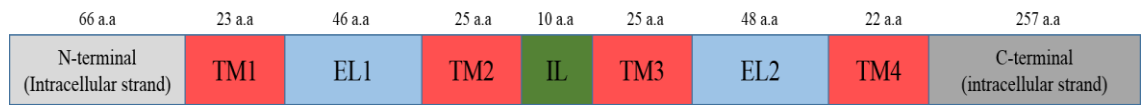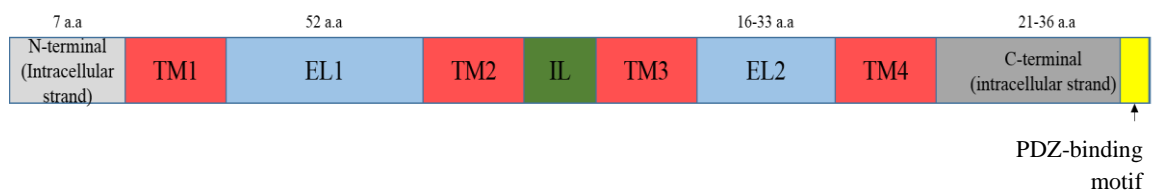
TM	Transmembrane domain
EL	Extracellular loop domain
IL	Intracellular loop domain

Figure 1-8: The arrangement of domains of occludin, claudin and JAM.

Occludin was the first membrane anchored protein localised at tight junctions of rat endothelial cells (Furuse et al., 1993). N-terminal and the extracellular domain of this TJP are important for a barrier function endothelium (Bamforth et al., 1999). The importance of occludin in an organism was demonstrated by the altered phenotype and postnatal growth retardation in occludin deficient mice (Saitou et al., 2000). Interestingly, occludin is not observed in normal new-born and foetal brain suggesting that it only synthesized in the developed brain (Papadopoulos et al., 2001).

Claudins are another family of transmembrane TJP found at the site of tight junctions between endothelial cells. 24 members of this protein family have been identified in mouse and human (Furuse et al., 1998, Morita et al., 1999). However, only three members, claudin-5, claudin-3 and claudin-12 were found at the site of the BBB (Nitta et al., 2003). Claudin is identified by the highly conserved PDZ-binding motif on its C-terminal, which serves as a binding site for PDZ-domain containing protein including ZO-1, ZO-2 and ZO-3 (Itoh et al., 1999).

Loss in both occludin and claudin-5 has been observed in a number of BBB pathologies including brain tumour, stroke and neural inflammation (Liebner et al., 2000, Lippoldt et al., 2000). The expression of occludin and claudin-5 in mice are also affected by the exposure to the human immunodeficiency virus type-1 (HIV-1) Tat protein, which may contribute to the breakdown of the blood-brain barrier in a HIV-1 infected patient (Pu et al., 2007, András et al., 2005). In addition, both of these TJP can be degraded by matrix metalloprotease-2 (MMP-2) which inhibited by the addition of broad spectrum MMP inhibitor BB1101, as seen in rat model of stroke (Rosenberg and Yang, 2007).

.

The cytoplasmic accessory tight junction proteins are made up of zonula occludens proteins and cingulin. Zonula occludens (ZO) is a member of the membrane-associated guanylate kinase-like (MAGUK) homolog family (Hawkins and Davis, 2005). It provides linkage between transmembrane TJ to the cytoskeletal actin. Three members of zonula occludens family have been identified, ZO-1, ZO-2, and ZO-3. Experimental diabetes in rat showed a significant reduction of ZO-1 and occludin in the compromised BBB suggesting that the reduction in ZO-1 and occludin at the BBB may affect the tightness and permeability of the BBB (Hawkins et al., 2007).

1.4.2 Adherens Junction Proteins (AJPs)

Like TJP, adherens junction proteins (AJP) also play a functional role in maintaining cell-cell adhesion by its molecular interaction. There are three AJP associated with brain microvascular endothelial cells which are VE-cadherin, catenin and vinculin (as reviewed in Stamatovic et al. (2008)).

Cadherin is a Ca^{2+} dependent transmembrane glycoprotein. To date 80 proteins have been identified in this protein family (Angst et al., 2001). Cadherins can be found in the brain endothelial cells, peripheral blood vessel endothelial cells (Bazzoni and Dejana, 2004), epithelial cells (E-cadherin) and neuronal cells (N-cadherin). In the brain endothelial cells, it is called vascular endothelial (VE)-cadherin. The involvement of cadherin in BBB is not clear since it is found in all endothelial cells. At the inter-endothelial junction, the cytoplasmic end of VE-cadherin is linked to the cytoskeleton with the help of catenin and vinculin, which can also be found at intercellular junction of cultured brain endothelial cells.

Vinculin is homologous to catenin and is regarded as adhesion junctional accessory protein located in the endothelial cytoplasm. It is a 116 kDa protein and provides a site of interaction between VE-cadherin and F-actin (Abe and Takeichi, 2008). The actual function of vinculin remains unclear, but when coupled with VE-cadherin, it may be involved in junction remodelling by distributing mechanical force between the cytoskeleton and the cell membrane to protect the endothelial cell junction (Huveneers et al., 2012). Rodríguez Fernández et al. (1993) demonstrates that the attachment of epithelial 3T3 cell line to the semi-solid culture surface and the attachments between neighbouring cells were significantly reduced when the vinculin expression was compromised, suggesting the involvement of vinculin in cell-cell and cell-matrix adhesion.

1.5 Breakdown of BBB in cerebral malaria

There are various way was used to assess the BBB function in human including; immunohistochemical analysis of the post-mortem brain section for a sign of BBB alterations, measurement of the ratio of IgG or albumin between cerebrospinal fluid (CSF) and plasma for permeability assessment, and recently the brain imaging for the detection of physical damage in the brain.

The association between *P.falciparum* infection and BBB damage in CM has been evidenced in a number of studies to date. The CSF/serum ratio of albumin in adult CM patients in Thailand showed a slight increase compared to the non-CM control patients, indicating the increase in the BBB permeability to allow serum albumin to infiltrated into CSF (Polimeni and Prato, 2014). Similarly, the CSF/plasma ratio of IgG among Vietnamese adults increased in CM compared to control (Brown et al., 2000). This however was found

not significant among Zairean children (as reviewed in Polimeni and Prato (2014)) suggesting that the impairment of BBB function was varies between adults and children.

Examination of post-mortem brain tissue, demonstrated three major patterns of BBB breakdown (Dorovini-Zis et al., 2011, MacCormick et al., 2014). The first is the fibrinogen extravasation that co-localised with ring haemorrhages (RH), second is the fibrinogen leakage around the blocked microvessels by fibrin thrombi, and the third is the deposition of fibrinogen around sequestered vessel but without fibrin thrombi. RH frequently occurs in the paediatric CM in the developing brain while the other two patterns of BBB damage are more frequent in adult CM, where the leakage is associated with the loss in the TJP. Immunohistochemical analysis of post-mortem brain section from Malawian children and Vietnamese adults for fibrinogen, a large serum protein that normally maintained within blood vessels, was showed leaked out into perivascular space indicating the leakage of BBB (Brown et al., 2001, Dorovini-Zis et al., 2011). This study also revealed reduction in BBB tight junction proteins (occludin, claudin, ZO-1) and adherens junction protein (vinculin) co-localised with the sequestered PRBC.

Evidence for BBB disruption also comes from a number of animal model studies. However, since *P.falciparum* only causes malaria in human a different *Plasmodium spp*. was used to study the effect of CM in mouse. It is well established that only *Plasmodium berghei* (ANKA) can induce cerebral malaria in mice with the similar symptoms as in human such as convulsion and coma (Rénia et al., 2012). Similar to the human CM, induction of CM in mouse results in BBB damage with severe impairment of BBB function. Although the mouse model shows similar evidence in BBB damage as seen in human, however, the mechanism contributing to this detrimental effect remains unclear because of the inability of the

Plasmodium berghei (ANKA) to sequester in the brain microvessel, which is a characteristic feature of human *Plasmodium falciparum*-mediated CM.

In line with the post-mortem study, an *in vitro* study demonstrated reduction in occludin, ZO-1 and vinculin mRNA in HUVEC when co-cultured with peripheral blood PRBC isolated from adult CM patients in Thailand (Susomboon et al., 2006). Interestingly, in the same study, no significant changes in the occludin, ZO-1 and vinculin mRNA were observed when the HUVEC was co-cultured with PRBC from non-CM patients. This suggests a potential strain specific effect that differentiates between the CM and non-CM causing *P.falciparum*.

Since the TJP have a relatively high correlation with endothelial barrier permeability, measurement of trans-endothelial electrical resistance (TEER) is popular *in vitro* for the assessment of BBB integrity (Treeratanapiboon et al., 2005, Tripathi et al., 2007). The electrical resistance of human brain microvascular endothelial cell (HBMEC) monolayer was decreased with time, peaking at within 5 hours when co-cultured with PRBC but not when co-cultured with uninfected RBC (Tripathi et al., 2007). The TEER proceeded to increase after the initial 5 hours, suggesting recovery of BBB integrity occurs after the damage, which was also seen in the post-mortem brain tissue of CM patients (Brown et al., 1999). Treeratanapiboon et al. (2005) also using TEER measurements, demonstrated reduction in the integrity of porcine brain endothelial cells monolayer *in vitro,* when co-cultured with malaria parasite-activated peripheral blood mononuclear cells. Although the loss of BBB integrity was observed in CM patients and in the *in vitro* model of BBB, the question on the possible mechanisms underlying the depletion of TJP leading to BBB leakage is still unanswered and open for exploration.

Previous studies demonstrated that contact between PRBC and endothelial cells is essential at low parasitaemia for the induction of ICAM-1 upregulation in HUVEC, which was not seen when the contact was inhibited by using a transwell to separate the PRBC and HUVEC monolayer but permits the passive diffusion of soluble factors between them (Chakravorty et al., 2007). This study also suggested that at low parasitaemia, the soluble factors from PRBC are unable to caused HUVEC activation. However, in a different system, Tripathi et al. (2007) suggested that parasite derived soluble proteins may be responsible for the loss of BBB integrity. In this study, HBMEC co-cultured with PRBC culture supernatant resulted in reduction in HBMEC monolayer TEER. In separate experiments, the investigator found that partial reduction of HBMEC electrical resistance could be induced by addition of artemisinin-treated PRBC, demonstrating that disruption of the BBB can also be induced by molecules on the surface of inactivated intact PRBC. Since the study only shows the TEER data, with no further examination on junctional complex composition and cell morphology, or characterisation of the possible soluble proteins released by PRBC, no further explanation can be made.

These collective evidences show that the leakage is mainly due to the loss of function of the endothelial cells monolayer making up the BBB; either directly due to the sequestration, inflammatory mediators or other soluble components.

1.6 Proteases and BBB damage in cerebral malaria

This thesis explores potential mechanisms for the loss of BBB integrity in CM. There is some evidence to suggest a potential role of proteases in a number of neurological disorders. Proteases are a superfamily of enzymes that are able to degrade a polypeptide by the

hydrolysis of peptide bonds between amino acids. There are several classes of proteases, categorised according to substrate specificity, molecular characteristics, and functions. A variety of proteases are expressed by endothelial cells either constitutively or due to activation including urokinase-type plasminogen activator (uPA) and the metalloproteases, collagenases, gelatinases and stromelysin (Menashi et al., 1993). This thesis focuses mainly on metalloproteases. Metalloproteases are a group of proteases containing divalent metal (*metallo*) ion at its active site. There are three closely similar metalloprotease families: matrix-metalloproteases (MMPs), a disintegrin and metalloproteases (ADAMs) and a disintegrin and metalloprotease with thrombospondin motifs (ADAMTS). A number of metalloproteases have been associated with the neurological disorders where the BBB is compromised such as multiple sclerosis, Alzheimer's disease and brain ischaemia.

1.6.1 Matrix metalloproteases (MMP).

Matrix-metalloproteases (MMP) or matrixins are a group of metalloproteases that function in the degradation of both extracellular matrix and non-matrix protein (Nagase et al., 2006). MMP are secreted in an inactive form (Sternlicht and Werb, 2001), and activated either by autocatalytic or non-proteolytic compounds such as reactive oxygen and denaturants (Springman et al., 1990, Van Wart and Birkedal-Hansen, 1990, Ogata et al., 1992, Nagase and Woessner, 1999). MMPs are secreted by various cells including endothelial cells. There are more than 23 members of the MMPs family which are categorised into 8 different sub-groups, according to their domain structures (Egeblad and Werb, 2002, Nagase et al., 2006). Of these subgroups, this thesis will focus mainly on the MMPs from gelatinase subgroup, of which there are two, MMP-2 (Gelatinase A) and MMP-9 (Gelatinase B). Both MMP-2 and MMP-9 show a high association with many vascular and neurodegenerative disorders (Gijbels et al., 1992, Wee Yong et al., 1998, Nakaji et al., 2006). MMP-2 is encoded by a

single copy gene (Collier et al., 1988) and regulated by various transcription factors such as AP-1, AP-2 and SP-1 (Qin et al., 1999). It is expressed and secreted as an inactive 70-72 kDa proMMP-2 molecule which is cleaved to form the 62-65 kDa active MMP-2 (Baramova et al., 1997). The main substrate for MMP-2 is collagen and fibronectin, which are extracellular matrix (ECM) proteins (Collier et al., 2001). Similarly, MMP-9 is secreted as a 92 kDa inactive proteases and undergoes proteolytic activation to form the 84 kDa active MMP-9 (Ogata et al., 1992). The expression of MMP-9 can be up-regulated by inflammatory cytokines namely IL-1α and TNF-α, as seen in fibroblast cells (Bond et al., 1998). Active MMP-9 may exist as a monomer or a homodimer (Van den Steen et al., 2002) and primarily hydrolyses ECM proteins, collagen and elastin (Murphy et al., 1991). Both MMP-2 and MMP-9 are secreted by various cell types including endothelial cells.

Involvement of MMP-2 and MMP-9 in the BBB damage in cerebral malaria has also been speculated in a number of studies. The level of MMP-9 in CSF from CM patient with minimal BBB breakdown was similar to the control, but significantly higher in the CSF from meningitis group which positive for the sign of BBB breakdown (Brown et al., 2000). Genomewide analysis of Kenyan children with malaria using microarray shows the upregulated level of MMP-9 compared to non-malaria control (Griffiths et al., 2005). Interestingly, significant relationship between upregulation of MMP and loss of ZO-1 and claudin has been observed in damaged BBB caused by West-Nile virus (Verma et al., 2010b). The involvement of matrix metalloproteases (MMP) in the breakdown of BBB also has been discussed by using mice model of CM with *Plasmodium berghei* ANKA (Van den Steen et al., 2006). Van den Steen et al. (2006) demonstrated the upregulation of MMP-2 and MMP-9 in the mice brain tissue following eight days of infection with *Plasmodium berghei* (ANKA), however further investigation using MMP-9 knock-out mouse showed no

difference in the mortality compared to wild-type mice, suggesting the minimal role of MMP-9 in CM pathogenesis in mice.

In multiple sclerosis (MS), the microglia and astrocyte isolated from the active brain lesions from MS patients show significant upregulation of MMP-1, -2, -3 and -9 compared to non-MS control (Cuzner et al., 1996). Interestingly, the breakdown of BBB in rat with MS is inhibited with the administration of GM6001, a synthetic hydroxamate inhibitor of MMP (Gijbels et al., 1994). In AD, MMP-2 and MMP-9 were localised highly in the region with elevated deposition of amyloid-β protein (Miyazaki et al., 1993). Additionally, these MMP including MMP-3 has the capability to degrade the amyloid-β proteins (Yoshiyama et al., 2000). The involvement of MMP in Alzheimer's disease (AD) however is unclear.

1.6.2 ADAMTS

There are at least 19 ADAMTS genes that have been identified in human (reviewed in Porter et al. (2005)). ADAMTS is differentiated from ADAM, another metalloprotease family by carrying the thrombospondin 1-like motifs near its C-terminal. Interestingly, in contrast to ADAM, all ADAMTS lack the transmembrane domain suggesting that the ADAMTS are a non-membrane bound protease. ADAMTS contains a signal peptide at N-terminal, which is cleaved during maturation process inside the cytoplasm before being secreted out of the cell as mature ADAMTS (Porter et al., 2005).

ADAMTS-1, -4 and -5 may be involved in the BBB damage and remodelling due to their ability to degrade extracellular matrix (ECM) proteins aggrecan (Tortorella et al., 1999) and versican (ADAMTS-1 and ADAMTS-4) (Matthews et al., 2000, Westling et al., 2004) which are the components of the BBB extracellular matrix (ECM). Additionally, the level of

ADAMTS-4 was found to be upregulated in MS plaques in MS post-mortem brain tissue where the BBB function is compromised, compared to control. Both ADAMTS-1 and ADAMTS-4 mRNA are upregulated in the brain tissue of the mice following induction of cerebral ischaemia (Cross et al., 2006). The upregulation of these ADAMTS was also shown in the brain tissue of monkeys with retroviral encephalitis (Medina-Flores et al., 2004). Additionally, activity of ADAMTS-4 from injured spinal cord tissue are increased after 7 days from the onset of injury, suggesting the involvement of ADAMTS-4 in the recovery of rat spinal cord following injury (Tauchi et al., 2012). Of interest, ADAMTS-1 and ADAMTS-4 inhibited endothelial cells proliferation and able to inhibit the VEGF-induced angiogenesis through its thrombospondin-1 motif (Vázquez et al., 1999) and, these proteases may also involves in the breakdown of BBB in cerebral malaria. This accumulating evidence on ADAMTS proteases may have significant roles in tissue damage in the CNS.

The gene encoding ADAMTS-1 was firstly identified in mouse (Kuno et al., 1997). In that study, ADAMTS-1 mRNA was demonstrated to be upregulated by the addition of pro-inflammatory cytokines such IL-1. ADAMTS-1 are secreted as 87 kDa proform which activated by proteolytic processing to the 65 kDa active form. ADAMTS-1 is found to be partially inhibited by TIMP-2 and TIMP-3 but not TIMP-1 (Carlos Rodríguez-Manzaneque et al., 2002). ADAMTS-4 activation involves the cleavage of the C-terminal protein, which reduces the size of inactive 75 kDa ADAMTS-4 into 60-50 kDa active form. The proteolytic function of ADAMTS-4 can be inhibited with very low concentration of TIMP-3 (Kashiwagi et al., 2001).

The potential involvement of MMP-2 and MMP-9 in CM pathogenesis was demonstrated in many malaria studies either using samples from malaria patients or

appropriate animal model of CM as previously mentioned, however only limited data on the potential association of both ADAMTS-1 and ADAMTS-4 with BBB damage in CM can be retrieved. Since ADAMTS-1 and ADAMTS-4 shares the majority of their substrates with MMPs (Fosang et al., 1996) and the link between the upregulation of these proteases and BBB damage in several neurological disorders as mentioned before, it is desirable to investigate their involvements in the mechanism of BBB damage in CM. This thesis hypothesized that the interaction between PRBC and HBEC induces the release of a group of soluble mediators including proteases, which may contribute to the BBB breakdown in Cerebral Malaria.

1.7 Aim of the thesis

Utilising tHBEC as an *in vitro* model of BBB, this thesis aims to:

1.   Investigate the effect of co-culture between PRBC and tHBEC to the expression of inflammatory mediators including cytokines and proteases (MCP-1, IL-8, MMP-2, MMP-9, ADAMTS-1 and ADAMTS-4) by ELISA and Western blotting.

2.   Investigate the effect of co-culture supernatant on the tHBEC integrity by TEER measurement in the absence and presence of protease inhibitors.

3.   Investigate the effect of co-culture supernatant on the tHBEC permeability using FITC-dextran permeability assay the absence and presence of protease inhibitors.

4.   Investigate the effect of co-culture supernatant on the expression of key TJP (Claudin-5, Occludin, ZO-1 and Vinculin) using cell-based ELISA.

CHAPTER TWO: GENERAL MATERIALS AND METHODS

Chapter 2: General Materials and Methods

2.1 Introduction

Throughout the experiments in this study, few methods were frequently used. This chapter will cover the methodology used in the maintenance of tHBEC and *Plasmodium falciparum*, the identification of tHBEC and the co-culture experiment. The specific material and methods for each other experiment can be found in each specific chapter. All kits, chemical and reagents, antibodies, materials and, equipment are listed in this chapter.

2.2 Endothelial cell culture

The transformed human brain endothelial cell (tHBEC) used in this study was kindly supplied by Dr. Monique F. Stins of John Hopkins University, Baltimore, USA. The brain endothelial cells were originally isolated from human and immortalised *via* transformation with the SV40 large T antigen. The cells were also thoroughly characterised by other research group (Stins et al., 1997, Callahan et al., 2004). However, the responsiveness of the tHBEC in to TNF-α, IL-1β and the uptake of Dil-Ac-LDL we regularly checked in this study. In this study, tHBEC from passage 20 to 30 was used as an *in vitro* model of human blood-brain barrier.

2.2.1   Endothelial cell growth medium

The tHBEC growth medium was formulated for the optimal growth of tHBEC. It comprised RPMI-1640 containing 10% (v/v) foetal bovine serum, 5% (v/v) new born-calf serum, 2 mM L-glutamine, 100 unit/ml penicillin and 100 μg/ml streptomycin.

2.2.2 Quiescent medium (Q-medium)

The tHBEC quiescent medium was formulated for culturing the tHBEC under resting condition for the co-culture experiments. It was a RPMI-1640 supplemented with 1% (v/v) foetal bovine serum, 2 mM L-glutamine, and 100 unit/ml penicillin and 100 µg/ml streptomycin, referred to as $Q_{1\% \text{ FBS}}$-medium. For the transendothelial electrical resistance (TEER) and permeability studies, the quiescent medium was supplemented with 5% (v/v) foetal bovine serum (referred to as $Q_{5\% \text{ FBS}}$-medium) in order to optimise the monolayer integrity.

2.2.3 Seeding endothelial cells from frozen stabilate

The tHBEC stabilates were kept at -80°C or liquid nitrogen storage in the cryopreservation medium (Cryo-SFM). Each vial contains 1 ml of cell suspension at the density between 2.0 to 3.5 x 10^6 cell/ml. To reconstitute the tHBEC, a stabilate was thawed in 37°C water bath. The cell suspension was then resuspended in 2 ml of pre-warmed growth medium before being transferred into three 25 cm^2 cell culture flasks containing 2 ml of pre-warmed growth medium. The flask was pre-coated with 1% (v/v) gelatine solution prepared in 1X sterile phosphate buffered saline (PBS), pre-incubated at 37°C for a minimum of 20 minutes before the cells were plated. The flask with the cells were incubated at 37°C and 5% CO_2 atmosphere, for a minimum of 2 hours to allow viable cells to adhere. After that, the initial growth medium in each flasks containing non-adherent and non-viable cells were replaced with 4 ml of pre-warmed growth medium and incubated until confluence, monitored every 48 hours using an inverted light microscope at a magnification of 10X objective.

2.2.4 Passaging the tHBEC

Each flask containing confluent tHBEC were passaged into new flask or plate (summarised in figure 2-1) for the cell culture continuation or subsequent experiment. First, the culture medium in the flask with confluent tHBEC monolayer was removed using a pump aspirator. Then, the cells monolayer was quickly washed in 1.5 ml of sterile phosphate buffered saline (PBS). To detach the cells from each other and from the culture surface, 1.5 ml of 0.25% (w/v) trypsin-EDTA solution was added evenly onto the cells monolayer and incubated at room temperature for 1 minute. To assist the cell detachment, gentle mechanical force was applied by tapping the side of the flask with the palm. The detached cells were observed under the inverted microscope as free-floating round cells. After that, 1.5 ml of pre-warmed growth medium was added into the flask to stop the trypsin digestion by a substrate competition mechanism. The detached cells were transferred into a 15 ml centrifuge tube and centrifuged at 480 x g (1500 rpm) for 3 minutes. The cell pellet was recovered by removing the supernatant using a pump aspirator. The pellet then suspended in 0.5 ml pre-warmed growth medium before being diluted with an additional volume of pre-warmed growth medium, depending on the culture plate required for the subsequent study (See figure 2-1). Once plated onto a gelatine coated plate, they were cultured as described in section 2.2.3.
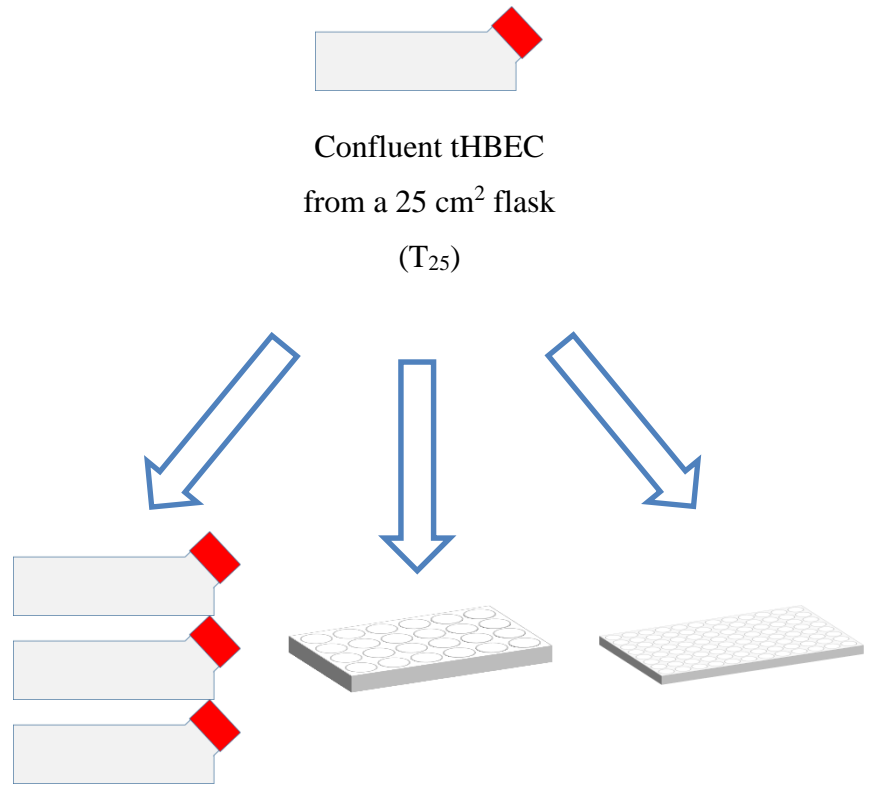
New culture plate:	Three T25 flask	One 24 well plate	One 96 well plate
Cell density:	1.5×10^6 cell/flask	1.0×10^5 cells/well	20 000 cell/well
Seeding volume (for 2 hour incubation):	3000 µl/flask	500 µl/well	100 µl/well
Culture volume (1-2 days culture):	4000 µl/flask	1000 µl/well	200 µl/well

Figure 2-1: The ratio of endothelial cell passage from single 25 cm^2 Flask.

Cell density referring to the number of cells seeded in each flask or plate. Seeding volume is lower than the culturing volume to facilitate the quicker endothelial cell attachment to the culture surface.

2.2.5 Cell counting

To count the cells, the cells need to be trypsinised as in section 2.2.4. Following trypsin treatment, the cells pellet was first suspended in 0.5 ml of pre-warmed growth medium. 10 µl of cell suspension was then diluted 1:10 in fresh growth medium and counted using a haemocytometer. All cells in the regions marked 1 to 4 in figure 2-2 were counted and averaged. The formula for cells count is as below. The cells were resuspended in appropriate volume of growth medium depending on the cell culture plate used for subsequent experiments (Figure 2-1).

Cell count formula:

$$\text{Cell density (cells/ml)} = \text{average number of cells} \times 10^4 \times \text{dilution factor}$$

$$\text{Where dilution factor} = 10$$
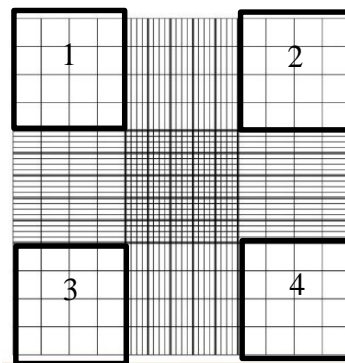
Figure 2-2: The layout of haemocytometer for cells counting.

Only cells in region 1 to 4 were counted, averaged and multiplied with dilution factor to give the approximate number of cells. The image taken from www.hawksley.co.uk/cell-count_glassware (last accessed on 03 March 2014)

2.2.5.1 Detection of ICAM-1 expression

The up regulation of tHBEC ICAM-1 in response to TNF-α and IL-1β was measured using cell-based ELISA on the fixed confluent culture (figure 2-3). First, the tHBEC was cultured in 96 well plate and maintained until confluent. After 24 hours, the medium was changed to $Q_{5\% \; FBS}$-medium to bring the tHBEC into resting condition for another 24 hours. This step is important to reduce the noise of the basal value due to active replicating cells. After that, 100 µl/well of 10 ng/ml TNF-α or 1 ng/ml IL-1β that was prepared in $Q_{5\% \; FBS}$-medium was added to the cells and incubated for 24 hours. Following the incubation, the supernatant was removed and the cells were gently washed in 150 µl cold PBS containing 0.1% (v/v) bovine serum albumin (BSA) per well. The cells then fixed with ice-cold methanol 100% (v/v), for five minutes at room temperature before being washed in 0.1% (v/v) BSA in PBS. To reduce the non-specific binding of the antibodies, the cells were blocked with 50 µl of 1% (v/v) BSA in PBS per well for 1 hour at room temperature. After that, the blocking solution was aspirated and 50 µl/well of anti-human ICAM-1 antibody was added to the cell at the concentration of 1 µg/ml prepared in 0.1% (v/v) BSA/PBS and incubated for two hours at room temperature on a rocking platform. Then, the cells were washed three times with PBS before the secondary antibody, horseradish peroxidase (HRP) conjugated- goat anti-mouse IgG at dilution of 1:3000 in 0.1% (v/v) BSA/PBS was added to the wells. At this stage, the plate was wrapped in tin foil to reduce the light exposure and incubated for 1 hour at room temperature on a rocking platform. After that, the cells were washed three times using PBS and in the low light condition and 100 µl of TMB (tetramethylbenzidine) substrate was added to each well. The substrate changes its colour from clear to blue, demonstrating a positive reaction. The magnitude of the blue colour correlates with the concentration of ICAM-1. Then, 100 µl concentrated sulphuric acid was added into each well to stop the reaction and change the blue colour of reaction product to yellow. The absorbance was measured at the

wavelength of 450 nm using an ELISA plate reader (GLOMAX™ Multi+ detection system, Promega). The measurement of the yellow colour correlated with the concentration of ICAM-1.

| Endothelial cells fixed in the well | Probing with primary antibody | Detection using HRP-conjugated secondary antibody |
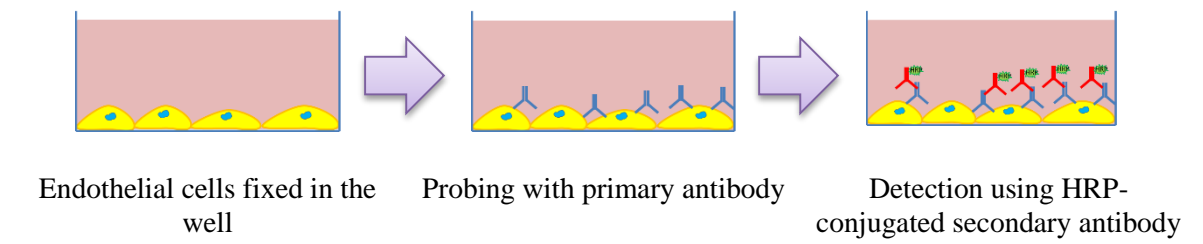
Figure 2-3: The principle of cell-based ELISA.

In cell based ELISA, the detection of an antigen is done directly on the fixed cells. First the probing of an antigen by specific antibody and then detected using HRP-conjugated secondary antibody. HRP on the secondary antibody is responsible for the colour change reaction of the TMB substrate.

2.2.5.2 Von Willebrand factor (vWF)

The endothelial nature of the tHBEC was confirmed by assessing the appearance of the von Willebrand Factor (vWF) using immunocytochemistry technique. First, the tHBEC were cultured to confluent on sterile round thermanox coverslips pre-coated with 1% (v/v) gelatine in a 24 well culture plate as in section 2.2.4. Once confluent, the cells were washed with pre-warmed PBS containing 1% (v/v) BSA. After that, the cells were fixed with 1%

(v/v) gluteraldehyde. To allow the antibody to reach the vWF in the cell cytoplasm, the tHBEC were permeabilised using 250 µl/well of 0.2% (v/v) triton X-100 prepared in 0.1% (v/v) BSA/PBS for 10 minutes at room temperature. Then, the cells were washed twice with 250 µl/well of 0.1% (v/v) BSA/PBS before been blocked with 250 µl/well of 1% (v/v) BSA/PBS for 1 hour at room temperature. After that, 1 µg/ml of monoclonal mouse anti-human vWF were applied on to the cells and incubated at room temperature for 2 hours on a rocking platform. After the incubation, the cells were washed twice with 250ul/well of 0.1% (v/v) BSA/PBS and incubated in the dark for 1 hour at room temperature with the secondary antibody, FITC-labelled goat anti-mouse IgG at a dilution of 1:250. The cells on the coverslip were washed twice with PBS. In control wells, the tHBEC were also stained with primary antibody only and secondary antibody only. Finally, the coverslip with the stained tHBEC were carefully transferred onto a microscope glass slide with the surface containing cells facing up. The nucleus of the cells were counterstained with fluorescent blue 4',6-diamidino-2-phenylindole (DAPI) in mounting reagent, Vectashield ™. The cells then covered with a rectangular glass coverslip and sealed with nail varnish to restrict the movement of the assembly when visualising under a fluorescent microscope. To image the vWF and cell's nucleus, sets of fluorescent filter as in table 2-1 were used.

Table 2-1: The list of the fluorochrome and its appropriate filter set used in the immunocytochemistry experiment for the detection of endothelial cell vWF.

Molecule and Fluorochrome	Filter set (Leica)	Wavelength (nm)	
		Excitation	Emission
vWF (FITC)	Green	467-498	513-556
Nucleus (DAPI)	Blue	352-402	417-477
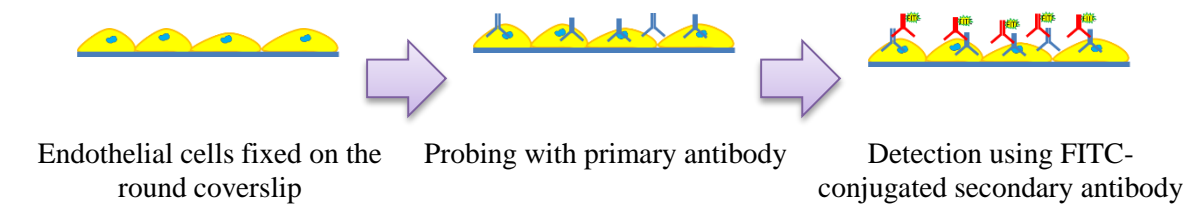
Figure 2-4: The principle in the immunofluorescence technique.

The primary antibody probing the antigen on the fixed cells, followed by the detection using fluorescence conjugated secondary antibody. The localisation of the fluorescein can be visualised using fluorescence microscope with appropriate filter set.

2.2.5.3 Dil-Ac-LDL uptake

The endothelial nature of the tHBEC was also confirmed by cytochemistry for its ability to uptake the acetylated-low density lipoprotein (Ac-LDL). For this assay, Ac-LDL labelled with fluorescent 1,1'-dioctadecyl-3,3,3',3'-tetramethyl-indocarbocyanine perchlorate (Dil-Ac-LDL) was used. First, the tHBEC was cultured in a sterile flat bottom 96-well culture plate as section 2.2.4 to confluent. Once the tHBEC reached more than 90% confluency, the growth medium was replaced with $Q_{5\% \text{ FBS}}$-medium and cultured for another 24 hours. After that, the medium was replaced with growth medium containing 10 µg/ml of Dil-Ac-LDL and incubated for 4 hours in culture condition. Then, the media containing Dil-Ac-LDL were removed and the cells monolayer was washed three times with $Q_{5\% \text{ FBS}}$-medium. By using a fluorescence microscope set at Rhodamine filter with excitation wavelength range between

515 nm and 560 nm, and emission at 590 nm, the tHBEC that is able to uptake the Dil-Ac-LDL appeared as red in its cytoplasm. The cells were imaged using Leica FW4000 imaging software.

2.3 *Plasmodium falciparum* culture

In this study, the *Plasmodium falciparum* ItG strain was used. This strain was derived from Brazilian line IT4/25/5 (Ockenhouse et al., 1992a). The *Plasmodium falciparum* were cultured in the laboratory according to the *in-vitro Plasmodium falciparum* culture method (Trager and Jensen, 1976). This strain has been characterised to have strong binding capability to ICAM-1 molecule on the endothelial cell surface, which may have significant role in PRBC sequestration in severe malaria (Ockenhouse et al., 1991, Gray et al., 2003, Chakravorty et al., 2007). Cultures were supplemented regularly with freshly isolated red blood cells every 48 hours and maintained in 96% N_2, 3% CO_2, and 1% O_2 at 37°C. *Plasmodium falciparum* was kept frozen at -80°C for long-term storage at the ring stage. The *Plasmodium falciparum* culture was performed in the CAT III cell culture suite which is a Health and Safety Executive approved facility for the use of *Plasmodium falciparum* according to local rules as laid out in the CAT III suite code of practice. The provision of screened leukocyte-depleted blood and serum by the National Blood and Transfusion service (NBTS) UK for *Plasmodium falciparum* culture is approved in this facility. All storage and disposal of blood was done in accordance with the Human Tissue Authority (HTA) licence held by Keele University. Detailed protocol for the culture of *Plasmodium falciparum* from frozen is described below in section 2.3.3.

2.3.1 Preparation of *Plasmodium falciparum* culture medium.

Plasmodium falciparum growth medium was prepared by modifying RPMI-1640 to contain 37.5 mM HEPES, 7 mM Glucose (Filter sterilised), 6 mM NaOH (Filter sterilised), 2 mM L-glutamine, 25 µg/ml gentamicin solution and 10% (v/v) pooled human serum. This medium is hereafter referred as *Pf* G-medium. Similar to this, serum free medium was prepared but without the addition of human serum and referred as *Pf* G-SF, which was used for all washes in PRBC culture.

2.3.2 Preparation of 50% (v/v) washed red blood cells (50% WRBC).

Plasmodium falciparum require red blood cells for its intra-erythrocytic life cycle. To fulfil this requirement, the parasite cultures were supplemented with red blood cells. To prepare 50% (v/v) washed red blood cells, 5 ml of leukocyte-depleted red blood cells (Type O) was mixed with an equal volume of *Pf* G-SF in a sterile tube. After that, the mixture was carefully layered onto 5 ml of histopaque (at a density of 1.077 g/ml) in a new 50 ml centrifuge tube (Figure 2-5). The tube was then centrifuged at 2000 x g (3000 rpm), for 15 minutes at room temperature. The supernatant (containing plasma, lymphocytes, monocytes and histopaque) was then removed by aspiration and leaving the red blood cells pellet (see figure 2-5). 25 ml of *Pf* G-SF was added to the pellet, mixed well and centrifuged at 2500 x g (3500 rpm) to remove any redual histopaque which is toxic to the cells. Finally, the volume of the red blood cells pellet was estimated and an equal volume of *Pf* G-SF was added to it to prepare a 50% (v/v) washed red blood cell suspension, and stored at 4°C for no longer than one week. This was referred as 50% WRBC in this thesis.

| Before centrifugation | After centrifugation |
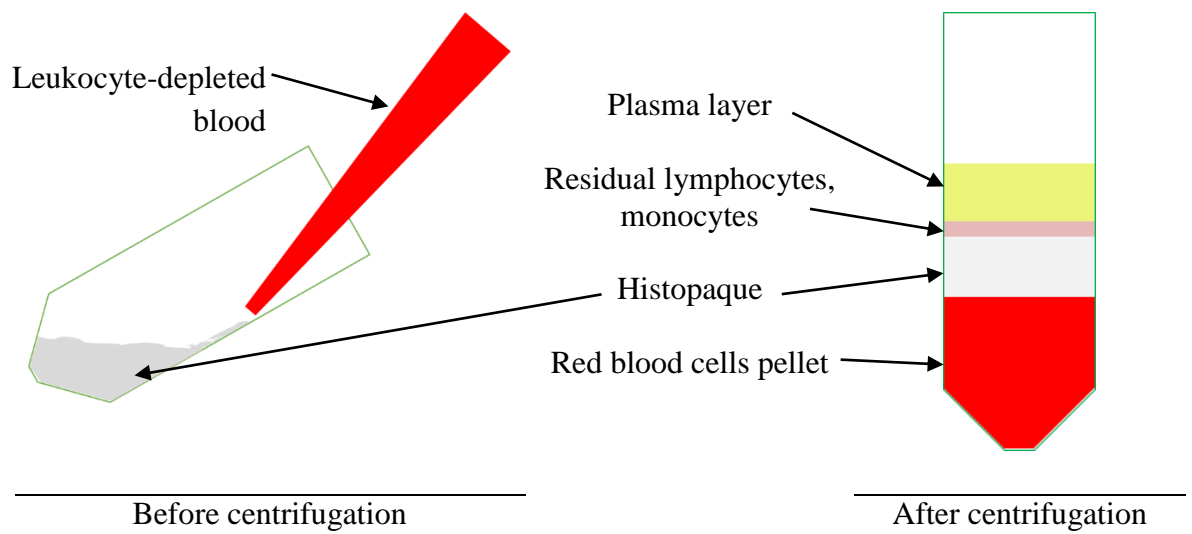
Figure 2-5: Preparation of 50% WRBC.

The process of layering the red blood cells on the histopaque in a 50 ml centrifuge tube. This process need to be very carefully done where the red blood cells were added slowly on the slanting wall of the tube to avoid them to form a mixture of histopaque and the red blood cells which can reduce the quality of the product.

2.3.3 Reconstitution of frozen *Plasmodium falciparum* stabilates

To start a fresh *Plasmodium falciparum* culture, the frozen stabilate was slowly thawed at 37°C. This was followed by addition of decreasing concentration of salt solutions from 12% to 0.9%. The salt solutions were filter sterilised (0.2 µm pore size). All solutions and medium used were pre-warmed at 37°C prior to use. Once the stabilate was completely thawed in a 37°C incubator, it was then transferred to a new 50 ml centrifuge tube. Then, 12% (w/v) NaCl was added drop wise into it with the ratio of 1 part of 12% (w/v) NaCl for every 5 part of starting stabilate volume and incubated at room temperature for 5 minutes. After that, pre-

warmed 1.8% (w/v) NaCl was added drop wise at the same ratio and incubated at room temperature for another 5 minutes. Next, the final salt solution at the concentration of 0.9% (w/v) NaCl in 0.2% (w/v) glucose was added to the parasite as before. The parasite suspension was then centrifuged at 1200 x g (2800 rpm) for 5 minutes and the supernatant was removed. The parasite suspension was washed with excess volume of *Pf* G-SF and centrifuged as above to remove any excess salt. After the supernatant was removed, the parasite pellet then suspended in 3 ml of *Pf* G-medium and transferred into a fresh non-vented 25cm^2 culture flask. The total volume of the parasite culture in the flask was adjusted to 5 ml before gassed with 96% N_2, 3% CO_2, and 1% O_2. The culture was incubated at 37°C for at least 24 hours and the progress monitored by preparing a smear and examine by light microscopy. Parasites at the trophozoites stage were expected.

The parasite was maintained for its optimal growth at a haematocrit of 1-2% and examined every 48 hours, reflecting the complete intra-erythrocytic cycle of *Plasmodium falciparum*. In this study, *Plasmodium falciparum* at the trophozoites stage was used for all experiments. The maintenance of *Plasmodium falciparum* involves preparation of a smear to estimate the parasitaemia, changing the medium and addition of fresh red blood cell supply for continued invasion by the parasite.

To prepare the smear, firstly, 100 µl of *Plasmodium falciparum* culture was transferred into a 1.5 ml micro centrifuge tube and centrifuged for 1 minute using a small bench top centrifuge (maximum 14 500 rpm). After that, the supernatant was removed and the pellet was suspended in 200 µl of *Pf* G-SF. Then, 10 µl of the parasite suspension was transferred onto a clean glass slide and a thin smear was prepared by using another clean glass slide to function as spreader. The smear was air dried before being fixed using 100%

(v/v) methanol for 1 minute. As soon as the methanol evaporated, the smear was stained with 10% (v/v) Giemsa for 5 minutes. Finally, the excess stain was removed by rinsing the smear using tap water and dried using hair a dryer. The appearance of life stage was observed under a compound microscope with the 100X objective oil immersion lens. The parasitaemia was calculated by counting the number of *Plasmodium falciparum* infected red blood cell (PRBC) out of 200 total cells using the following equation:

$$\text{Parasitemia (\% P)} = \frac{\text{number of PRBC}}{\substack{\text{number of total cell count} \\ \text{(PRBC+uRBC)}}}$$

To change the *Plasmodium falciparum* culture medium, first, the culture was transferred into appropriate size of sterile centrifuge tube. The culture then centrifuged at room temperature with the speed of 1200 x g (2800 rpm) to separate the red blood cells (RBC) and *Plasmodium falciparum* infected red blood cells (PRBC) from the *Pf* G-medium. After that, the supernatant was aspirated and leaving the mixture of RBC and PRBC pellet. The pellet was then resuspended in appropriate volume of pre-warmed *Pf* G-medium. The volume of fresh *Pf* G-medium added was determined according to the percentage of parasitaemia. After that, the parasite was transferred into a sterile non-vented culture 25 cm² flask. The parasitaemia of the culture was maintained at 5 to 10% in 1000 μl pack cell volume (PCV) for co-culture experiments. The parasitaemia was adjusted by adding an appropriate volume of 50% (v/v) washed RBC. Finally, the culture were re-gassed for 20 seconds and incubated at 37°C for another cycle.

2.3.4 Trophozoite enrichment by plasmagel floatation.

For the co-culture experiments, the mature trophozoite stage of *Plasmodium falciparum* was harvested from the culture by using the plasmagel floatation technique. This technique selects the less dense trophozoite stage and knob positive PRBC. To obtain more than 50% parasitemia after the enrichment, the *Plasmodium falciparum* culture was expanded to 10-15% parasitemia at trophozoite stage in 1000 μl packed cell volume (PCV), prior to plasmogel floatation.

First, the culture was transferred into a centrifuge tube and centrifuged at 1430 x g (2000 rpm) for 5 minutes. The pellet was recovered by aspirating the supernatant and washed with 20 ml of pre-warmed *Pf* G-SF. Then, the parasite suspension was centrifuged at 1430 x g for five minutes. The pellet was suspended in 6 ml of *Pf* G-SF and divided into two sterile 15 ml centrifuge tube. The tubes were then centrifuged at 1430 x g for 5 minutes and the PCV of PRBC was estimated. After removing the supernatant, 1.5 ml of pre-warmed *Pf* G-SF and 2.5 ml of pre-warmed plasmagel was added per one millilitre PCV of PRBC. The mixture was thoroughly mixed to form a homogeneous suspension and incubated for 1 hour at 37°C in upright standing position. During this step, the suspension will form a clear demarcation between the top and bottom layer. Top layer containing trophozoites was carefully transferred into a sterile 15 ml centrifuge tube and centrifuged at 1430 x g for 5 minutes. To remove any plasmagel carryover, the pellet was washed twice in *Pf* G-SF. To wash, the pellet was suspended in 10 ml *Pf* G-SF and centrifuged at 1430 x g for 5 minutes. Finally, the parasitaemia and the development stage of parasite were assessed under the light microscopy as in section 2.3.3.

2.4 The co-culture experiment

Co-culture experiment is an experiment where the tHBEC were co-cultured either with *Plasmodium falciparum* infected red blood cells (PRBC) or uninfected red blood cells (uRBC), as control.

For the co-culture experiment, the tHBEC was cultured in a 25 cm^2 cell culture flask for 48 hours to reach confluence. The medium was replaced with $Q_{1\% FBS}$-medium for a minimum of four hours prior to the start of the co-culture.

The enriched trophozoite suspension at a minimum of 50% parasitemia was diluted in an appropriate volume of $Q_{1\% FBS}$-medium to give a final haematocrit of 1%. All co-culture experiments were done in 3 ml of the prepared PRBC suspension of more than 50% and haematocrit of 1% for 20 hours.

To be a consistent control to the experiment, uRBC was prepared with the same procedure as PRBC. First, the uRBC suspension was cultured as in section 2.3.3 and subjected to the plasmagel floatation step as in section 2.3.4. The uRBC was diluted in $Q_{1\%}$ $_{FBS}$-medium to give a final of 1% haematocrit.

2.4.1 The co-culture condition

The resting tHBEC was co-cultured with either PRBC or uRBC for 20 hours at 37°C with 5% CO_2 supply. To serve as an activation control, the tHBEC was cultured in $Q_{1\% FBS}$-medium containing 10 ng/ml of TNF-α. For the experiment control, the PRBC and uRBC was cultured in the same condition but without tHBEC. The co-culture conditions in each experiment are summarised in table 2-2.

Table 2-2: The co-culture condition in this study.

Five co-culture experiments were done in this study to yielding 10 sets of co-culture supernatant and lysate. The uninfected red blood cells (uRBC) only and the *Plasmodium falciparum* infected red blood cell (PRBC) only culture experiment was only done twice.

Components	Co-culture condition					
	Control (Negative)	tHBEC/ uRBC control	tHBEC/ PRBC	tHBEC/ TNF-α activation	uRBC only control	PRBC only control
tHBEC	✓	✓	✓	✓	✗	✗
uRBC	✗	✓	✗	✗	✓	✗
PRBC	✗	✗	✓	✗	✗	✓
TNF-α	✗	✗	✗	✓	✗	✗

Legend:

 The tHBEC

 The uninfected red blood cells (uRBC)

 The *Plasmodium falciparum* infected red blood cell (PRBC)

TNF-α   Tumour necrosis factor – alpha

2.4.2 Harvesting the cell lysate and co-culture supernatants

Following 20 hours incubation, the supernatant and endothelial cell lysates were harvested. First, the supernatant from the flask was transferred into a sterile 15 ml centrifuge tube and was kept on ice for processing later. As soon as the supernatant was transferred, the cell in the flask was washed twice with cold cell wash buffer (RPMI1640 containing 2 mM L-glutamine, and 100 unit/ml penicillin and 100 µg/ml streptomycin). To assist the adhered PRBC to detach from the tHBEC, the flask was gently rocked ten times while in cell wash buffer. After that, the cell wash buffer was removed by aspiration and 100 µl of ice cold RIPA was added dropwise onto the cell monolayer and incubated at 4°C for 3 minutes. The cells were observed under light microscope with the appearance of tHBEC nucleus in round shape indicating the tHBEC were lysed. Then, the cells were scraped from the flask using clean cell scraper and the lysate was transferred into a sterile centrifuge tube. The nucleic acid, which appears as a cloudy white sticky clump, was removed from the lysate before being stored at -20°C for later use.

The co-culture supernatant that was kept on ice earlier was centrifuged at 478 x g (1500 rpm) for 3 minutes to clarify the co-culture supernatant from uRBC, PRBC and any cell debris. The co-culture supernatant then recovered from the pellet into three sterile 1.5 ml centrifuge tubes, with one ml in each tube.

2.5 List of kits

Table 2-3: The list of kits used in the study.

No.	Name	Catalogue Number	Manufacturer
1	DuoSet® ELISA human ADAMTS-1	DY2197	R&D Systems
2	ELISA IL-8 Eli-pair	Ab48481	Abcam
3	Human MCP-1 ELISA	650 110 096	Diaclone
4	Quantikine ® ELISA MMP-2	DMP2FO	R&D Systems
5	Quantikine ® ELISA MMP-9	DMP900	R&D Systems

2.6 List of chemicals and reagents

Table 2-4: The list of chemicals and reagents used in the study.

No.	Name	Catalogue Number	Manufacturer
1	10% (w/v) Sodium Dodecyl Sulphate	BP2436	Fisher Scientific
2	10x Blocking Buffer	B6429	Sigma-Aldrich
3	2-Mercaptoethanol	M7154	Sigma-Aldrich
4	Acetic acid	A/0360/PB17	Fisher Scientific
5	Acrylamide solution	BP1408	Fisher Scientific
6	Albumin solution from bovine serum	A7284	Sigma-Aldrich
7	Ammonium persulfate	A/P470/46	Fisher Scientific
8	Brij 35.30 % (w/v)	3.3E+08	Acros Organics
9	Bromophenol Blue	114391	Sigma-Aldrich
10	Calcium Chloride	BP510	Fisher Scientific
11	Cyro-SFM (Endothelial cryopreservative)	C-29910	Promocell
12	Dextran-FITC conjugate (MW 70 000)	FD70S	Sigma-Aldrich
13	D-Glucose	G/0500/61	Fisher Scientific
14	Dil-Ac-LDL	BT-902	Biomedical technologies
15	Dulbecco's Phosphate buffered saline	D8537	Sigma-Aldrich
16	ECL Western blotting substrate	32209	Thermo Scientific
17	Foetal Bovine Serum	F9665	Sigma-Aldrich
18	Gelatine solution (Type-B)	G1393	Sigma-Aldrich
19	Giemsa stain	295595000	Acros Organics
20	Glycerol	BPE229	Fisher Scientific
21	Glycine	BP381	Fisher Scientific
22	GM6001	364206	Calbiochem

No.	Name	Catalogue Number	Manufacturer
23	HEPES buffer solution	H0887	Sigma-Aldrich
24	Histopaque ®	10771	Sigma-Aldrich
25	Hydrogen Peroxide solution	H1009	Sigma-Aldrich
26	IL-1β (Human, Recombinant)	201-LB	R&D System
27	L-Glutamine	G7513	Sigma-Aldrich
28	Methanol	BP110	Sigma-Aldrich
29	New born-calf serum (Bovine)	N4762	Sigma-Aldrich
30	Paraformaldehyde	P6148	Sigma-Aldrich
31	Penicillin-streptomicine	P0781	Sigma-Aldrich
32	Plasmagel		Sigma-Aldrich
33	Ponceau S	81462	Fluka
34	Precision Plus ™ Protein Ladder	161-0375	Bio Rad
35	Protein Assay Reagent	500-0006	Bio Rad
36	Protein assay standard (II)	500-0007	Bio Rad
37	Restore plus Western blot stripping buffer	46430	Thermo Scientific
38	RIPA buffer	R0278	Sigma-Aldrich
39	RPMI-1640	R0883	Sigma-Aldrich
40	Sodium Chloride	BPE358	Fisher Scientific
41	Sulphuric acid	J/8420/17	Fisher Scientific
42	TEMED	T9281	Sigma-Aldrich
43	TIMP-3 (Human, Recombinant)	973-TM	R&D System
44	TMB peroxidase substrate	172-1068	Bio Rad
45	TNF-α (Human, Recombinant)	PHC3015	Life Technology
46	Tris Base	BP152	Fisher Scientific
47	Tris Hydrochloric	BP153	Fisher Scientific
48	Triton X-100	BP151	Fisher Scientific
49	Trypsin-EDTA solution	T4049	Sigma-Aldrich
50	Tween 20	BPE337	Fisher Scientific
51	X-ray film developer	P7042	Sigma-Aldrich
52	X-ray film fixer	P7167	Sigma-Aldrich

2.7 List of antibodies

Table 2-5: List of the primary and secondary antibodies used in the study.

No.	Name	Catalogue No.	Manufacturer
1	Anti-ADAMTS-1 (C-13)	sc-5463	Santa Cruz Biotechnology
2	Anti-ADAMTS-4 (K-20)	sc-16533	Santa Cruz Biotechnology
3	Anti-CD54 Mouse mAb (8.4A6)	217677	Calbiochem
4	Anti-human CD31 FITC conjugate	852.561.010	Diaclone
5	Anti-mouse-FITC	F7512	Sigma-Aldich
6	Anti-rabbit-FITC conjugate	F0257	Sigma-Aldich
7	Anti-β-actin	A2228	Sigma-Aldich
8	Anti-Claudin-5 (H-52)	sc-28670	Santa Cruz Biotechnology
9	Donkey anti-goat IgG-HRP	sc-2020	Santa Cruz Biotechnology
10	Goat anti-mouse-HRP conjugate	170-6516	Bio-Rad
11	Goat anti-rabbit-HRP conjugate	172-1019	Bio-Rad
12	Anti-human MMP-2 antibody	MAB903	R&D System
13	Anti-human MMP-9 antibody	MAB936	R&D System
14	Anti-vinculin antibody	V9264	Sigma-Aldich
15	Anti-PECAM-1 antibody (E-8)	Sc-133091	Santa Cruz Biotechnology
16	Rabbit anti-goat-HRP conjugate	172-1034	Bio-Rad
17	Rabbit anti-occludin	71-1500	Invitrogen
18	Anti-vWF antibody (G-11)	Sc-271409	Santa Cruz Biotechnology
19	Anti-ZO-1antibody (C-19)	Sc-8146	Santa Cruz Biotechnology

2.8 List of materials

Table 2-6: The list of materials used in the study.

No.	Name	Manufacturer
1	24 well culture plate	Sarstedt
2	25 cm2 culture flask (non-vented cap)	Sarstedt
3	25 cm2 culture flask (vented cap)	Sarstedt
4	6 well culture plate	Sarstedt
5	96 well culture plate (Flat bottom, cell-culture)	Sarstedt
6	96 well plate (Flat bottom, ELISA)	NUNC
7	96 well plate (Flat bottom, solid black)	Sarstedt
8	Blot paper	Bio-Rad
9	Cells scraper	Star Lab
10	Centifuge tubes (15 ml and 50 ml)	Scientific lab
11	ECIS 8 wells array	Applied Biophysics
12	Hanging cell culture insert	Millipore
13	Microcentrifuge tube (500 µl and 1500 µl)	Star lab
14	Micropipette tips (various sizes)	StarLab
15	Micropippettes (various sizes)	BioPette
16	Multichannel pipette	CAPP Denmark
17	Nitrocellulose membrane	GE Healthcare
18	Pump pipette	StarLab
19	Pump pipettes tips (various sizes)	Sarstedt
20	Round glass coverslip	VWR
21	Round thermanox cover slip	NUNC

2.9 List of equipment

Table 2-7: The list of equipment and instrument used in the study.

No.	Name	Manufacturer
1	37°C Incubator (*P.falciparum* culture)	Thermo Scientific
2	Benchtop centrifuge(Endothelial culture)	SiGMA
3	Benchtop centrifuge, Midispin (*P.falciparum* culture)	Eppendorf
4	Benchtop centrifuge, Minispin (*P.falciparum* culture)	Eppendorf
5	Biosafety cabinet (Endothelial culture)	SterilGard
6	Biosafety cabinet, Category III (*P.falciparum* culture)	NuAIRE
7	CO_2 Incubator (Endothelial culture)	Galaxy R
8	Compound microscope	CETI
9	Deionised water system	ELGA
10	ECIS Zθ™	Applied Biophysics
11	EVOM	Precesion instrument
12	FluorChem M	Protein simple
13	Glomax Multi+ Detection System	Promega
14	Heat block	Grant
15	Inverted fluorescence microscope (FW4000)	Leica
16	Inverted microscope	Motic
17	Mini Protein Plus tetra cell	Bio-Rad
18	pH meter	Denver instrument
19	Rocking platform	Luckham
20	Western Blot Scanning system	Bio-Rad
21	Wet protein transfer system	Bio-Rad
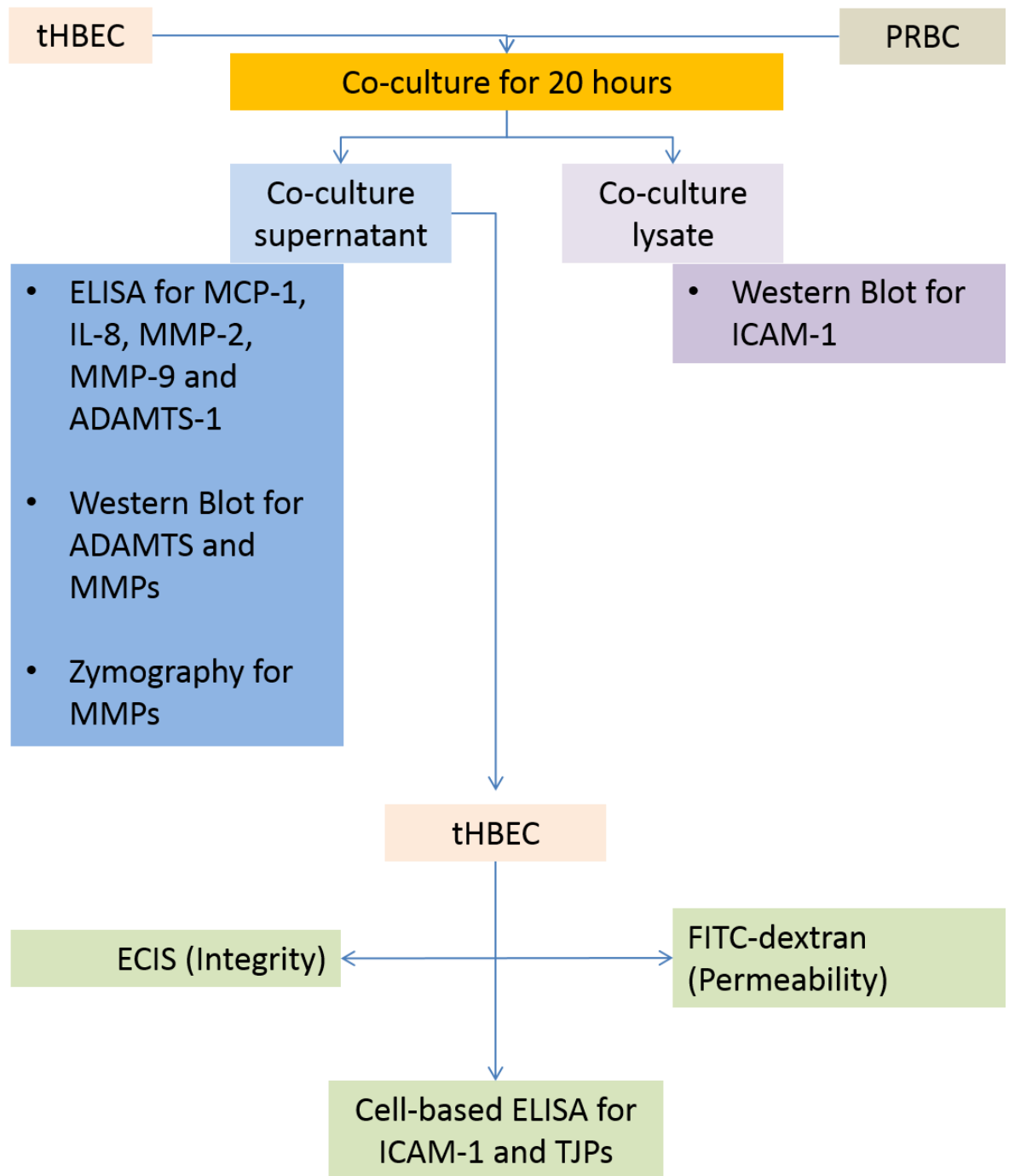
Figure 2-6: The flow chart of the methodology used to achieve the aim of the thesis.

CHAPTER THREE: THE ACTIVATION OF ENDOTHELIAL CELLS BY PRBC

Chapter 3: The activation of endothelial cells by PRBC

3.1 Introduction

In many *in vitro* cerebral malaria studies, PRBC was found to upregulate the expression of ICAM-1 in various endothelial cells including HUVEC (Viebig et al., 2005, Chakravorty et al., 2007) and human brain microvascular endothelial cells (HBMEC) (Tripathi et al., 2006). The upregulation of ICAM-1 by endothelial cells is one of the signs of endothelial cell activation. The activation of BBB endothelial cells was consistently seen in the post mortem study of CM patients (see section 1.2). Further, the activation of endothelial cells may also cause the alteration in the regulation of other molecules especially those that are important in an inflammatory response.

In this study, tHBEC monolayer was used to represent the endothelial cells of the BBB. This immortalised human brain endothelial cell line is more stable and display consistent properties compared to the primary cell line. Additionally, the tHBEC has been widely characterized in various *in vitro* studies of the BBB (Callahan et al., 2004, Tripathi et al., 2006, Tripathi et al., 2007). Primary cell lines are difficult to isolate and can be maintained for a very short number of passages for the multiple assay, which is also compromising the consistencies between isolates. The other popular option in examining the alteration in BBB structure and function is the use of an animal model, especially mice. It is however, generally known that the CM in the animal model is not the same pathology as in human as the major event in human is the sequestration of *P.falciparum* in the brain microvessels which the animal model lacks (Van den Steen et al., 2006, van der Heyde et al., 2006).

To elucidate the activation of tHBEC in cerebral malaria, the tHBEC was co-cultured with PRBC to mimic sequestration in CM. Following co-culture, the supernatants and the endothelial cell lysates were harvested, and analysed for ICAM-1 expression, to determine endothelial cell activation. The supernatants were also analysed for MCP-1 and IL-8 to elucidate any inflammatory responses to the PRBC. In addition, supernatants were also analysed for the presence of candidate proteases (ADAMTS-1, ADAMTS-4, MMP-2 and MMP-9) to elucidate their potential role in alteration to the BBB during sequestration.

3.2 Material and methods

3.2.1   Sandwich ELISA

Enzyme-linked immunosorbent assay (ELISA) for the detection of cytokines and some proteases was done by using commercially available kits. The kits used for these experiments were summarised in chapter 2, table 2-3. All sandwich ELISA were done according to the manufacturer's instructions. In principle, the antigen of interest was firstly immobilised by the capture antibody attached to the well (Figure 3-1). This was then detected by the detection antibody. There were two detection systems used in these studies, the direct detection by a HRP-conjugated antibody (for MCP-1, MMP-2 and MMP-9) and detection using biotinylated antibody which later interacted with HRP-conjugated streptavidin (for IL-8 and ADAMTS-1). In all cases, 100 µl TMB was added into each well as the substrate for HRP and the plate was incubated in the dark for 10 minutes. The colour change from the catalytic conversion of TMB substrate by HRP was stopped by the addition of 50 µl of either stop solution (supplied with kit) or concentrated sulphuric acid. The colour change was measured using 96 well plate reader (GloMax Multi+ system, Promega) at a wavelength of 450 nm. The absorbance of the standard solution (provided in the kit) was plotted against concentration to give an assay standard curve. The standard curve generated for each test antigen was used to calculate the concentration of each antigen in the samples assayed.

Detection using HRP-conjugated antibody		Detection using biotinylated antibody
	Well coated with capture antibody	
	Antigen captured by the immobilised capture antibody	
HRP-conjugated	Detection of the antigen by conjugated antibody	Biotin-conjugated
	Signal amplification by streptavidin-HRP	HRP-Streptavidin binds biotin
	Colour reaction from TMB substrate by HRP	
MCP-1, MMP-2 and MMP-9	Used for:	IL-8 and ADAMTS-1

Figure 3-1: The detection systems of sandwich ELISA.

For MCP-1, the ELISA was done using Human MCP-1 ELISA kit (Diaclone). The 96 well ELISA plate was pre-coated with mouse monoclonal anti-human MCP-1 capture antibody by the manufacturer. All buffers and reagents were supplied with the kit. For the assay standards, a series of serial dilution of MCP-1 standard reagent from 16 pg/ml to 1000 pg/ml in assay buffer was prepared in duplicate. The samples were also prepared in duplicate but at a 1:5 dilution in assay buffer to avoid over saturation of the samples. Once all standards and samples were pipetted into the plate (20 µl/well), 50 µl of HRP-conjugate anti-MCP-1 (1:100) were added into each well and incubated in dark for 2 hours at room temperature. After that, the wells were emptied rapid flipping of the plate and washed three times by the addition of 150 µl wash buffer in each well. For the final wash, the plate was dried by dabbing it onto a clean paper towel. The colour development was done as mentioned before.

The interleukin 8 (IL-8) was detected using IL-8 Eli-pair kit (Diaclone). Only capture antibody, biotinylated detection antibody, IL-8 standard and Streptavidin-HRP was supplied in the kit. First, the 96 well ELISA plate was coated with 100 µl/well of capture antibody prepared in coating buffer (PBS, pH 7.4), and incubated at 4°C for overnight. After that, the plate was washed two times with wash buffer (0.05% (v/v) Tween 20 in PBS) and blocked with 250 µl/well of saturation buffer (5% (w/v) BSA in PBS) for two hours at room temperature. For the assay, IL-8 standard ranging from 62.5 pg/ml to 2 000 pg/ml in standard diluent buffer (1% (v/v) BSA in PBS) was prepared by serial dilution and all co-culture supernatant samples were diluted 1:4 in standard diluent buffer. After these standards and samples were transferred into ELISA plate at 50 µl/well, 50 µl of biotinylated detection antibody was added into each well. This set up was incubated for one hour at room temperature. After that, the plate was washed three times with 150 µl wash buffer per well and properly dried before the 100 µl of streptavidin-HRP was added into each well and

incubated for 20 minutes. The unbound streptavidin-HRP was removed by washing as before. The plate then subjected for colour development as mentioned before.

The MMP-2 and MMP-9 ELISA was done using the Quantikine® ELISA kit (R&D systems). These kits came with a pre-coated ELISA plate and all the reagents and buffers required. First, standards and samples were prepared in duplicate in assay diluent buffer. Standards for MMP-2 were ranging from 0.78 ng/ml to 50 ng/ml and MMP-9 from 0.312 ng/ml to 10 ng/ml. All samples were diluted in the ratio of 1:2 with assay diluent. These standards and samples were transferred into the ELISA plate at 50 µl in each well. The set-up was incubated at room temperature for two hours before being washed four times with 150 µl per well of wash buffer. After that, the plate was dried by dabbing it onto a clean paper towel and incubated for two hours with the HRP-conjugated detection antibody. Once the incubation finished, the plate was washed again as before, followed by colour development.

The concentration of ADAMTS-1 in co-culture supernatant was measured using DuoSet® ELISA for human ADAMTS-1 (R&D Systems). First, the 96 well ELISA plate was coated with 100 µl per well of 1µg/ml of capture antibody and incubated at room temperature overnight. Then, the unbound capture antibody was removed by four washes with wash buffer. The plate was then blocked with 200 µl of reagent diluent in each well for 1 hour. For the assay, first, the ADAMTS-1 standards were prepared by serial dilution in reagent diluent over a range of 93.75 pg/ml to 6 000 pg/ml. Then, the co-culture supernatant was diluted 1:1 in reagent diluent. These standards and samples were then pipetted into respective wells and incubated at room temperature for two hours. Once finished, the plate was washed three times to remove the unbound proteins. After that, 100 µl of biotinylated

detection antibody (200 ng/ml) was added into each well and incubated in the dark for another two hours. The unbound antibodies were removed by washing three times as before. Next, 100 µl of streptavidin-HRP was added into each well and incubated for 20 minutes in the dark before continuing with the colour development steps.

3.2.2 Sample preparation for SDS-PAGE and Western blot

The total protein of the tHBEC lysate harvested from the co-culture experiment was determined using Bradford's protein assay (Bio-Rad) and equally load into each well of SDS-PAGE gel. First, a series of BSA standards ranging from 0.05 mg/ml to 0.50 mg/ml were prepared by serial dilution. Then, the cell lysate samples were prepared in 1:10 and 1:25 dilution to avoid the absorbance reading exceeding the standard range. After that, 10 µl of standards and samples were transferred in triplicate into 96 well plate. 200 µl of diluted dye reagent was then added to each well. The mixture was thoroughly mixed using the mixing function of 96 well plate reader before being incubated in the dark for five minutes. The colour change was measured at 595 nm. Absorbance of the BSA standards was plotted against concentration and a standard curve was prepared to determine the total protein concentration in each cell lysate sample.

All samples for SDS-PAGE were prepared as following. For cell lysate sample, 30 µg of protein was loaded into each well after mixing the sample with equal volume of 2x sample buffer (1% (w/v) SDS, 20 % (v/v) glycerol, 0.01 % (w/v) bromophenol blue in 120 mM Tris buffer (pH 6.8)) and boiled for 5 minutes. All co-culture supernatants were analysed by loading equal volumes into each well. To achieve this, 15 µl of each sample was mixed with 15 µl of 2x sample buffer and boiled for five minutes. 30 ml of each mix was loaded into each well. In each gel set up, 5 µl of a protein marker was added into one well

to allow determination of molecular weight of any positive bands. The samples were electrophoresed by amperage constant at 35 mA for each gel.

3.2.3 SDS-PAGE and Western Blot

The samples (cell lysate or co-culture supernatant) harvested previously was electrophoresed using SDS-PAGE (Sodium dodecyl sulphate-polyacrylamide gel electrophoresis), transferred onto a nitrocellulose membrane and then specific proteins detected using antibodies.

3.2.3.1 SDS-PAGE

The polyacrylamide gel was prepared using the gel cast apparatus (Tetra cell, Bio-Rad). To prepare the gel, first, the thick and thin glass plates with the 1.0 mm spacer were aligned using the glass plate clamp. The bottom part of the assembly was then sealed by the rubber pad on the glass plate assembly stand. After that, the resolving gel mixture as table 3-1 was prepared and slowly filled into the space between the two glass plates assembly until 1.5cm from the top. The mixture was layered with water to level the top edge and to remove any bubbles. The gels were left to set for about 30 to 45 minutes. As soon as the gel was set, the water was removed by pouring and the stacking gel mixture as table 3-2 was prepared and added into the top part of the assembly. The gel combs were placed into the stacking gel while the mixture is still in the liquid form to allow wells to form when the gel set. Stacking gel took approximately 30 minutes to set. After the gel was set, the glass plate with gel was taken out from the clamp and transferred into the gel holder in the tank. Then, the comb was removed and SDS-PAGE running buffer added.

Table 3-1: The recipe for the preparation of 10% resolving gel for SDS-PAGE using the Bio-Rad mini gel system.

Component	Concentration	Volume (ml)
Acrylamide: Bis-acrylamide (29:1) 40% solution	10 % (v/v)	5
1.5 M Tris-Cl (pH 8.8)	375 mM	5
dH$_2$O	-	9.59
10% (w/v) SDS	2.5 % (w/v)	0.2
10% (w/v) APS	2.5 % (w/v)	0.2
TEMED	-	0.013
TOTAL volume		20

Table 3-2: The recipe for the preparation of 5% stacking gel for SDS-PAGE using the Bio-Rad mini gel system.

Component	Volume (ml)
Acrylamide: Bis-acrylamide (29:1) 40% solution	1.25
1.0 M Tris-Cl (pH 6.8)	1.25
dH$_2$O	7.3
10% (w/v) SDS	0.1
10% (w/v) APS	0.1
TEMED	0.007
Total volume	10

3.2.3.2 Western blot

As soon as the electrophoresis was completed, the gels were removed from SDS-PAGE assembly and transferred onto a nitrocellulose membrane for Western transfer as figure 3-2, using wet transfer system (Bio-Rad) in Western transfer buffer (25 mM Tris-Base, 192 mM Glycine in 10% (v/v) methanol). The transfer was performed at 300 mA for 60 minutes.

After that, the blot was stained with Ponceau S to check for optimal transfer and equal loading in each well. Next, the blot was washed with water and blocked with 1x blocking solution (Sigma) for one hour on a rocking platform at room temperature. After that, the blot was incubated with the primary antibody (Table 3-3) overnight. Then, the blot was washed three times with 10 ml wash buffer (20 mM Tris-base, 150 mM NaCl in 0.001% (v/v) Tween-20 at pH 7.6) to remove any weakly or unbound primary antibody. After the third wash, the blot was incubated with the HRP-conjugated secondary antibody for two hours. The blot was then washed again as previous and transferred onto a clean cling film with the protein side facing upward (figure 3-3). The enhanced chemiluminescence (ECL) reagent was mixed as per manufacturer's instructions. 750 µl of the mixed ECL reagent was then added onto each blot before being imaged using blot imager (FluorChem M, Protein Simple) or exposed to an x-ray film. In all Western blot analysis of cell lysate, the blots were stripped and reprobed with β-actin, a housekeeping protein. The ratio between densities of the β-actin band and the band of test antigen (e.g. ICAM-1) was used to derive semi-quantitative measurement of expression of each antigen tested.
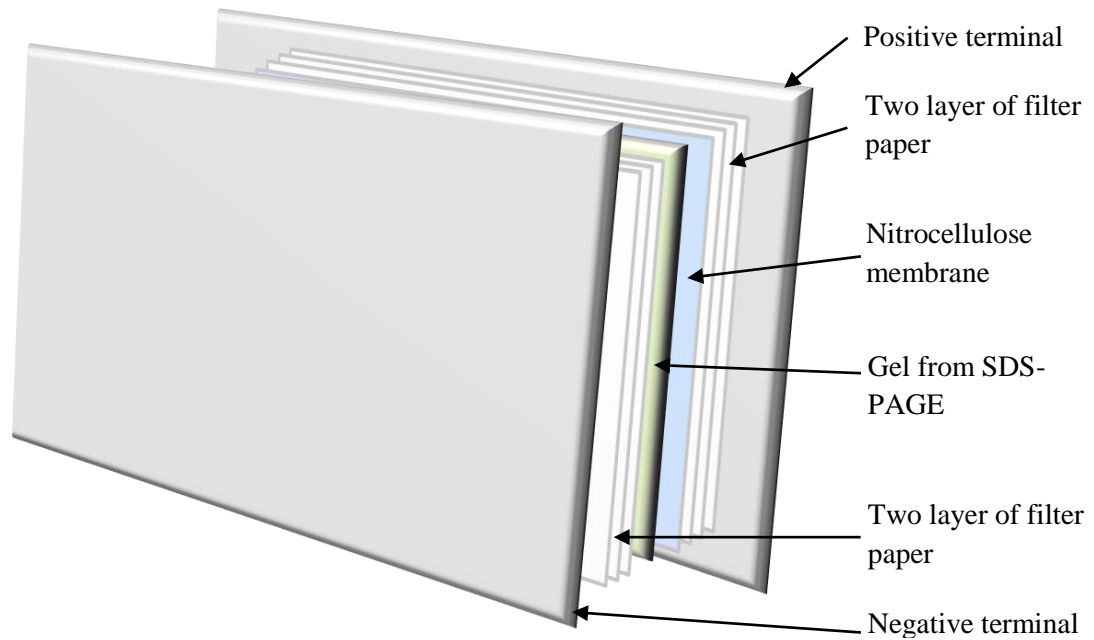
Figure 3-2: The positioning of the western transfer system.

The negatively charged proteins in the gel were moved to the positive terminal and transferred onto the nitrocellulose membrane by the electrophoresis. These layers of filter paper, nitrocellulose membrane and gel were carefully layered and aligned between each other to avoid the formation of trapped air in between them.

Table 3-3: Antibodies used in Western blot.

Antigen	Sample tested	Primary antibody		Secondary antibody	
		Name	Dilution	Name	Dilution
ADAMTS-1	Supernatant	Anti-ADAMTS-1 (C-13)	1:250	Rabbit anti-goat	1:1000
ADAMTS-4	Supernatant	Anti-ADAMTS-4 (K-20)	1:250	Donkey anti-rabbit	1:1000
MMP-2	Supernatant	Anti-human MMP-2	1:500	Goat anti-mouse	1:1000
MMP-9	Supernatant	Anti-human MMP-2	1:500	Goat anti-mouse	1:1000
ICAM-1	Supernatant* and lysate	Anti-CD54	1:1000	Goat anti-mouse	1:1000
β-actin	Lysate	Anti- β-actin	1:1000	Goat anti-mouse	1:1000

Note: * from previous studies in the lab (not shown).
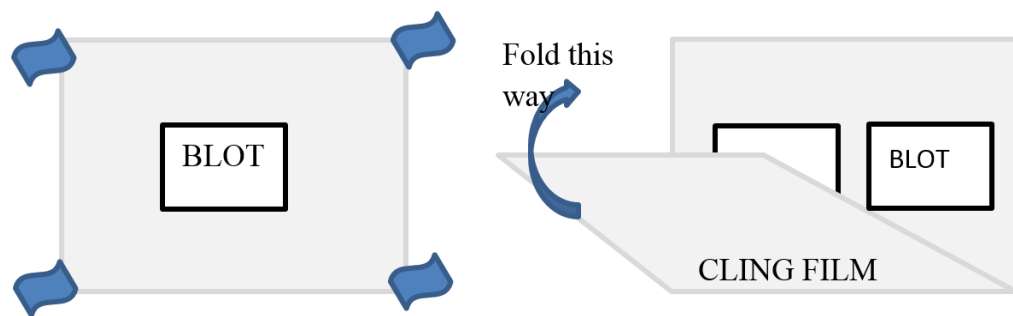
Figure 3-3: The set up for the addition of ECL reagent onto the blot.

3.2.3.3 Densitometric analysis of the western blot images.

The density of the bands of interest from western blot experiments were analysed using a specialised computer software (AlphaView, Protein simple). First, the image captured by FluorChem was cropped to the size of one blot. Then, the rectangular tools were utilised to mark the band of interest. To maintain the same size of selected area, multiple plot tools were used. Since the blot was captured with some background, the density of the background was deducted from the density of each band value by the background analysis tools. The value from these normalisation were recorded in excel and GraphPad (Prism) for statistical analysis.

3.2.4 Zymography for the MMP-2 and MMP-9 in the co-culture supernatant

Zymography was used to screen the gelatinase activity of the MMP-2 and MMP-9 in the co-culture supernatant. The gel was called zymogram. The gelatine zymogram was prepared similar to the SDS-PAGE gel as in section 3.2.3.1 with some modification. In zymography, 2 mg/ml of gelatine was added to the resolving gel mix in table 3-1. After the gel was set, supernatant samples were treated as before with an equal volume of 2X sample buffer. In this assay, the sample mix was not boiled to preserve the gelatinase activity. The samples were then pipetted into respective wells and electrophoresed at 35 mA for each gel until the lowest molecular weight marker reached the bottom edge of the gel. Following electrophoresis, the gel was transferred into a clean container and soaked in renaturation buffer (2.5% (v/v) Triton X-100) for 30 minutes, with the buffer change in every ten minutes. To allow the digestion of gelatine, the zymogram was incubated at 37°C in developing buffer (50 mM Tris-HCl, 10 mM $CaCl_2.H_2O$, 0.05% (v/v) Brij 35 and pH adjusted to 7.6) for overnight with gentle shaking. To visualise the area with digested gelatine from the activities of active MMP-2 and MMP-9, the zymogram was stained for 15 minutes with Coomassie

blue staining solution (5% (w/v) Coomassie R-250, 40% (v/v) methanol and 10% (v/v) acetic acid) on a rocking platform. The area with the undigested gelatine was stained blue and the area with the digested gelatine appeared as clear band after being destained in destaining solution (40% (v/v) methanol and 10% (v/v) acetic acid).

3.2.5 Results

3.2.6 Activation of tHBEC in response to PRBC.

Following the co-culture experiment the tHBEC lysates were analysed using western blotting technique for the cell associated ICAM-1 (ICAM-1), one of the endothelial cell activation markers. A best representative western blot image is shown in figure 3-4. A number of bands were detected for each lane with the biggest band at 80 kDa (approximate). The size of full length ICAM-1 is between 80-114 kDa and depending on the glycosylation of its structure (Van de Stolpe and Van der Saag, 1996). Western blot analysis showed that ICAM-1 was constitutively expressed by tHBEC (as the positive band for ICAM-1 in the resting tHBEC lysate). However, there was no significant upregulation of ICAM-1 expression when co-cultured with either PRBC or URBC, in these studies (1 way ANOVA, $P > 0.05$). The densitometry data on the immunoblot images of lysates from five different co-culture experiments is shown in figure 3-5. .
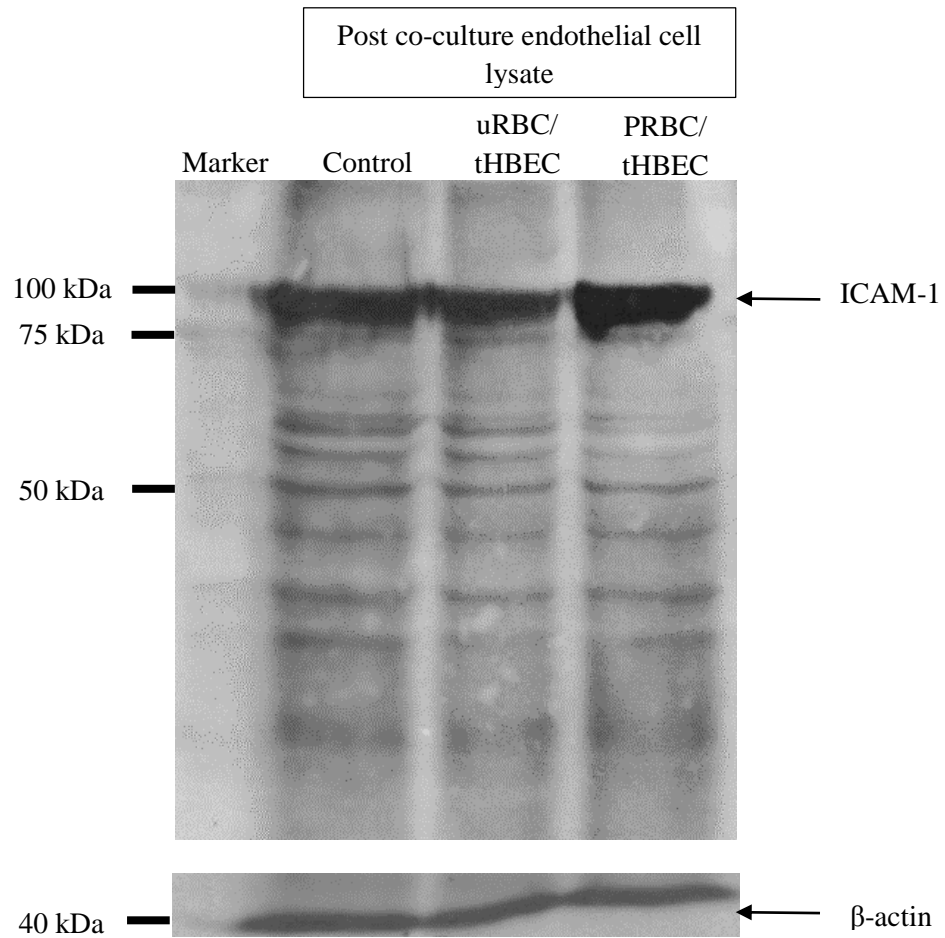
Figure 3-4: Western blot of post co-culture endothelial lysate for ICAM-1.

Top panel shows the ICAM-1expression from the tHBEC lysate after the co-culture experiment. The total amount of proteins loaded in each well is 30 µg. The first lane is protein marker (Bio-Rad), followed left to right by, control lysate, uRBC-tHBEC co-culture lysate and PRBC-tHBEC co-culture lysate. Lysate of the tHBEC co-cultured with PRBC shows a darker band at 80 kDa compared to control and uRBC-tHBEC lysate. As the loading control, the same blot was stripped and re-probed with anti-β-actin antibody, which gave a band at 40 kDa.
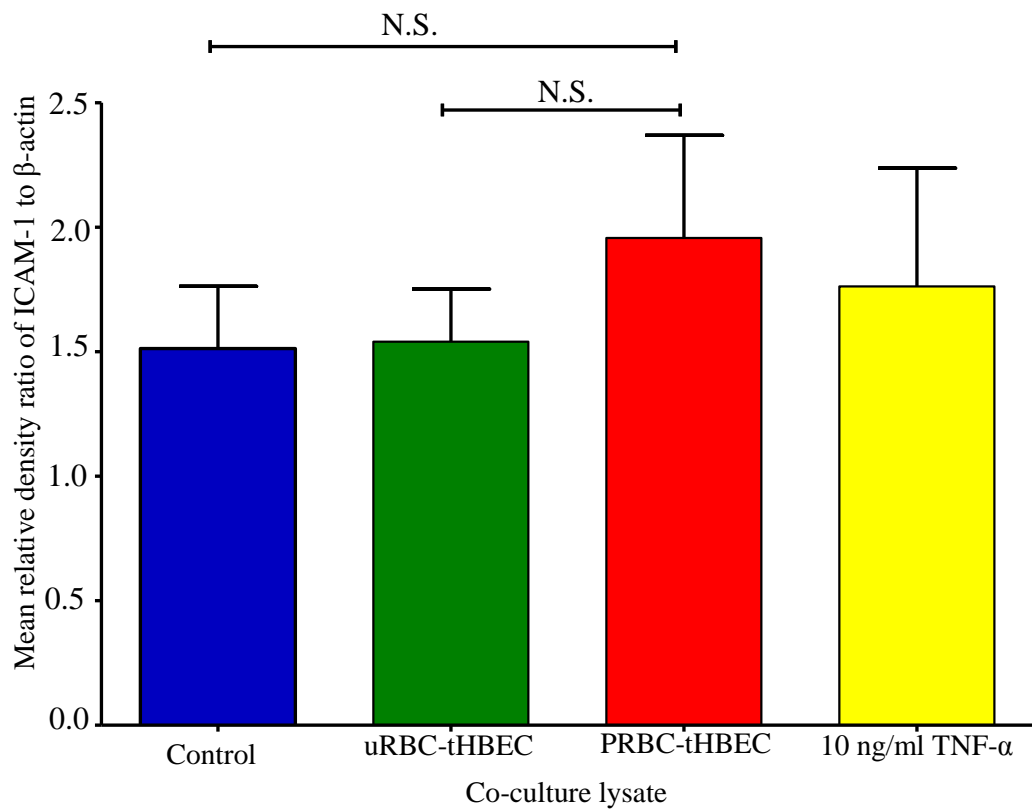
Figure 3-5: Densitometry of ICAM-1.

The graph shows the average of density ratio between the bands of the 80 kDa ICAM-1 to

the 40 kDa β-actin from five separate co-culture experiments. Level of ICAM-1 was

slightly higher in the tHBEC co-cultured with PRBC compared to the activation by 10

ng/ml TNF-α. The level of ICAM-1 from control was similar to the tHBEC co-cultured

with uRBC, which was lower than the PRBC-tHBEC lysate (N.S. is for not significant, 1

way ANOVA, error bar is at 1 S.E.M)

3.2.7 PRBC mediated increase in secretion of MCP-1 and IL-8 by tHBEC.

Supernatants from ten separate co-culture experiments were analysed for MCP-1 and IL-8. The level of MCP-1 in the PRBC-tHBEC co-culture supernatant was twofold higher compared to control supernatant (Figure 3-6). Exposure to uRBC for 20 hours, however, did not increase the secretion of MCP-1 by tHBEC. In resting condition, the tHBEC was found to secrete a basal level of MCP-1 (800 pg/ml) into supernatant indicating that the MCP-1 is produced constitutively by tHBEC. Activation of tHBEC by 10 ng/ml TNF-α also upregulated MCP-1 production by tHBEC.

The level of IL-8 was found to be significantly increased by ten fold in the PRBC-tHBEC co-culture supernatant (2916.6 pg/ml) compared to control (272.6 pg/ml), indicating the activation of tHBEC in response to PRBC (Figure 3-7). The co-culture with uRBC for 20 hours was unable to change the basal secretion of IL-8 by tHBEC showing that interaction between tHBEC and uRBC did not cause endothelial activation, as expected. 10 ng/ml TNF-α caused a slight increase in the level of IL-8 compared to the activation by PRBC. These data demonstrate that upregulation and releases of MCP-1 and IL-8 by tHBEC, is a specific response to PRBC.
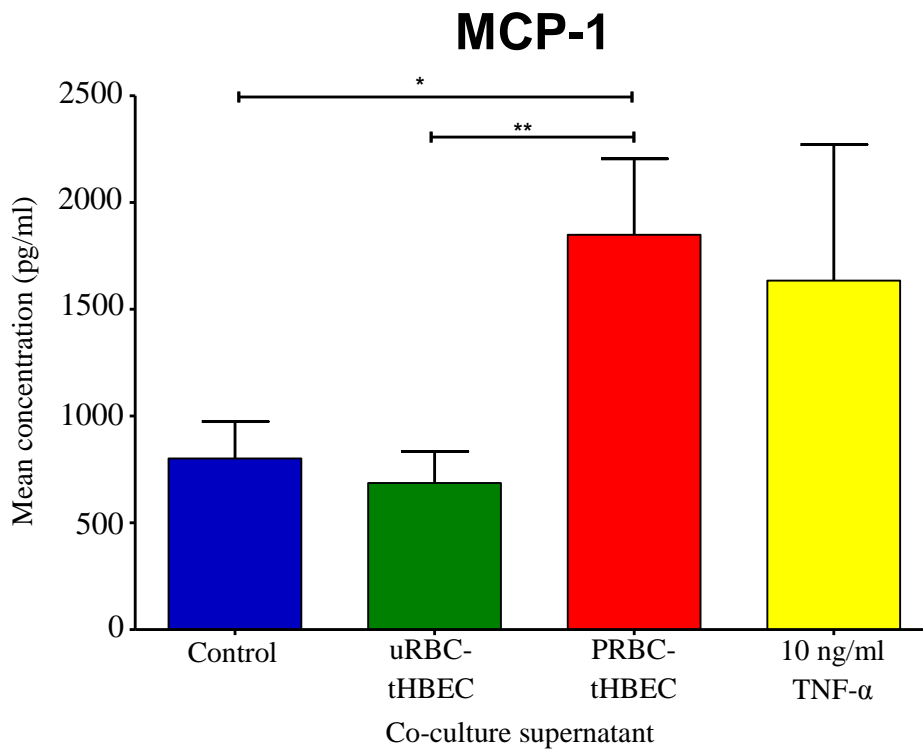
Figure 3-6: ELISA of MCP-1 in co-culture supernatant.

The graph shows the average concentration of MCP-1 secreted by tHBEC from ten separate co-culture experiments. Bars represent 1 S.E.M. and the significant difference between treatments was analysed using 1 way ANOVA with Turkey's multiple comparison test. (n=10, * is P ≤ 0.05 and ** is P ≤ 0.01).
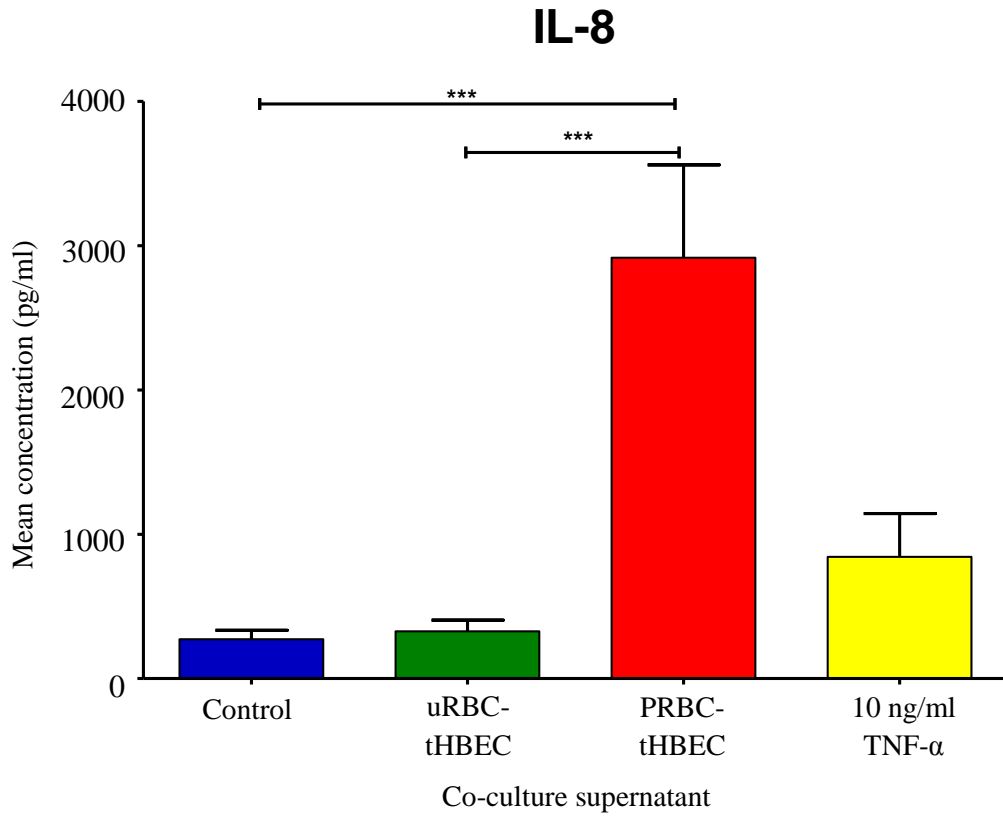
Figure 3-7: ELISA of IL-8 in co-culture supernatant.

The graph shows the average concentration of the IL-8 from 10 separate co-culture experiments. Bars represent 1 S.E.M. and the significance difference between treatments was analysed using 1 way ANOVA with Turkey's multiple comparison test. (n=10, and *** is P $\leq$ 0.001).

3.2.8 PRBC mediated regulation of ADAMTS-1 and ADAMTS-4 of tHBEC.

Western blot analysis of the co-culture supernatant for ADAMTS-1 gives three bands at different size; 110 kDa, 60 kDa and 30 kDa (Figure 3-8A). Visually, there are no major differences in the densities of these bands between different co-culture conditions. Across supernatants from five different co-culture experiments, there were variations in the pattern of regulation of ADAMTS-1. Semiquantitative analysis of the western blot by densitometry for all three different bands was done. The 30 kDa band of ADAMTS-1 is markedly upregulated in the PRBC-tHBEC co-culture supernatant compared to uRBC-tHBEC co-culture supernatant (Figure 3-8B). In contrast, the 60 kDa (figure 3-8C) and 110 kDa (figure 3-8D) bands showed no significant difference between co-culture conditions. Activation of tHBEC by TNF-α also increased the release of 30 kDa ADAMTS-1 into supernatant compared to resting tHBEC, but this was not different compared to uRBC-tHBEC co-culture supernatant.

Further analysis of the co-culture supernatant using sandwich ELISA showed that the release of ADAMTS-1 was slightly upregulated in uRBC-tHBEC co-culture supernatant but markedly upregulated in PRBC-tHBEC co-culture supernatant, compared to resting tHBEC (Figure 3-9). These changes were statistically tested using 1 way ANOVA with Turkey post-hoc test however shows no significant difference ($P > 0.05$) was apparent. In line with the western blot data, ADAMTS-1 was constitutively released by tHBEC and not upregulated by TNF-α.
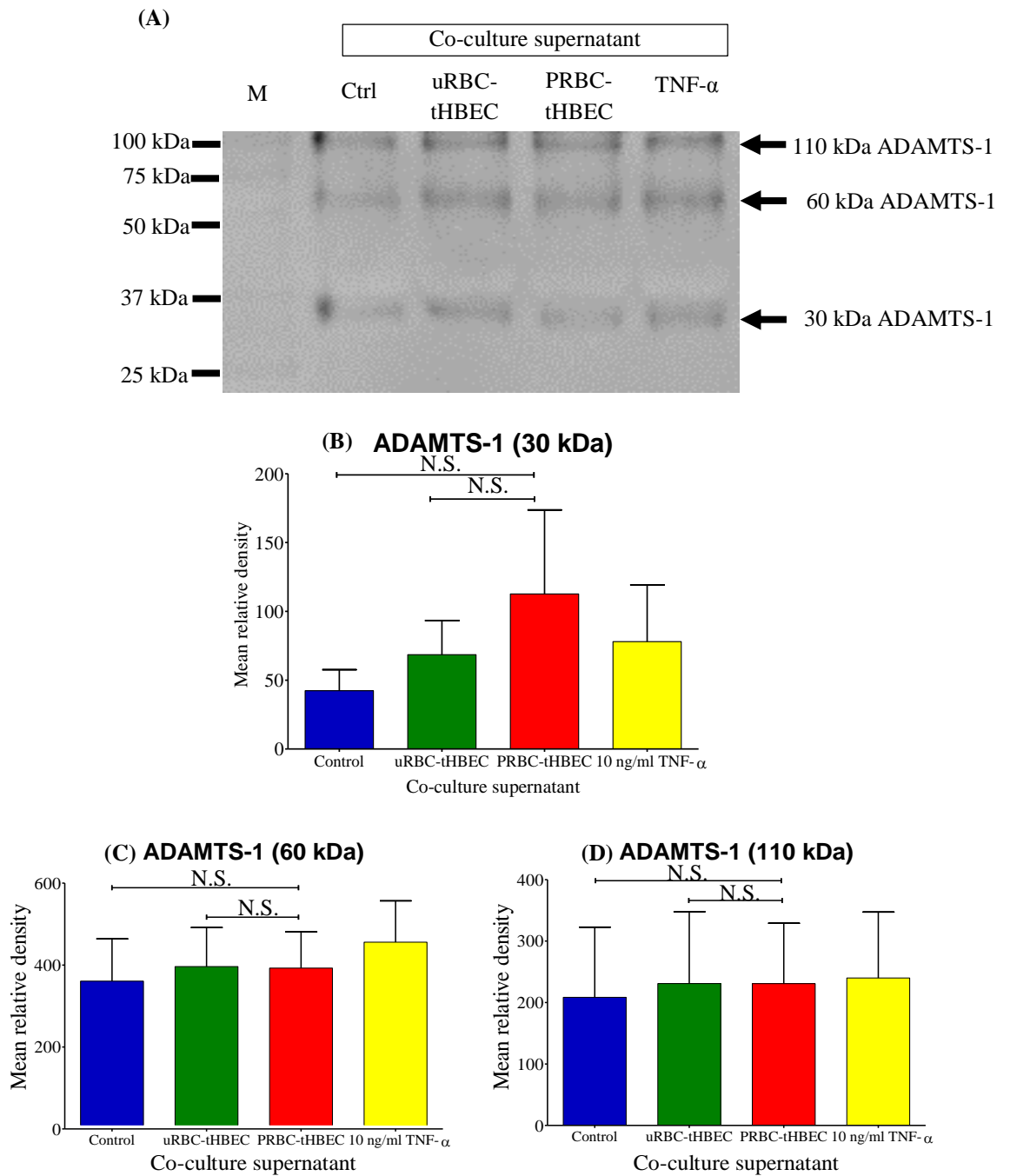
Figure 3-8: Western blot and densitometry of co-culture supernatants ADAMTS-1.

A: A representative western blot image for ADAMTS-1. From left protein marker (M), control supernatant (Ctrl), uRBC-tHBEC co-culture supernatant, PRBC-tHBEC co-culture supernatant and TNF-α activation supernatant. The graph shows the relative density of the 30 kDa band (B), 60 kDa (C) and 110 kDa (D) of the ADAMTS-1 blots (n = 5).
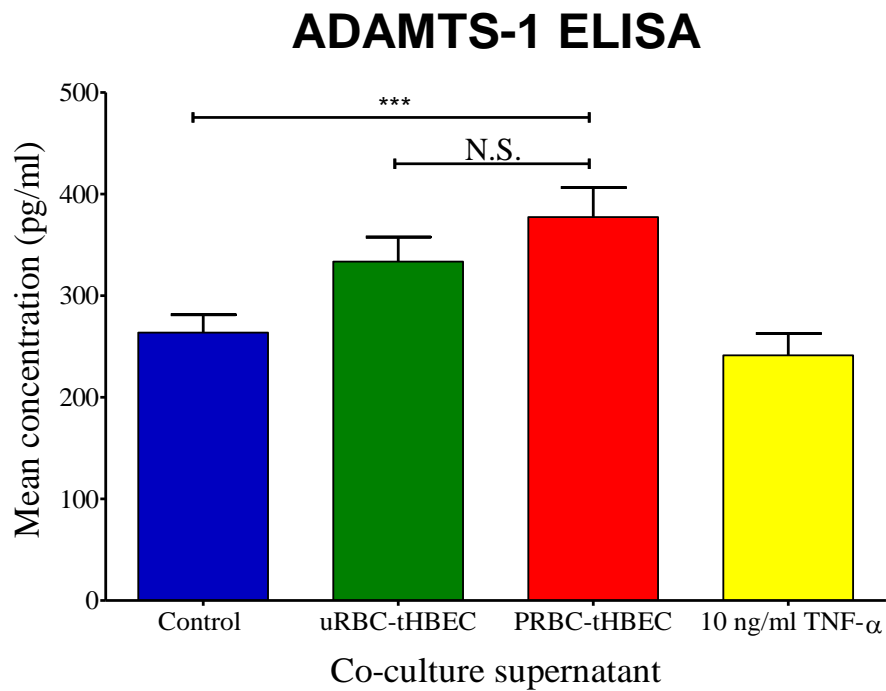
ADAMTS-1 ELISA

Figure 3-9: ADAMTS-1 ELISA.

The graph shows the mean concentration of ADAMTS-1 in the co-culture supernatant from ten separate experiments. Error bar is 1 S.E.M. The significant differences between co-culture treatments was tested using 1 way ANOVA with Turkey's multiple comparison test (n = 10, *** is P ≤ 0.001).

ADAMTS-4 in co-culture supernatants were screened using western blot (Figure 3-10A). Two main bands were detected in the uRBC-tHBEC and PRB-tHBEC co-culture supernatants, at 60 kDa and at 30 kDa. Interestingly, the 30 kDa band was absent in control supernatant and is markedly upregulated in PRBC co-culture supernatant tested from seven different experiments. The densitometric analysis of this band shows the upregulation of ADAMTS-4 is statistically significant compared to control co-culture supernatant ($P \le 0.05$), but not significant compared to uRBC-tHBEC co-culture supernatant ($P > 0.05$) (Figure 3-10B). Analysis of the 60 kDa band (figure 3-10C) shows no significant difference between the co-culture condition, analysed using 1 way-ANOVA with Turkey's multiple comparison post hoc test.
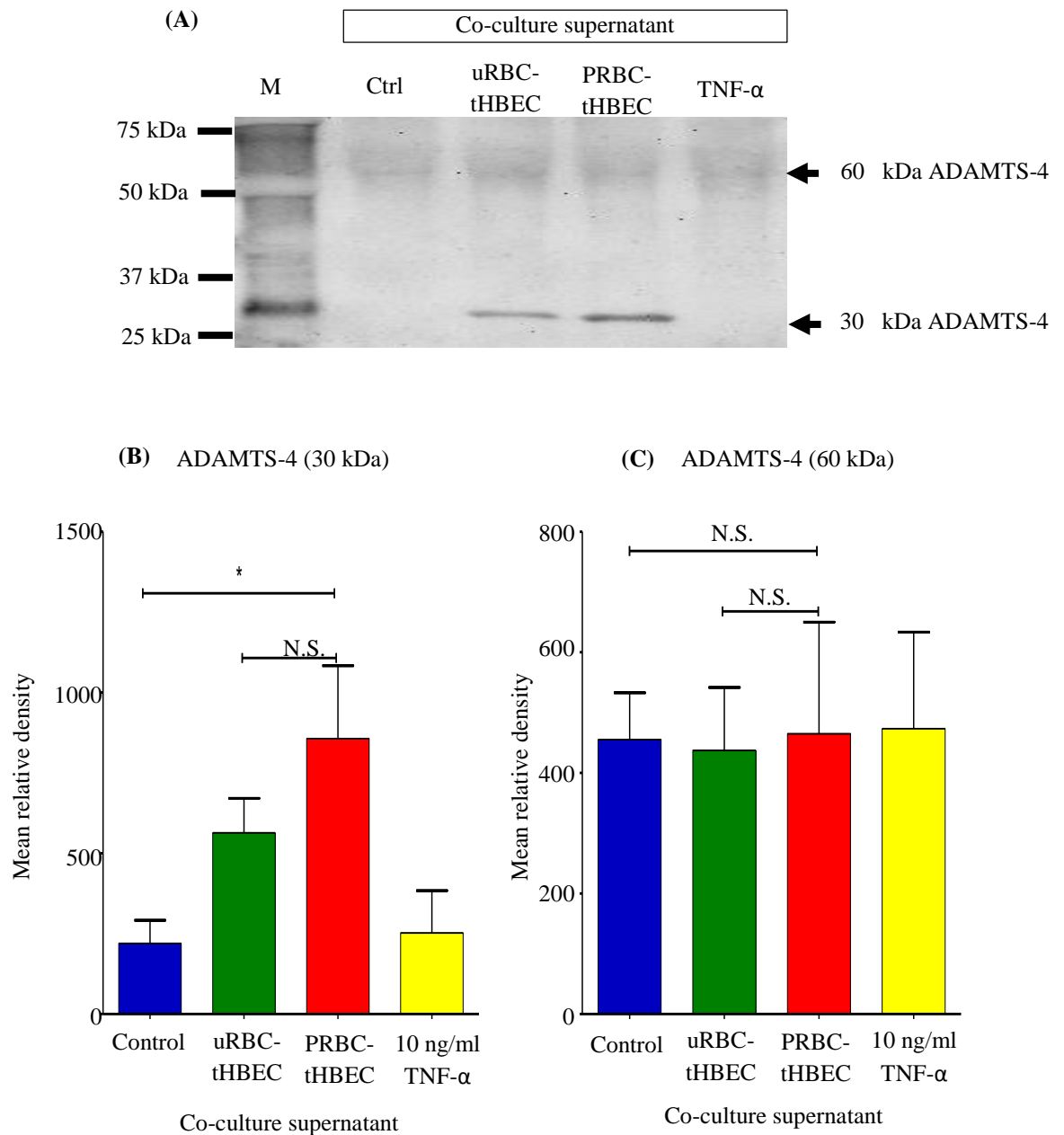
Figure 3-10: Western blot and densitometry of ADAMTS-4.

A: A representative western blot image for ADAMTS-4. From left protein marker (M), control supernatant (Ctrl), uRBC-tHBEC co-culture supernatant, PRBC-tHBEC co-culture supernatant and TNF-α activation supernatant. The graph shows the relative density of the 30 kDa (B) and 60 kDa (C) of the ADAMTS-1 blots. Error bars represent 1 SEM. The significant differences were tested using 1 way ANOVA with Turkey's post hoc test. (n = 7, * is P ≤ 0.05).

3.2.9 PRBC cause differential regulation of tHBEC MMP-2 and MMP-9.

The level of MMP2 in the co-culture supernatants was detected using western blotting and measured using sandwich ELISA. Western blotting of the co-culture supernatant for MMP-2 showed a major band at 60 kDa (Figure 3-11A). Densitometry analysis on the 60 kDa bands of MMP-2 from five different co-culture experiment did not show any significant difference between the co-culture conditions (Figure 3-11B). This was tested using 1 way ANOVA with Turkey's multiple comparison test. In contrast, the measurement of MMP-2 concentration using a commercial ELISA kit gave a very different finding (Figure 3-12). Interestingly, the level of MMP-2 in the PRBC-tHBEC co-culture supernatant (17.9 ng/ml) was significantly increased ($P \leq 0.001$) compared to the resting tHBEC control (0.45 ng/ml). The concentration of MMP-2 in the uRBC-tHBEC co-culture supernatant was slightly higher than in the control co-culture supernatant, however this was not significant. Similarly, the activation by 10 ng/ml TNF-α only cause slight increase in the concentration of MMP-2 in the co-culture supernatant compared to the resting tHBEC control.
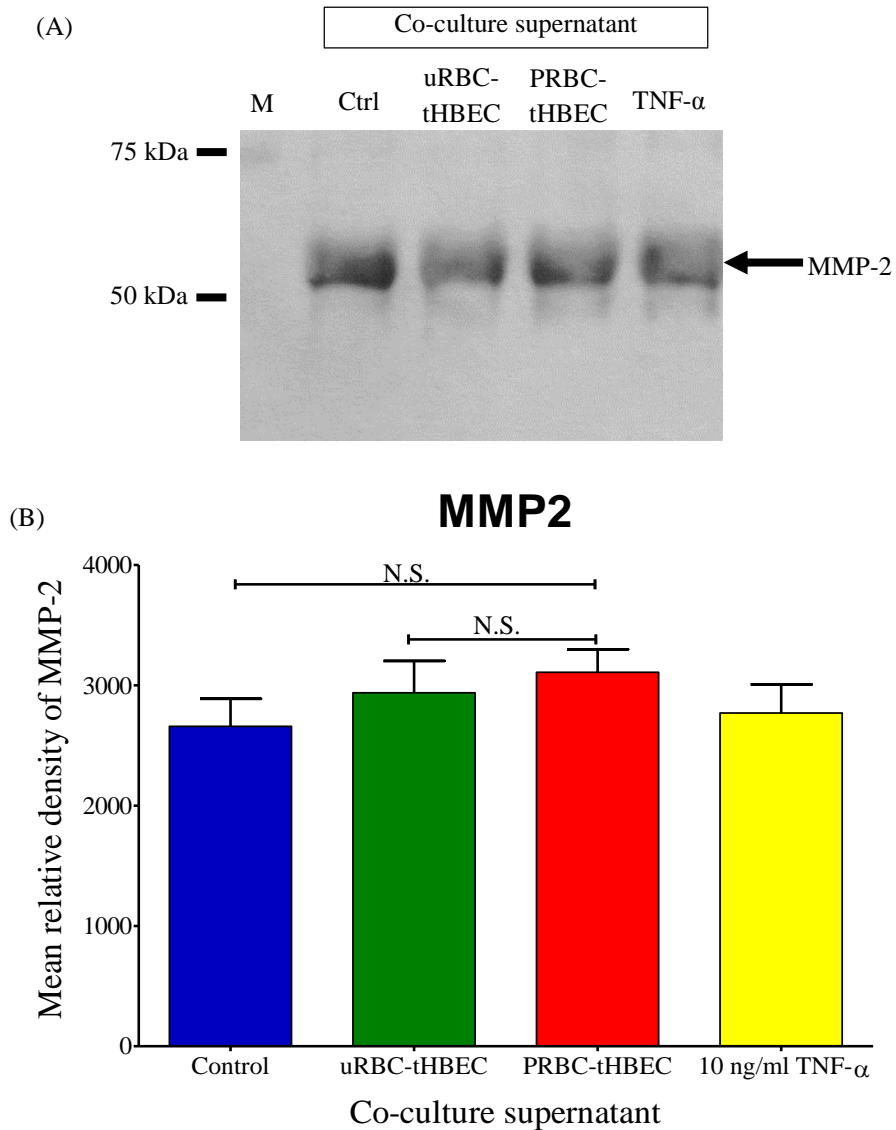
Figure 3-11: Western blotting of MMP-2 in the co-culture supernatant.

A: A best western blot image for MMP-2. From left protein marker (M), control supernatant (Ctrl), uRBC-tHBEC co-culture supernatant, PRBC-tHBEC co-culture supernatant and TNF-α activation supernatant. B: The graph shows the relative density of the 60 kDa band of the MMP-2 blot (n = 5, N.S. is for not significant).
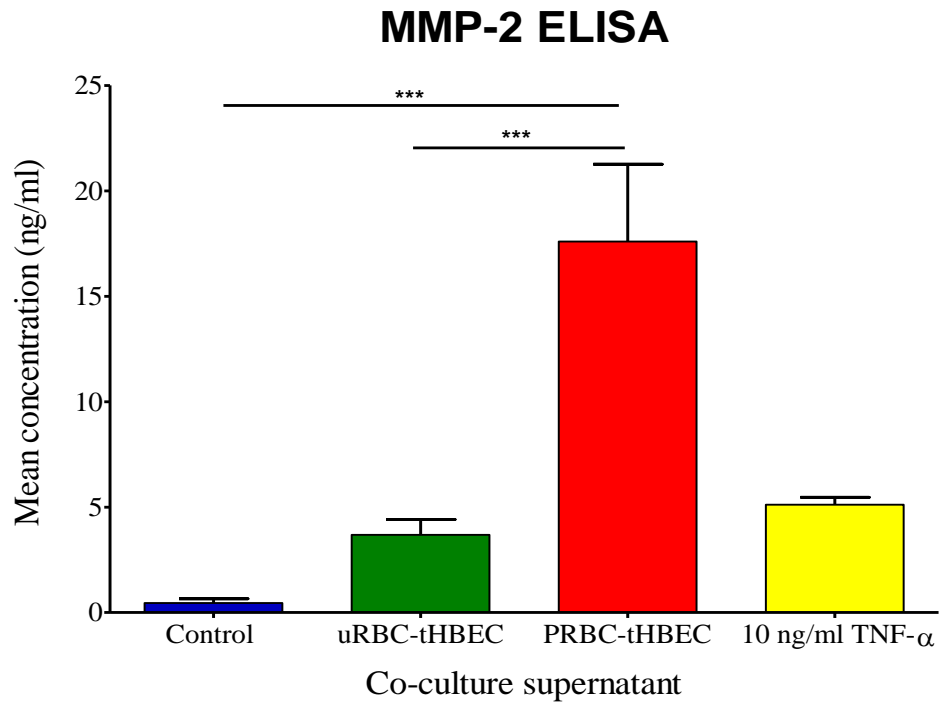
Figure 3-12: ELISA of MMP-2 in the co-culture supernatant.

The graph shows the averaged concentration of MMP-2 in the co-culture supernatant from ten separate experiments. Error bar is +1 SEM. The significant differences between co-culture treatments was tested using 1 way ANOVA with Turkey's multiple comparison test (n = 10, *** is P ≤ 0.001).

The western blot for MMP-9 in co-culture supernatant gives two different sizes of bands; 60 kDa and 30 kDa (Figure 3-13A). The biggest band was at 60 kDa and the band intensities were inconsistent in every supernatant tested. Interestingly, the 30 kDa band was found only in the lane for uRBC-tHBEC co-culture supernatant and PRBC-tHBEC co-culture supernatant. The densitometric analysis shows that 30 kDa MMP-9 significantly upregulated in the PRBC-tHBEC co-culture supernatants ($P \leq 0.001$) compared to control co-culture supernatant, however this was not significant compared to the uRBC-tHBEC co-culture supernatants ($P > 0.05$) (Figure 3-13 B). The densitometry of the 60 kDa band shows there are no significant differences between the co-culture conditions. These statistics were tested using 1 way-ANOVA with Turkey's multiple comparison test.

Further analysis using sandwich ELISA (Figure 3-14) showed that the concentration of MMP-9 was significantly higher in the PRBC-tHBEC co-culture supernatants compared to the concentration of MMP-9 in resting tHBEC supernatants ($P \leq 0.01$). The secretion of MMP-9 into supernatant was also increased by the tHBEC when co-cultured with uRBC. The regulation pattern in the ELISA quantitation was similar to the regulation pattern seen in the densitometry of 30 kDa MMP-9.
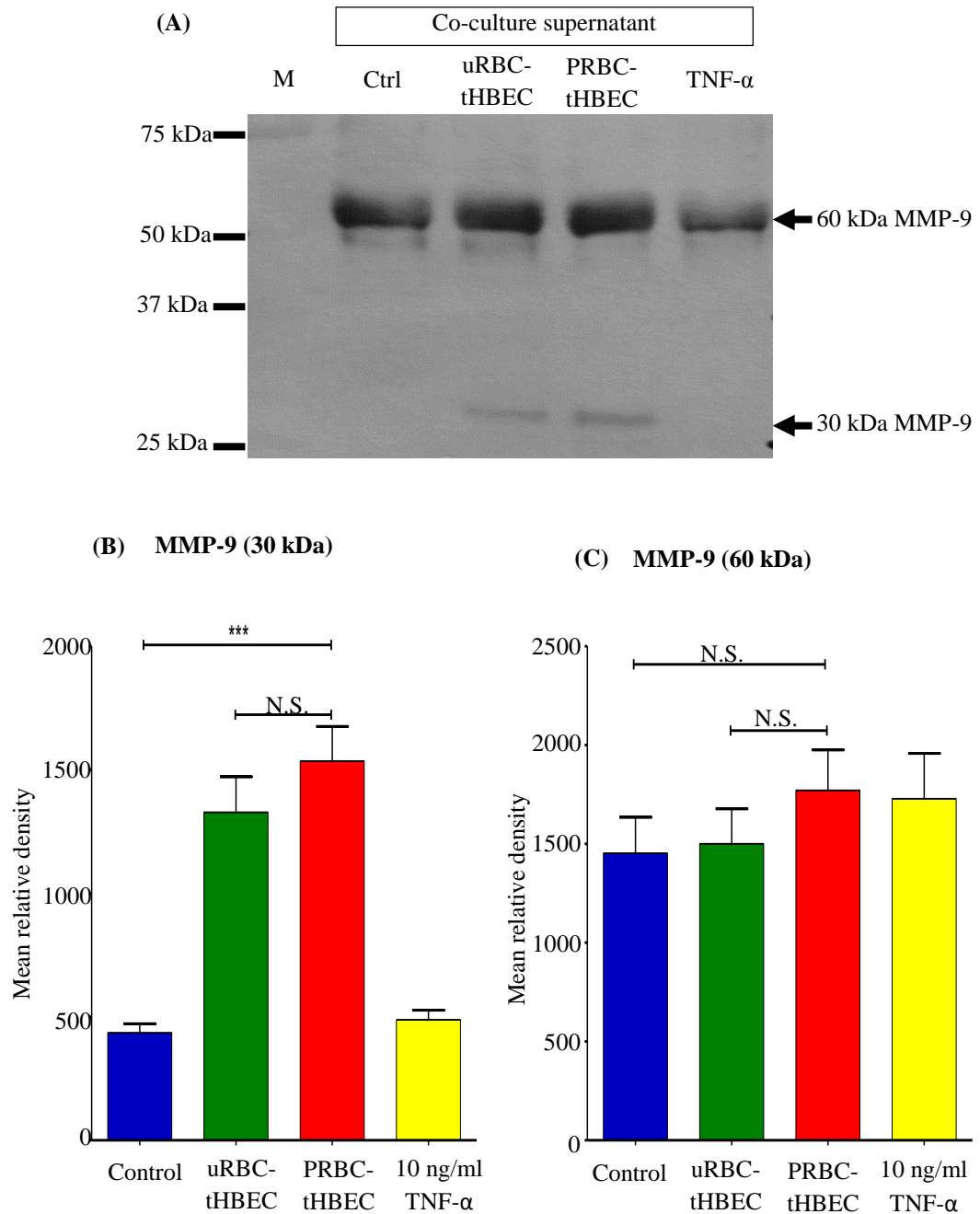
Figure 3-13: Western blotting of MMP-9 in co-culture supernatant.

A: A representative western blot image for MMP-9. From left, protein marker (M), control

supernatant (Ctrl), uRBC-tHBEC co-culture supernatant, PRBC-tHBEC co-culture

supernatant and TNF-α activation supernatant. The graph shows the relative density of the

30 kDa band (B) and 60 kDa (C) of the MMP-9 blot (n = 9).
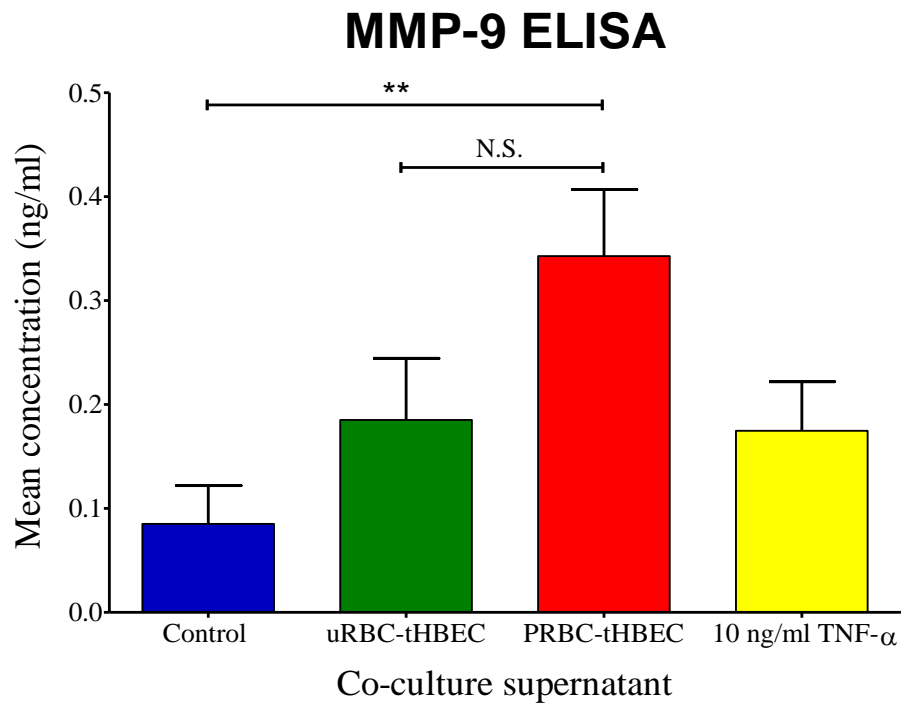
Figure 3-14: ELISA of MMP-9 in co-culture supernatants.

The graph shows the averaged concentration of MMP-9 in the co-culture supernatant from ten separate experiments. Error bar is 1 S.E.M. The significant differences between co-culture treatments was tested using 1 way ANOVA with Turkey's multiple comparison test (n = 10, *** is $P \leq 0.001$).

3.2.10 The gelatinase activity of co-culture supernatant.

The gelatinase activity of the co-culture supernatant was examined using gelatine zymography (Figure 3-15). Two main bands were visualised using this method; 90 kDa and 60 kDa. The 90 kDa band is the MMP-9 and the 60 kDa is the MMP-2. In co-culture supernatant tested from four separate experiments, there were consistently no differences in the band intensities between the different co-culture conditions. There are no gelatinase activities were observed from 30 kDa MMP-9, a band which appears in western blots (figure 3-13A).
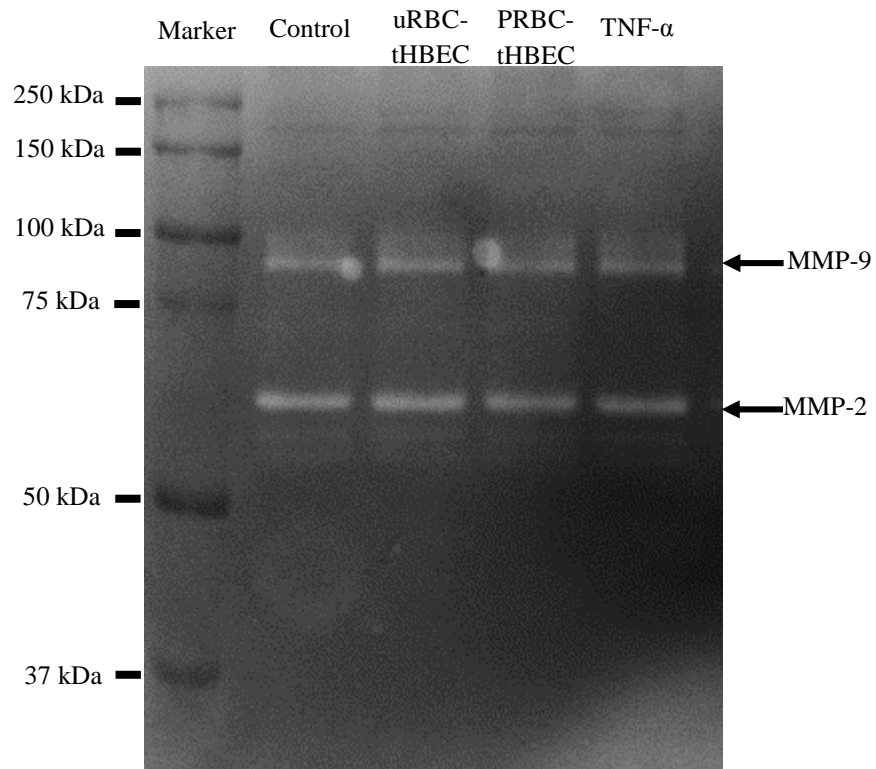
Figure 3-15: MMP-2 and MMP-9 gelatine zymography.

A representative zymogram shows the MMP-2 (60 kDa) and MMP-9 (90 kDa) in the co-culture supernatant are function and active in degrading gelatine substrate.

3.3 Chapter discussion

In this study, western blot analysis did not demonstrate clear and significant upregulation of ICAM-1 in tHBEC following direct exposure to the trophozoite stage of PRBC at a high parasitemia for a prolonged period (20 hours). Although the western blot analysis consistently shows the largest band for ICAM-1 in the endothelial cell lysate treated with PRBC and the densitometry analysis shows a tendency towards an increase in ICAM-1 expression (figure 3-5), this was not significant. This may be a reflection of the quality of the western blot images and background noise. This data is contrary to previously reported effect of PRBC activation on HUVEC (Viebig et al., 2005) and Human brain endothelial cells (Tripathi et al., 2006), under conditions of high parasitaemia. In comparison, Chakravorty et al. (2007) found that when parasitaemia is low (i.e. 3% in these studies) the up-regulation of ICAM-1 by HUVEC can only be seen when the HUVEC were co-cultured with PRBC in the presence of a basal concentration of TNF-α. This difference may also be due to the difference in the endothelial cell line, *Plasmodium falciparum's* strain, culture medium as well as the parasitaemia. However, all these studies demonstrate the ability of PRBC to activate endothelial cells which is in line with the observed activation of the endothelial lining of the brain vessels in cerebral malaria post-mortem studies (Turner et al., 1994).

Although the increase in ICAM-1 was not apparent in the cell lysate (this study) additional analysis of the PRBC-tHBEC co-culture supernatant demonstrated significant upregulation of soluble ICAM-1 (sICAM-1) compared to control tHBEC supernatant using a R&D Systems ELISA kit (performed by undergraduate placement student; data not shown). This finding represents the release of sICAM-1 from tHBEC in response to PRBC

which is also observed in the plasma of children with cerebral malaria (Conroy et al., 2010). In addition, the concentration of sICAM-1 in the plasma and CSF of Vietnamese adults with CM was found to be significantly higher than the concentration of sICAM-1 in the control (Adults from UK) (Brown et al., 2000). This upregulation of sICAM-1 is however not unique to CM, but is also apparent in other neurological condition where the consciousness was decreased, indicating the disturbance in the normal function of CNS. It is also noteworthy that result from this study may not represent the sICAM-1 in the brain vessels as the study assessed sICAM-1 in the plasma of peripheral vessel.

Generally, all candidate proteases were analysed by 2 different methods, western blotting and ELISA. In contrast to the clear ELISA data, only minimal upregulation of all protease candidates are observed in western blotting analysis. This is due to the insensitivity of western blotting compared to the ELISA, especially in the detection step. Additionally, the protein sample may undergo further processing that gives several sizes of products which are later separated by SDS-PAGE, thus resulting in different intensities of different sizes of the same protein. This was overcome by the use of ELISA, where the colour change represents the total protease content, irrespective of any breakdown products.

These studies demonstrated significant increase in MCP-1 and IL-8 release from tHBEC in response to PRBC. MCP-1 is released by endothelial cells during inflammatory responses, including the activation by cytokine such as IL-1β, IFN-ɣ, TNF-α and angiotensin II (Rollins et al., 1990, Szmitko et al., 2003). During inflammation, MCP-1 is involved in monocyte transmigration via CCR2 receptors on monocytes (Boring et al., 1998). Both MCP-1 and IL-8 was found to be markedly elevated in the serum and cerebrospinal fluid of children who died due to cerebral malaria compared to the children

who died due to severe malarial anaemia or other causes (Armah et al., 2007). Additionally, serum IL-8 was also increased in children with severe malaria in a clinical study in Mali (Lyke et al., 2004a). Interestingly, level of IL-8 in the serum of non-survival cerebral malaria was significantly higher than the patients who survived in a study in India (Jain et al., 2008), suggesting the severity of the inflammation caused by *Plasmodium falciparum* in the non-survival CM cases. In an *in vitro* study, Chakravorty et al. (2007) demonstrated that direct exposure of HUVEC to PRBC for 20 hours not only increase the expression of endothelial ICAM-1 but also IL-8, which can be synergistically increased by the addition of low concentration TNF-α. Although this study is in line with the *in vivo* data, it is important to note that measurement of serum and CSF MCP-1 and IL-8 can represent non-specific generalised inflammation as opposed to being a reflection to the effect of sequestration of PRBC in the brain microvasculatures.

ADAMTS-1 and ADAMTS-4, which are aggrecanases were upregulated in PRBC-tHBEC co-culture supernatant. ADAMTS-1 is believed to be secreted as inactive aggrecanase at 110 kDa and the activation involves proteolytic digestion of a 25 kDa peptide to yield an active 85 kDa ADAMTS-1. Smaller than ADAMTS-1, ADAMTS- 4 is a 90 kDa protein which subjected to proteolytic activation to forms 60 kDa mature ADAMTS-4. Western blot of co-culture supernatant for ADAMTS-4 visualised bands at 60 and 30 kDa, relecting the cleavage products, however the full size 90 kDa band was not detectable showing that most of the ADAMTS-4 released by tHBEC is in the active form. Interestingly, all of the western blots consistently showed that the 30 kDa band of ADAMTS-4 was absent in resting tHBEC, and only detectable in uRBC-tHBEC and PRBC-tHBEC co-culture supernatants. To confirm that the 30 kDa ADAMTS-4 bands were not derived from either uRBC or PRBC, western blot for ADAMTS-4 was also done on supernatant from uRBC

alone and PRBC alone cultures. Both supernatants were negative for ADAMTS-4 (not shown). The blot was also probed with secondary antibody alone to confirm that the 30 kDa ADAMTS-4 band was not due to cross reactivity. A significant increase in both ADAMTS-1 and ADAMTS-4 was demonstrated in the brain section of a rat induced with stroke (Cross et al., 2006), suggesting the involvement of these proteases in the BBB damage, a characteristic of stroke. Additionally, both aggrecanases were also suggested to have strong association with the degradation of aggrecan and versican, a major ECM component at BBB, which was seen in Alzheimer's disease (Rauch, 2004). These data suggest the potential involvement of these aggrecanases in mediating BBB damage in CM.

Analysis of the co-culture supernatant for MMP-2 and MMP-9 showed a clear upregulation of both matrix metalloproteases in PRBC-tHBEC co-culture supernatant, although this was only observed in the ELISA data, which quantifies the total concentration of the proteins. These proteases may be involved in the pathogenesis of CM as activated MMP-9 in the brain tissue was found to be strongly upregulated in the mouse model of CM, infected with *Plasmodium berghei* ANKA, which shows similar neurological disturbances as in human CM (Van den Steen et al., 2006). The potential involvement of these proteases in the CM pathogenesis was discussed in chapter 1 (section 1.6).

In conclusion, the activation of tHBEC by direct exposure to PRBC for 20 hours increases the release of MCP-1, IL-8, ADAMTS-4, ADAMTS-1, MMP-2 and MMP-9 by tHBEC into supernatant while the expression of tHBEC ICAM-1 was not modified significantly in the western blot analysis in this thesis.

CHAPTER FOUR: ALTERATION IN THE INTEGRITY OF THE ENDOTHELIAL CELL MONOLAYER IN THE RESPONSE TO THE CO-CULTURE SUPERNATANT.

Chapter 4: Alteration in the integrity of the endothelial cell monolayer in response to the co-culture supernatants.

4.1 Introduction

Many post mortem studies on patients who died due to CM show association between sequestration and activation of endothelial cells of BBB, which usually co-localised with the site of the BBB leakage. Interestingly, the same damage can also be seen in some of the vessels that do not have sequestered PRBC (Brown et al., 1999, Brown et al., 2000, Brown et al., 2001). There is some suggestion that the damage of the BBB in CM occurs due to the soluble factors released during malaria infection, although sufficient evidence to prove this assumption is still lacking (Hunt and Grau, 2003, Idro et al., 2005, Medana and Turner, 2006, Clark and Alleva, 2009).

Results from post-mortem brain sections of patients who died due to CM also demonstrate that the PRBC could not be seen in the brain perivascular space. However, serum fibrinogen, one of the serum protein molecules which are normally maintained in the vessel lumen, was consistently observed to have leaked out of the brain microvessel into the brain parenchyma in cerebral malaria (Brown et al., 2001, Dorovini-Zis et al., 2011). This suggests that the BBB disruption is sufficient for the 250 kDa fibrinogen to move across the barrier.

The pathogenesis of cerebral malaria in human is still poorly understood which is mainly due to the limitation of the models that can be used. As *Plasmodium falciparum* is unable to cause malaria in rodent models, there is no specific *in vivo* model that can be used to study the mechanisms involved in human cerebral malaria (Hunt and Grau, 2003). As an alternative, *in vitro* models of BBB consisting of primary or immortalised human brain

endothelial cells has been widely used to study the interactions between PRBC and BBB (Wassmer et al., 2005, Tripathi et al., 2007). The properties of primary and immortalised brain endothelial cells were described in chapter 1.

By using such *in vitro* models, several methods can be used to assess the barrier function of the *in vitro* model of BBB. The changes in integrity of the intercellular junction can be assessed by measuring electrical resistance across a confluent monolayer. The measurement of transendothelial electrical resistance (TEER) utilises the concept that a confluent endothelial monolayer imposes a resistance to electrical current between electrodes and the current (at specific frequency) flows through the intercellular junction (Figure 4-1). With this concept, any reduction in the "tightness" of the intercellular junctions will reduce the resistance and increase the current flow, which can be measured by an amperage meter.
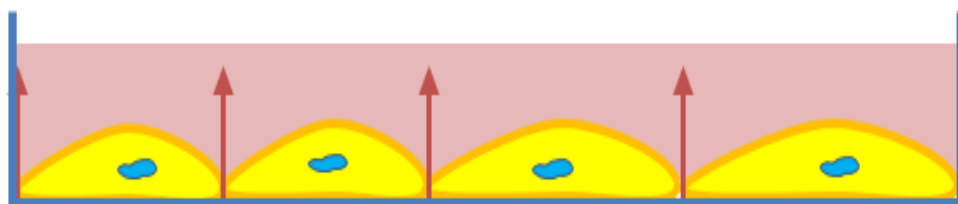
Figure 4-1: The concept of endothelial cells monolayer TEER.

The confluent brain endothelial cell poses an intense tight junction that imposes a high impedance towards conductance of an electrical current. At frequencies below 2000 Hertz, the current flows through intercellular junction (Red arrow) but not through the cell cytoplasm (Image was modified from http://www.biophysics.com/ecis-theory.php, last assed in 9th September 2014)

An important element of cerebral malaria is the interaction of PRBC with the brain endothelial cells. It was shown using TEER measurements that the integrity of the endothelial cells is decreased when co-cultured with PRBC (Tripathi et al., 2007). In the same study, it was demonstrated that soluble factors that can be precipitated using ammonium sulphate cause the reduction in endothelial cells monolayer integrity.

Results in the previous chapter demonstrated that the PRBC were able to induce an upregulation of release of MCP-1, IL-8, collagenases (MMP) and aggrecanases (ADAMTS) from tHBEC. To study the potential involvement of the proteases in causing alterations in tHBEC integrity, the co-culture supernatants harvested previously, were applied onto fresh tHBEC monolayers and the TEER measured. To determine the potential role of candidate proteases detected in the co-culture supernatants (chapter 3), specific inhibitors were used in this study. GM6001, a synthetic potent inhibitor for MMP while the ADAMTS and MMP-2 activities were inhibited using recombinant human TIMP-3 (rhTIMP-3). Previous studies demonstrated that 25 µM, GM6001 was able to inhibit the loss of endothelial cells tight junction proteins caused by MMP (Verma et al., 2010a). Similarly, rhTIMP-3 at 0.9 ng/ml efficiently inhibited ADAMTS activity, especially ADAMTS-4 (Wayne et al., 2007). Therefore, these concentrations were used in all the inhibition studies in this thesis.

4.2 Materials and methods

4.2.1   The electrical cell-substrate impedance sensing (ECIS™) equipment setting

The ECIS™ Zθ equipment was loaned from Applied BioPhysics, USA. The equipment set consists of a computer, a station controller and a station (figure 4-2). The computer was installed with the proprietary software for data acquisition and manipulation. The software used was from version 1.2.141.O PC. The computer is linked to the station controller and both of these components are located outside, but adjacent to the incubator. The station, which can hold a maximum of 2 arrays was placed inside the cell incubator and connected to the station controller by a cable through the door opening. Due to the thickness of the cable used, the incubator glass door's needed additional support to maintain the CO_2 and temperature inside the incubator. For noise reduction and statistical relevance of the transendothelial electrical resistance (TEER), 8 well arrays containing 40 electrodes in each well was used (8W10E+, Applied BioPhysics) (figure 4-3). Once the equipment was set up, it was calibrated using the test array as per manufacturer's instructions. The unit of the measured TEER is ohm (Ω).
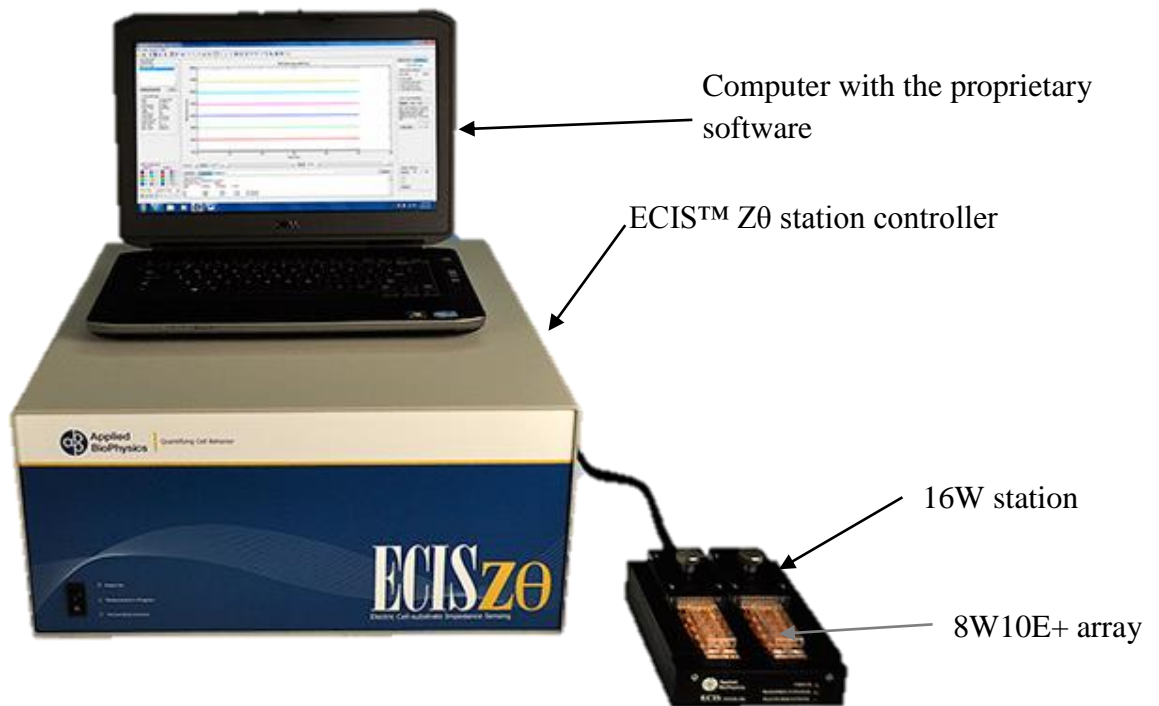
Figure 4-2: The components of the ECIS™ Zθ equipment.

The computer and the station controller are placed adjacent to the CO_2 incubator, while the station and the array are placed inside the CO_2 incubator. The image was taken from http://www.biophysics.com/products-ecisz0.php (Last accessed on 03 June 2014)
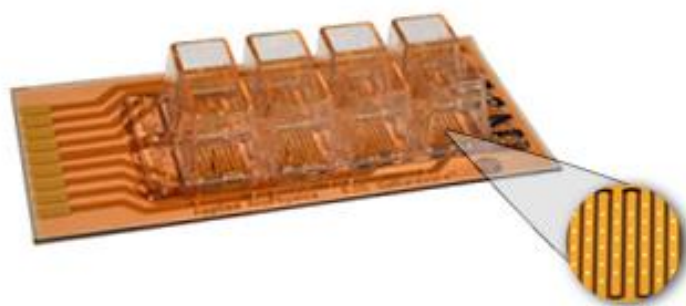
Figure 4-3: The appearance of the 8W10E+.

The small round image shows the arrangement of the electrodes on the gold plated array surface. The image was taken from http://www.biophysics.com/cultureware.php (Last accessed on 03 June 2014)

4.2.2 Seeding of tHBEC on the ECIS array.

First, the array was coated with 1% (v/v) gelatine prepared in sterile water and incubated for a minimum of 20 minutes. After that, the trypsin treated tHBEC were seeded at the density of 40 000 cell/ 400 µl of growth medium in each well of the 8 well array. The cells were maintained in growth medium for 24 hours. When a confluent monolayer was formed, the medium was replaced with 400 µl $Q_{5\% FBS}$-medium per well and the culture was maintained for another 20 hours. The timeline of the experiment is summarised in table 4-1.

Table 4-1: The typical timeline in the tHBEC maintenance for the ECIS experiment

Day	1	2	3	4
Morning	Seed cells		Change the $Q_{5\% FBS}$-medium. Start the ECIS for 4 hours stabilisation	Stop the ECIS measurement after 20 hours
Afternoon	Change the growth medium after 2 hours	Replace medium with $Q_{5\% FBS}$-medium	Add co-culture supernatant and treatments	

4.2.3 The measurement of HBEC monolayer TEER in response to the co-culture supernatant and selected protease inhibitors.

Before starting the TEER measurement, the medium in each well was replaced with 400 µl of pre-warmed $Q_{5\%FBS}$-medium. Two 8 well arrays were used for each experiment. The arrays were carefully reconnected to the station unit in the incubator and the connectivity

checked using the ECIS™ software. The station controller was set to record the time course measurement at 8 second intervals in the 16 wells, at 4000 Hz. To reduce the spike of unstable current following the medium change, the array was allowed to stabilise for 4 hours before the co-culture supernatant was added to the HBEC.

After the 4 hour stabilisation period, with the arrays still connected to the station, 80 μl of medium was removed from each well. This was carefully replaced with 40 μl of the pre-warmed co-culture supernatant and 40 μl of protease inhibitor respectively to achieve a 1:10 dilution. In the control wells, 40 μl of the inhibitor diluent control was added instead of the inhibitor. The inhibitor diluent controls were prepared as in table 4-2. The GM6001 was prepared in DMSO and TIMP-3 was prepared in dH_2O, thus the same dilution of DMSO or dH_2O in $Q_{5\% \, FBS}$-medium was used as the respective treatment control. A typical layout of the array for this experiment is shown in figure 4-4. Finally, the cells were incubated for 20 hours at 37°C, with 5% CO_2.

Table 4-2: The summary of concentration of the inhibitors and its diluent.

Inhibitor/ Diluent control	Dilution for experiment	Volume added (μl)	Final concentration (In each well)
GM6001 (10 mM)	250 nM	40	25 nM
DMSO (control for GM6001)	Equivalent to GM6001 dilution	40	Equivalent to GM6001 dilution
rhTIMP-3 (100 μg/ml)	0.4 nM (9 ng/ml)	40	0.04 nM (0.9 ng/ml)
dH_2O (control for rhTIMP-3)	Equivalent to rhTIMP-3 dilution	40	Equivalent to rhTIMP-3 dilution
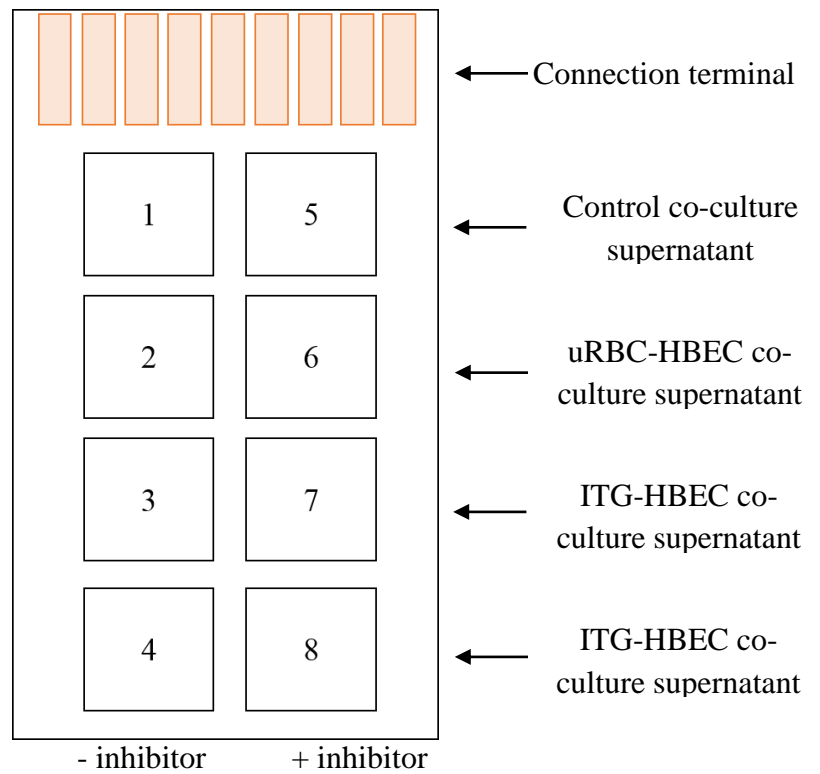
Figure 4-4: The typical layout of 8 well ECIS ™ array.

The wells are numbered from top to bottom. The top of the array is where the gold plated connection terminal is located. The correct positioning of array is crucial for the accurate reading of the TEER.

4.2.4   Acquiring the ECIS data

The TEER value during the time interval measurement was recorded using the ECIS™ software provided. The data was then exported to the Microsoft ® Excel spreadsheet for further calculation.

4.2.5   The calculation of TEER change

The raw data exported from ECIS™ software was calculated to determine the relative change in TEER from the treatment compared to control. First, the first five time point values from each well were averaged to give the baseline value. Then, the differences in TEER from the baseline were calculated by subtracting the baseline value from the TEER values of each time point. Finally, this TEER value was normalised to the value for the control at each time point.

4.3 Results

4.3.1 The optimal TEER of the confluent tHBEC.

In this study, the TEER of the tHBEC was measured and recorded in real-time by using the ECIS™, from two hours after seeding the cells until a confluent monolayer was formed as mentioned in section 4.4.1. The TEER measured from 16 wells of 2 different array were averaged and plotted against time in hour as shown in figure 4-5. The arrays were viewed by light microscopy through the transparent part of the array in each well prior to connecting the arrays to the ECIS station. The starting TEER was 310 Ω, which was recorded in the first TEER measurement, 24 hours after seeding. The TEER gradually increased to an average resistance of 553Ω after 23hours and the cells were more than 85% confluent at this time. The array was then disconnected from the station and the tHBEC growth medium was replaced with $Q_{5\% \ FBS}$-medium. The TEER then rapidly increased during the following 12 hours after the addition of $Q_{5\% \ FBS}$-medium, and started to plateau after that. The maximum TEER recorded by the confluent tHBEC was 1231Ω, which was achieved 48 hours after the cells were plated.
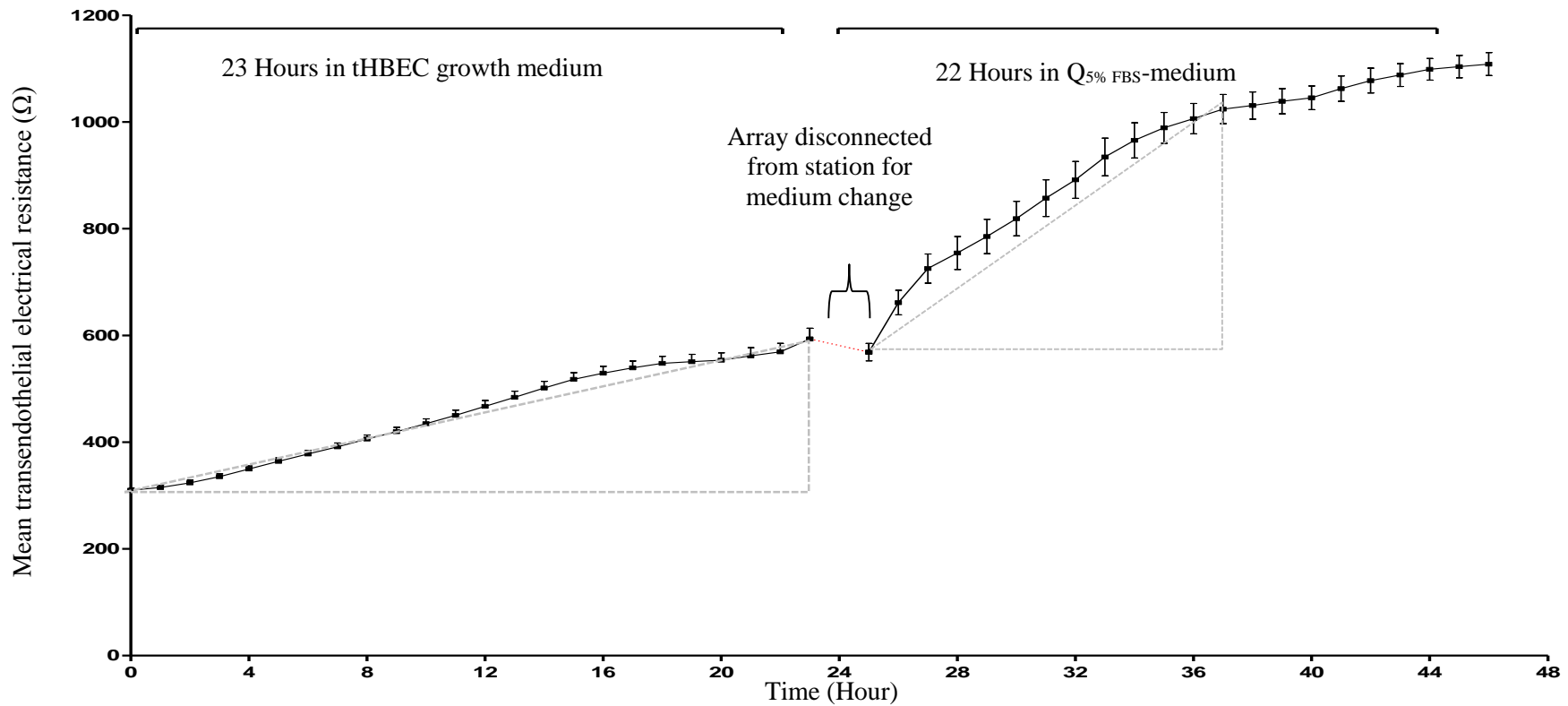
Figure 4-5: TEER of tHBEC.

The graph shows the increase in the transendothelial electrical resistance of tHBEC monolayer in 48 hours after inoculation. The graph

represents the average of TEER measured from 16 wells of two different array. The error bars represent ± 1 S.E.M.

4.3.2 Alterations in tHBEC transendothelial electrical resistance in response to the co-culture supernatants.

The alteration in transendothelial electrical resistance (TEER) of the resting tHBEC monolayer in response to the co-culture supernatants was measured over 20 hours. These experiements were only performed when the TEER of the tHBEC monolayer reached average of 1000 Ω or above. To investigate the role of GM6001 sensitive proteases, the co-culture supernatants were assessed by measuring TEER in the absence and presence 25 nM GM6001.

The mean normalised TEER from 6 different experiments using supernatants from 6 different co-culture experiment was plotted (figure 4-6). In general, the TEER reading during the first 4 hours gives huge variation between experiments. These TEER spikes were a result of the medium change and the addition of treatment. This shows that TEER measurement using ECIS is sensitive to the disturbances on its array. TEER value from the tHBEC treated with control co-culture supernatant was used as a baseline control.

PRBC-tHBEC co-culture supernatant was found to cause reduction in TEER compared to control co-culture supernatant after 3 hours of treatment. The TEER then steadily decreased and was lower than the TEER value from tHBEC treated with uRBC-tHBEC co-culture supernatant after 8 hours of treatment. After 20 hours of treatment, the TEER in response to PRBC-tHBEC co-culture supernatant was 2 fold lower than that with uRBC-tHBEC co-culture supernatant ($P \leq 0.005$, n=6). Treatment with uRBC-tHBEC co-culture supernatant only caused a slight reduction in TEER, which was lower than control

co-culture supernatant treatment throughout the ECIS experiments, however, there was no statistical difference between these two treatments as tested by 2 way ANOVA.

In adjacent wells, the experiment was with the addition of protease inhibitor GM6001 (dashed lines, Figure 4-6). Interestingly, the steady reduction in the TEER caused by the PRBC-tHBEC co-culture supernatant, was inhibited in the tHBEC treated with the same co-culture supernatant in the presence of GM6001. This inhibition was not significant from 0 hour to 12 hour ($P > 0.05$, n=6), however became more significant after 13 hour with the maximum of 2-fold inhibition at 18 to 20 hours ($P \leq 0.001$, paired t-test at the selected time point, n=6). The addition of GM6001 however, did not have any significant effect in the small TEER changes in response to by uRBC-tHBEC co-culture supernatant. For clarity, TEER data for the tHBEC treated with PRBC-tHBEC co-culture supernatant in the presence and absence of GM6001, was extracted and presented in figure 4-7.

Similarly, inhibition studies were performed using TIMP-3. TIMP-3 did not inhibit the effect of the PRBC-tHBEC co-culture supernatant. The data from these studies was difficult to interpret conclusively since, the distilled water, which was the diluent for the TIMP-3 and was added as a control to the wells without the inhibitor in these studies, appeared to interfere with the effect of the co-culture supernatants. Both the URBC-tHBEC co-culture supernatant and the PRBC-tHBEC co-culture supernatant caused an increase in TEER (Fig 4-8). For clarity, TEER data for the tHBEC treated with URBC-tHBEC co-culture supernatant and PRBC-tHBEC co-culture supernatant, was extracted and presented in Fig 4-9. These observations were contrary to previous experiments, where PRBC-tHBEC co-culture supernatant produced a significant reduction in TEER in studies where the supernatant was used with DMSO as in the GM6001 studies (Fig 4-6 & Fig 4-7) or without DMSO in preliminary experiments (data not shown). However, it was interesting to note,

that there was a smaller increase in TEER with PRBC-tHBEC co-culture supernatant than with URBC-tHBEC co-culture supernatant (Fig 4-9). It is possible that the disparate effect of the PRBC-tHBEC co-culture supernatant, compared to the other experiments is related to the addition of distilled water.
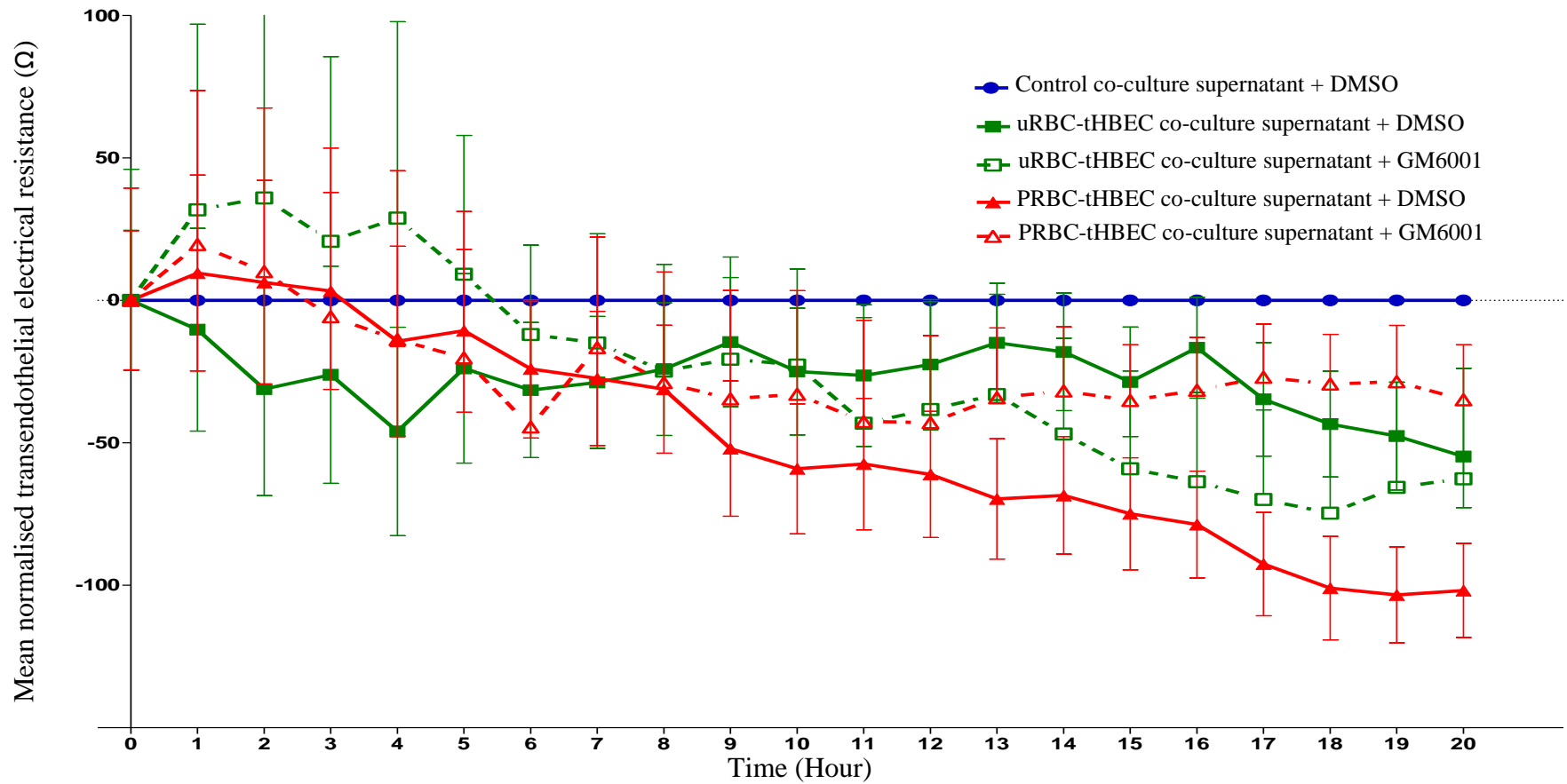
Figure 4-6: The line graph shows the alteration in tHBEC monolayer TEER treated with co-culture supernatants in the presence and absence of GM6001 over 20 hours. The error bars represent ± 1 S.E.M from 6 separate experiments.
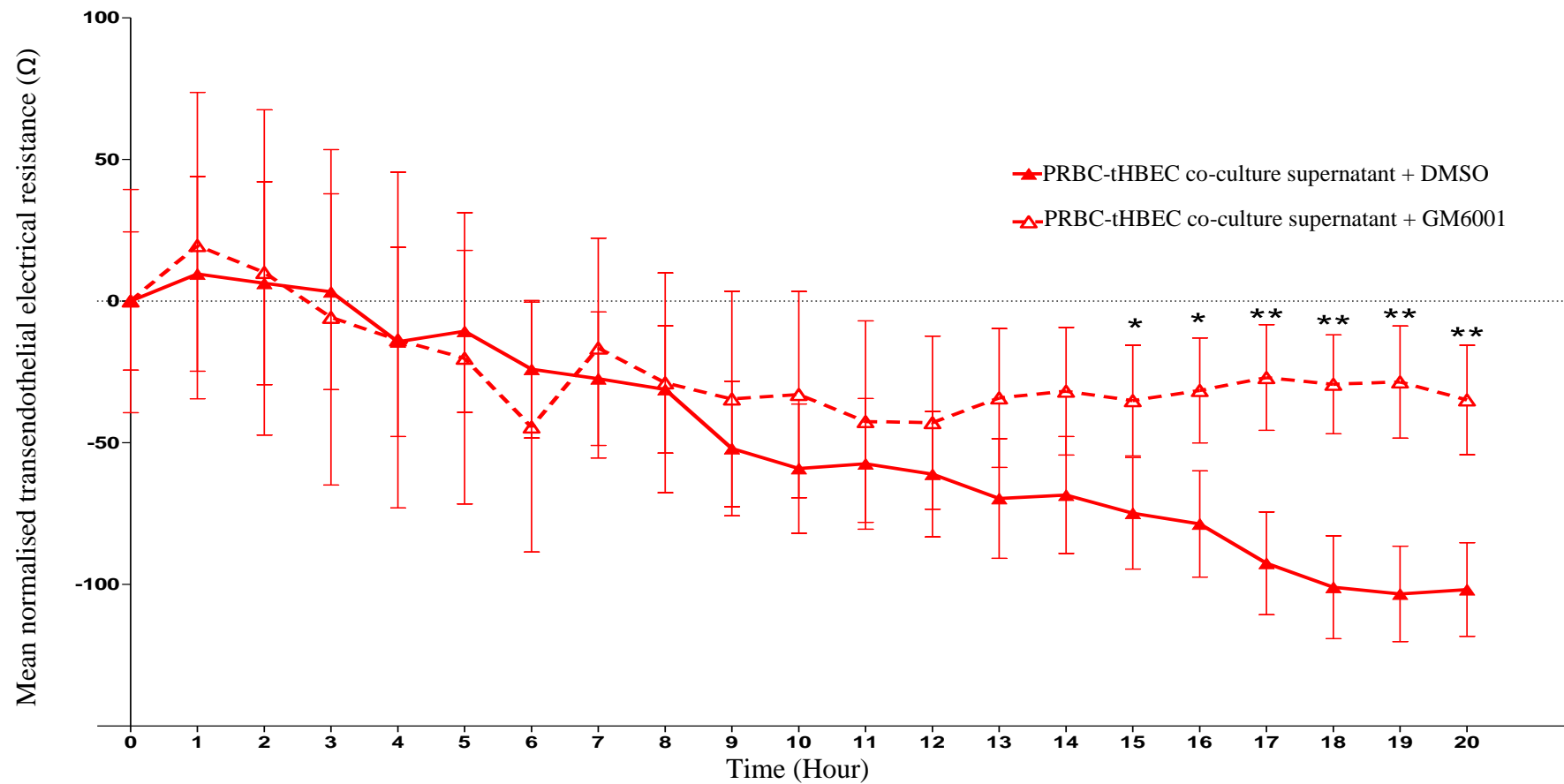
Figure 4-7: TEER data for the tHBEC treated with PRBC-tHBEC co-culture supernatant in the presence and absence of GM6001 (extracted from figure 4-6 for clarity). The error bars represent ± 1 S.E.M from 6 experiments.
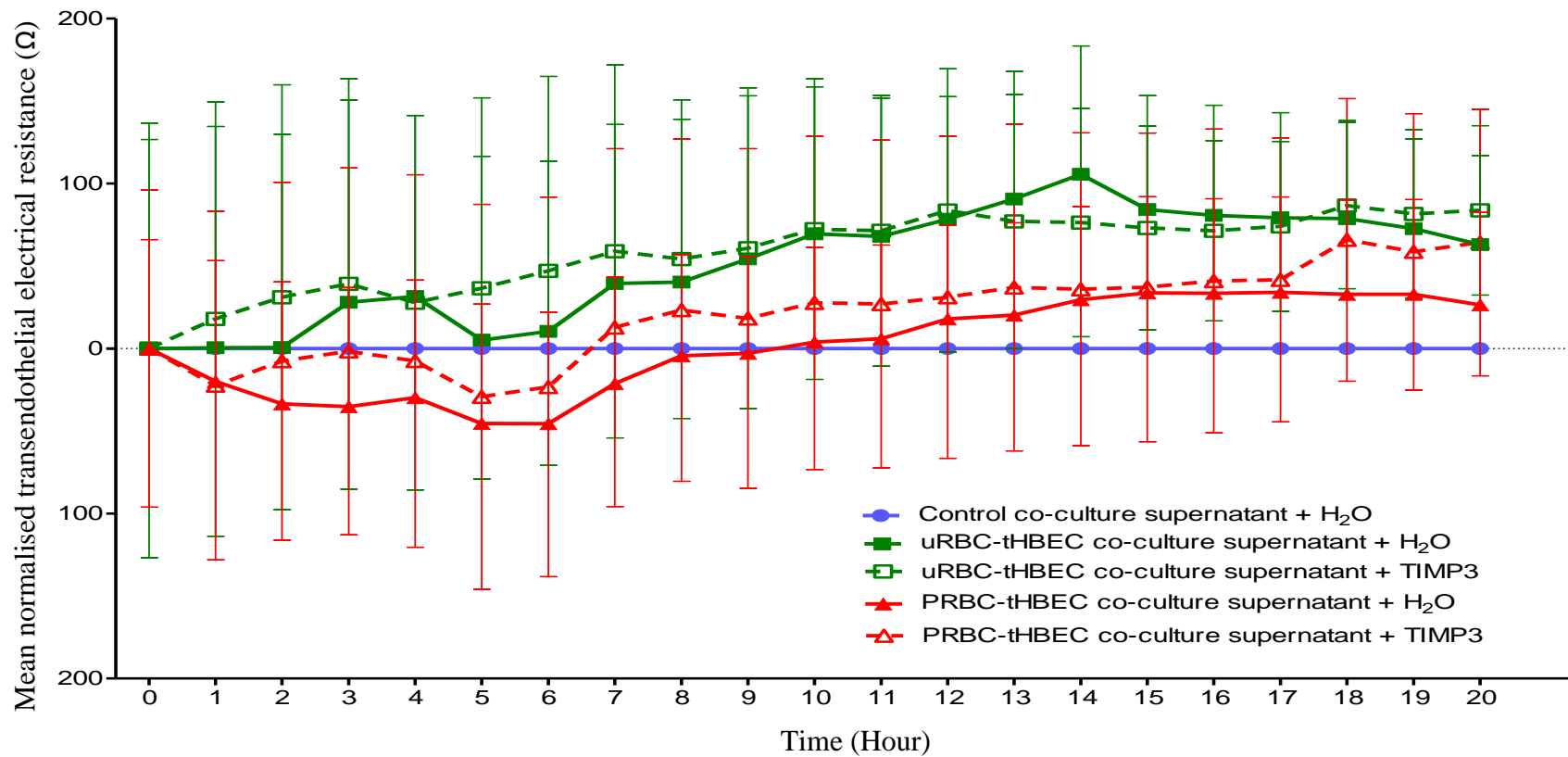
Figure 4-8: The line graph shows the alteration in tHBEC monolayer TEER treated with co-culture supernatants in the presence and absence of rhTIMP-3 over 20 hours. The error bars represent ± 1 S.E.M from 4 separate experiments.
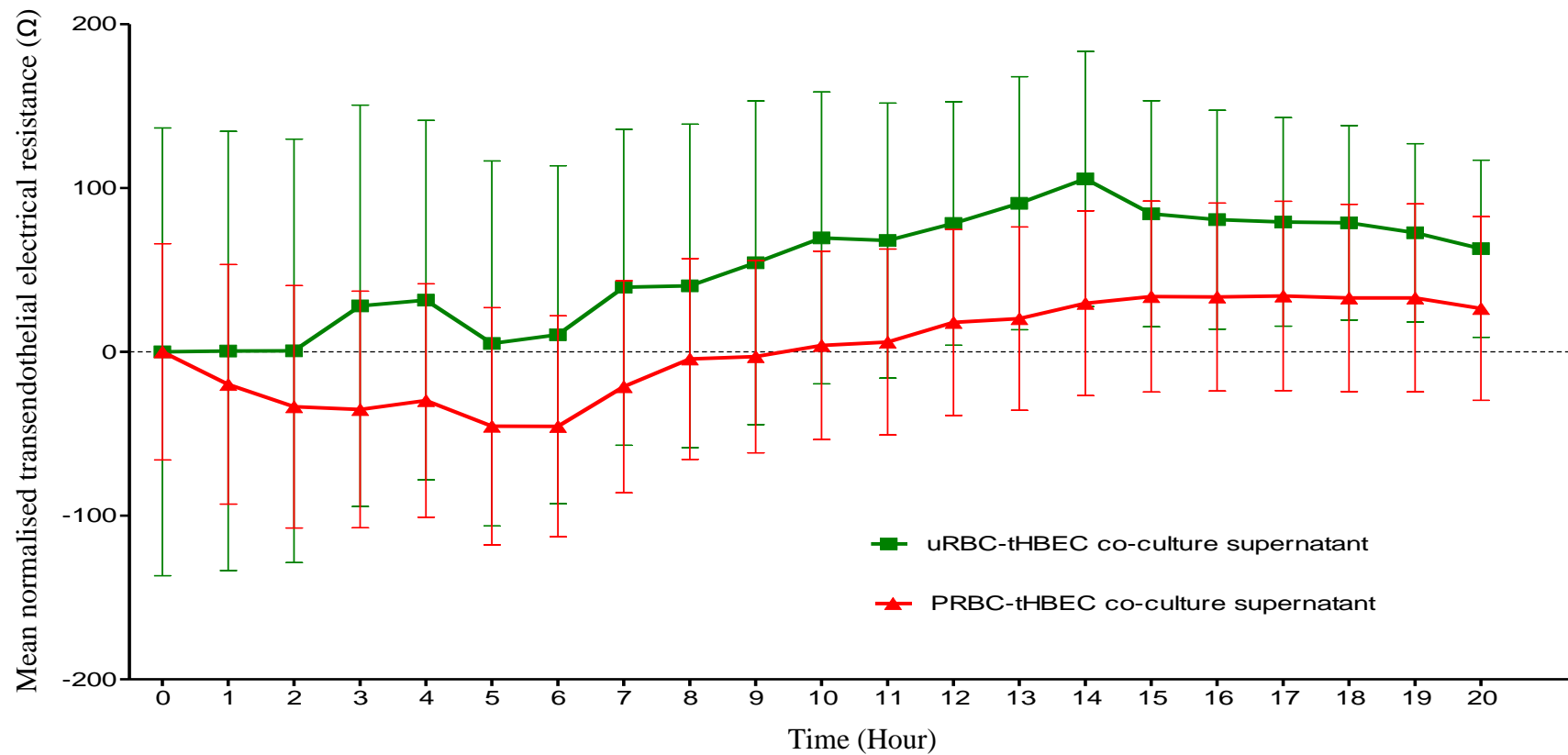
Figure 4-9: The graph shows the alteration in tHBEC monolayer TEER treated with uRBC-tHBEC co-culture supernatants and PRBC-tHBEC co-culture supernatants with the rhTIMP-3 diluent, dH_2O over 20 hours (extracted from figure 4-8 for clarity). The error bars represent $\pm$ 1 S.E.M from 4 separate experiments.

4.4 Discussion

In this chapter, it was demonstrated that the tHBEC could achieve a high TEER that suits an *in vitro* model of the blood-brain barrier. The tHBEC at passage between 19 and 28 was able to form a barrier of high integrity at 1000 to 1300 Ω after 48 hours of seeding, which was continuously measured using ECIS. This value is comparable to the primary brain endothelial cells monolayer (1500 Ω; (Tripathi et al., 2007)), and other immortalised brain endothelial cells used as an *in vitro* BBB model such as HBEC-5i (Wassmer et al., 2006), hCMEC/D3 (Weksler et al., 2013) and HBMEC-3 (Chaitanya et al., 2011).

The measurement of TEER using ECIS™ is sensitive and convenient as it can continuously measure the changes in endothelial cell monolayer TEER without the need to remove the cells set up from the incubator. This allows a stable endothelial cell growth to be maintained and reduces disturbances in CO_2 supply and the temperature compared to the measurement of TEER using the EndOhm-EVOM system.

By using the ECIS and tHBEC monolayer as an *in-vitro* BBB model, the data demonstrate that the PRBC-tHBEC co-culture supernatant at a dilution of 1: 10 has the ability to cause a 2- fold decrease in monolayer electrical resistance compared to the uRBC-tHBEC co-culture supernatant. The loss in the tHBEC electrical resistance by the PRBC-tHBEC co-culture supernatant can be seen clearly within 4 hours of treatment with the co-culture supernatant.

This shows that the endothelial monolayer integrity can not only be reduced directly by PRBC (Tripathi et al., 2007), or PRBC in the presence of platelets (Wassmer et al., 2006), but also indirectly by soluble factors produced during interaction between tHBEC and

PRBC. Interestingly, the ability of PRBC-tHBEC co-culture supernatant to reduce the TEER of endothelial cells monolayer is inhibited by the addition of 25 nM GM6001. GM6001 is a potent inhibitor of MMP and can inhibit different MMP at different concentrations.

The effect of rhTIMP-3 on the reduction of tHBEC monolayer TEER was also tested, however it is not conclusive (figure 4-8). In contrast to the pattern seen in figure 4-6, the addition of rhTIMP-3 caused a slight increase in TEER of tHBEC monolayer treated with uRBC-tHBEC co-culture supernatant and PRBC-tHBEC co-culture supernatant compared to control. Surprisingly, the average TEER of tHBEC monolayer treated with uRBC-tHBEC co-culture supernatant is slightly higher than the treatment with PRBC-tHBEC co-culture supernatant. However, there are no significant difference in TEER between the presence and absence of rhTIMP-3 on the same co-culture supernatant treatments. This effect however, varies between experiments, which can be seen by the bigger size of error bars.

In conclusion, the tHBEC forms a tight barrier with a high electrical resistance, suitable for monitoring changes in TEER. The integrity of tHBEC monolayer is compromised by the addition of PRBC-tHBEC co-culture supernatant, represented by a significant reduction in electrical resistance. This can be inhibited by the addition of 25 nM GM6001, thus protecting the barrier integrity. These studies suggest the involvement of proteases in the MMP family in mediating loss of BBB integrity seen in CM brain tissue.

CHAPTER FIVE: ALTERATION IN ENDOTHELIAL CELL MONOLAYER PERMEABILITY IN RESPONSE TO THE CO-CULTURE SUPERNATANTS.

Chapter 5: The alterations in endothelial cell monolayer permeability in response to the co-culture supernatants.

5.1 Introduction

BBB leakage in cerebral malaria is still not fully understood. Many hypotheses link the BBB damage in cerebral malaria with the activation of endothelial cells either directly by PRBC or indirectly by the activated platelet and up-regulation of pro-inflammatory cytokines. BBB damage not only occurs in CM, but also in other diseases such as multiple sclerosis and Alzheimer's disease (AD) (Lou et al., 1997, Minagar et al., 2002). In these non-infectious neuropathologies, the damage is believed to be caused by dysregulation of endothelial function due to over-activation of astrocytes and macrophages (For review see Ballabh et al. (2004)). This damage can increase the permeability of BBB, which can in turn have a negative impact on the normal function of the human brain.

In chapter 3, it was demonstrated that PRBC have the ability to induce endothelial cell activation and alter the expression of a member of pro-inflammatory cytokines and proteases that may mediates BBB damage. The soluble factors produced as a result of interaction between endothelial cells and PRBC were shown to be able to induce the reduction in the tHBEC monolayer integrity measured *via* the trans-endothelial electrical resistance (chapter 4). Thus, it is important to determine if the loss in the tHBEC integrity as suggested by the loss in electrical resistance is sufficient to cause leakage of molecules through the intercellular junctions, between endothelial cells, from the vessel lumen into the brain parenchyma as seen in CM.

There are several different methods that can be used to determine the permeability of an endothelial cells monolayer. One of the most widely used techniques is the culture of endothelial cells in a cell culture insert (transwell) which forms two different compartments, apical and basolateral. The permeability is then assessed by measuring the migration of molecules from the apical to the basolateral chamber. The solute must be water-soluble, cannot be actively transported by endothelial cells and must not be toxic to the cells. Examples include albumin or dextran labelled with a fluorescent tracer such as fluorescein isothiocyanate (FITC) or tetramethyl rhodamine iso-thiocyanate (TRITC) (Yuan and Rigor, 2010).

In this chapter, the permeability of the tHBEC cultured in a cell culture insert following treatment with co-culture supernatant was investigated using FITC labelled dextran. As in chapter 4, the inhibitory effect of GM6001 and rhTIMP-3 on the tHBEC permeability was also determined.

5.2 Material and methods

5.2.1 Preparations of cell culture insert and cells plating.

The cell culture inserts (Millipore) were arranged in a 24 well plate as in figure 5-1 by using sterile pointed tip forceps. The culturing surface (0.4 μm pore polyethylene terephthalate membrane) of the inserts was coated with 100 µl of 1% (v/v) gelatine and incubated at 37°C for the minimum of 20 minutes. After that, confluent tHBEC from a 25 cm^2 culture flask was trypsinised, counted and diluted to give a final concentration of 1 x 10^5 cells/ml as in section 2.7.4 and 2.7.5. Excess gelatine were removed from the insert (apical) by aspiration and replaced with 2 x 10^4 cells in 200 µl of tHBEC growth medium in each insert. The bottom chamber (basolateral) was filled with 1 300 µl of growth medium and the set up was incubated for a minimum of 2 hours to allow the cells to adhere on the culturing surface. The volume of medium used in apical and basolateral part of the culture was recommended by the manufacturer (Figure 5-2), to avoid non-specific diffusion due to change in hydrostatic pressure.
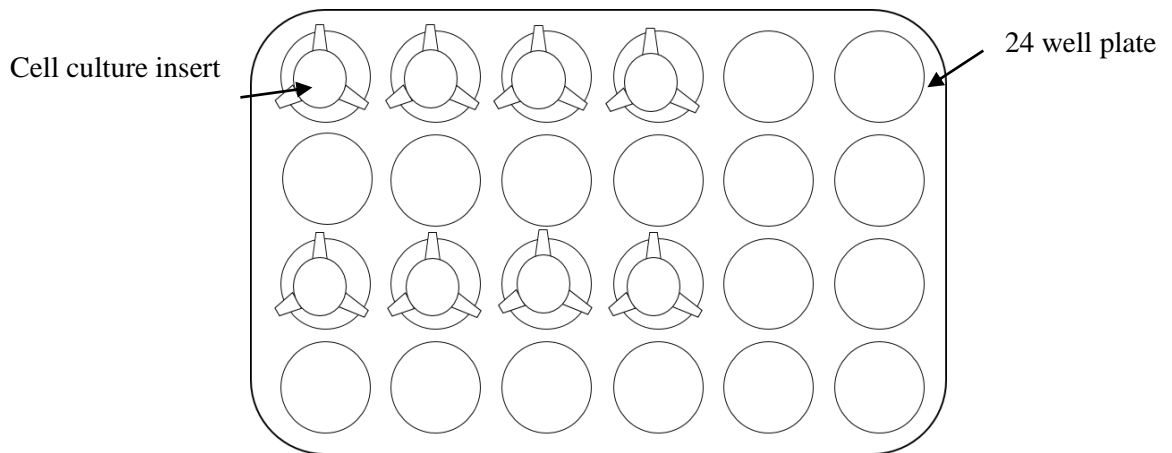
Figure 5-1: The figure shows the typical arrangement of insert in a 24 well plate.

The first and third row of well were used for culturing and assay while the second and

fourth row were used to hold the insert during medium change and assay sampling.
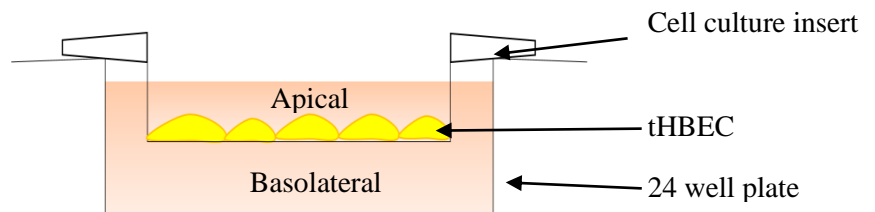
Figure 5-2: The diagram shows the side view of the hanging cell culture insert set up.

The culture medium in apical was level to the culture medium in the basolateral to

maintain its hydrostatic pressure.

5.2.2 The maintenance of tHBEC in the hanging culture insert.

After the cells were plated in the insert, the cells were maintained for 5 days before the assay was performed. The medium was changed after two hours of cell plating, then on day 3, day 5 and day 6 as summarised in table 5-1. To change the medium, the culture insert was firstly transferred into the adjacent empty well. Then, the medium in the basolateral chamber was aspirated and replaced with 1 300 µl of either tHBEC growth medium or $Q_{5\% \text{ FBS}}$-medium, depending on the stage of the culture (see table 5-1). After that, the medium in the apical chamber were carefully aspirated and replaced with 200 µl of the same medium. This sequence of medium change is important to preserve the positive pressure in the apical chamber. Finally, the insert was moved back to the culturing well and the set up was returned to the CO_2 incubator.

Table 5-1: The summary of the typical timeline in tHBEC maintenance for the FITC-dextran permeability assay.

Day	1	3	5	6
Morning	Seed cells			Change to the $Q_{5\% \text{ FBS}}$-medium 2 hours before treatments
Afternoon	Change the growth medium after 2 hours	Change the growth medium after 48 hours	Change to the $Q_{5\% \text{ FBS}}$-medium	

5.2.3 The permeability assay.

The permeability of the tHBEC monolayer as *in vitro* BBB model in response to the co-culture supernatant was assessed by measuring the accumulation of fluoresceinated dextran (Fluorescein isothiocyanate-conjugated dextran, referred to as FITC-dextran in this thesis) in the basolateral chamber. On day 6, the cells were stabilised in the fresh $Q_{5\% FBS}$-medium for 2 hours before the treatments were performed. The co-culture supernatants were added in 1:10 dilution to the medium in the apical chamber. 24 µl of the $Q_{5\% FBS}$-medium from the apical chamber was removed and replaced with 20 µl of the co-culture supernatant to achieve a 1:10 dilution and 4 µl of 20 mg/ml FITC-dextran to achieve a final concentration of 0.4 mg/ml. For the permeability assay with the addition of protease inhibitor GM6001 and rhTIMP-3, additional 20 µl of the $Q_{5\% FBS}$-medium from the apical chamber was removed and replaced with 20 µl of inhibitor. The final concentration of inhibitors used for this assay was 25 nM for GM6001 and 0.04 nM for rhTIMP-3 as in transendothelial electrical resistance experiment (chapter 4) (see table 4-2). As soon as the treatments were added, the insert was carefully removed to the adjacent well and 50 µl of the medium from basolateral chamber was removed and transferred into a flat bottom black 96 well plate. This was taken as the basal time zero sample for the experiment. To compensate for the loss of volume in the bottom chamber, 50 µl of pre-warmed $Q_{5\% FBS}$-medium was added into the basolateral chamber. Finally, the insert was carefully placed back into the culturing well and the set up was returned to the CO_2 incubator. The sampling was repeated every hour for 6 hours.

Table 5-2: The summary of concentration of the inhibitors and its diluent.

Inhibitor/ Diluent control	Dilution for experiment	Volume added (µl)	Final concentration (In each well)
GM6001 (10 mM)	250 nM	20	25 nM
DMSO (control for GM6001)	Equivalent to GM6001 dilution	20	Equivalent to GM6001 dilution
rhTIMP-3 (100 µg/ml)	0.4 nM (9 ng/ml)	20	0.04 nM (0.9 ng/ml)
dH$_2$O (control for rhTIMP-3)	Equivalent to rhTIMP-3 dilution	20	Equivalent to rhTIMP-3 dilution

5.2.4 Measuring the fluorescence intensity and associate calculation.

The fluorescence intensity of the collected samples from the basolateral chamber in permeability assay was quantitatively measured using a fluorescence reader (Glomax multi+ detection system, Promega). First, the fluorescence reader was set to measure the fluorescence from the FITC-dextran using a filter to 490 nm wavelength for excitation and between 510 nm and 570 nm for emission. To get normalised fluorescence change against time, the raw data was firstly normalised to the zero time point fluorescence for each respective treatment, which then normalised to the fluorescence value of the respective control. The normalised data was plotted against time.

5.2.5 Measurement of the tHBEC electrical resistance using EVOM reader.

The TEER of tHBEC cultured in the hanging culture insert system was measured to determine the optimal TEER, reflecting the confluent state of the tHBEC. First, the cells were cultured in the hanging cell culture insert as mentioned above (section 5.2.1). After 24 hours in culture, the first TEER measurement was taken using the EVOM and EndOhm-6

instrument. To measure the TEER, the culture insert containing the confluent tHBEC monolayer was placed inside the chamber of the EndOhm cup filled with 1.5 ml tHBEC growth medium. Then, the EndOhm cap containing top electrode was placed onto the insert and the electrical resistance was calculated by the EVOM voltohmmeter. The unit of the resistance given by this method is Ω/cm^2.
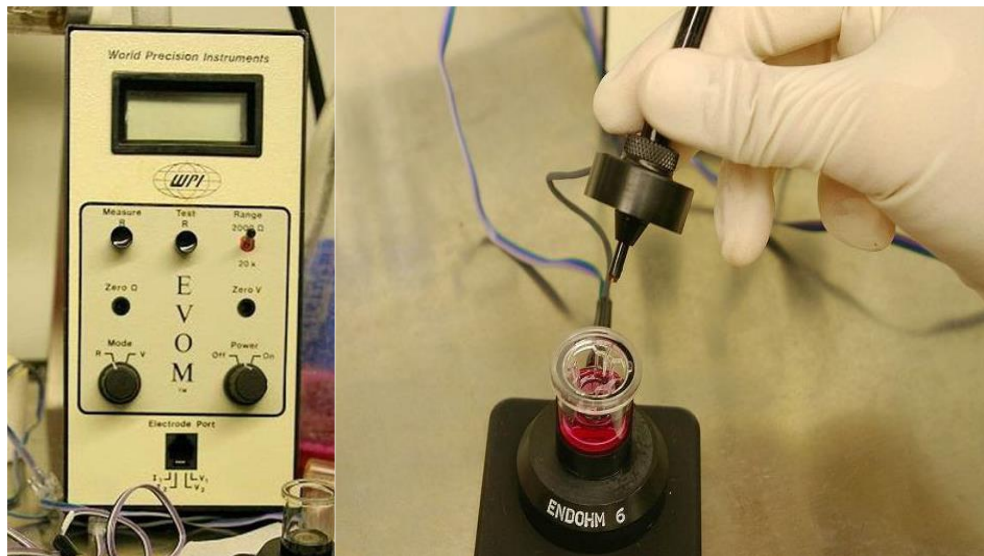
Figure 5-3: The EVOM voltohmeter and the EndOhm-6 measurement chamber are demonstrated in picture.

5.3 Results.

5.3.1 The integrity and permeability of the tHBEC monolayer in cell culture insert system

The culture surface of the cell culture insert used in this study was translucent and the confluency of the tHBEC cultured in it cannot be seen by light microscopy. Thus, TEER measurement using EVOM voltohmeter was used to determine the optimal electrical resistance of the tHBEC, which represents the integrity of a resting tHBEC monolayer. Electrical resistance from nine culture inserts from two different experiments was measured on day 2, 3, 4, 5 and 6 of culture (Figure 5-4). Electrical resistance of the culture insert only was measured as control and found to be consistent at 81 Ω cm^2 over the 6 days of the experiment. The lowest electrical resistance of the tHBEC monolayer was recorded in day 2 of culture with only 4.2 Ω cm^2 higher than the insert only control. The electrical resistance however gradually increased over time and reached a maximum resistance of 124 Ω cm^2 on day 5 of culture. Slight reduction in tHBEC monolayer electrical resistance was measured on day 6 (110 Ω cm^2). This result shows that the tHBEC cultured in the cell culture insert have the highest integrity after 5 days of culture.
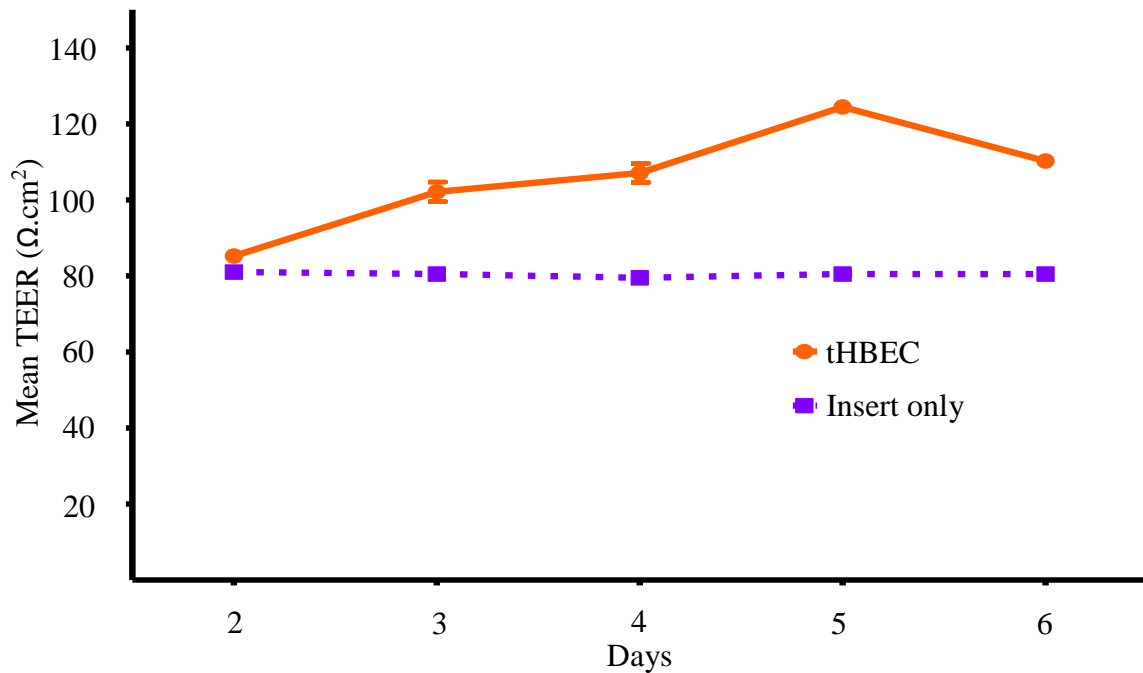
Figure 5-4: tHBEC TEER over 6 days.

The line chart shows the electrical resistance of the tHBEC in the culture insert over time

for six days. Empty insert coated with 1% (v/v) gelatine was used as negative control.

To support the finding from EVOM experiment, the permeability of the tHBEC

monolayer in hanging cell culture insert system was assessed by using FITC labelled dextran

(FITC-dextran) permeability assay. The fluorescence intensity of the medium in basolateral

chamber was measured from day 2 until day 5 of culture. The assay was done in duplicate

wells for each culture day and the average fluorescence intensity was measured (figure 5-5).

In this assay, the fluorescence intensity of the media in basolateral chamber decreases with

time suggesting an increase in barrier function of the tHBEC monolayer. Although the

tHBEC did not form a tight barrier on day two, the monolayer integrity became more

restricted after that. The movement of 40 kDa FITC-dextran across the tHBEC barrier in day

five was reduced up to three fold compared to day two of culture. These assays were important to determine when optimal barrier integrity is achieved. Both experiments suggest that the optimal barrier function of tHBEC monolayer in the cell culture insert system were formed on day four to day five of culture. Thus, all subsequent experiments were done five days after seeding into the cell culture insert.
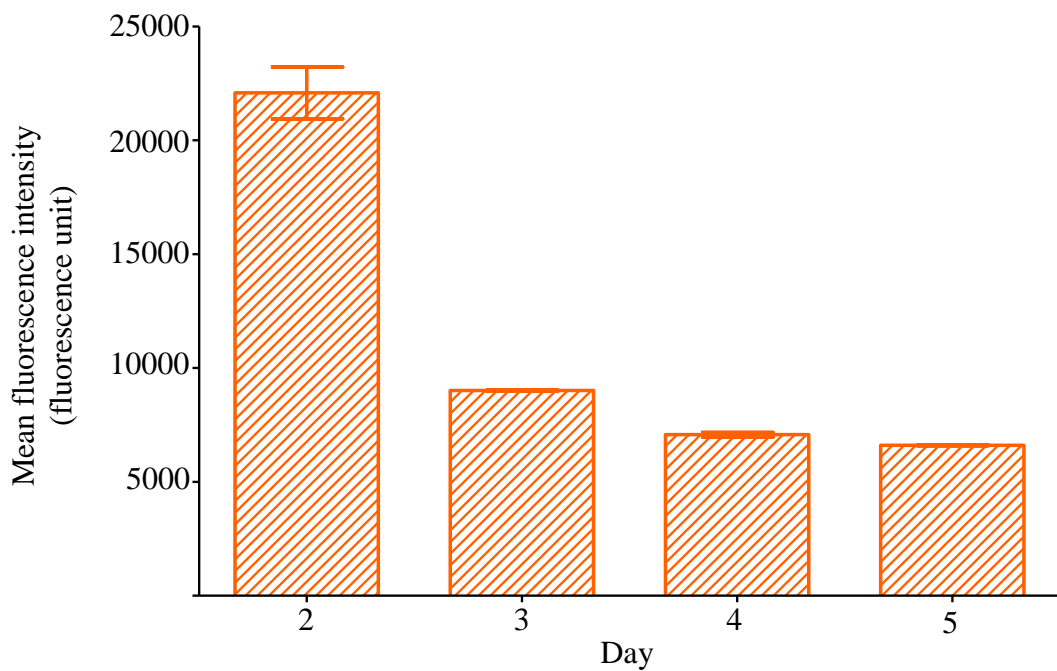
Figure 5-5: tHBEC permeability to FITC-dextran.

The reduction in the migration of the FITC-dextran from apical to basolateral chamber on day two to day five of tHBEC culture using cell culture insert. The bar chart represents the average from 2 replicate of experiment using 40 kDa FITC-dextran. (Error bars are ± 1 S.E.M)

5.3.2 Co-culture supernatant alters the permeability of the tHBEC monolayer

The co-culture supernatant together with 40 kDa FITC-dextran was added into the apical chamber and the fluorescence intensity of the medium in the basolateral chamber was measured every 1 hour for 6 hours. Collected supernatants from 10 separate co-culture experiments were analysed (Figure 5-6). Interestingly, the tHBEC monolayer barrier function was significantly disrupted after 3 hours of treatment with PRBC-tHBEC co-culture supernatant compared to control (P < 0.001, n=10) and uRBC-tHBEC co-culture supernatant (P < 0.001, n= 10). uRBC-tHBEC co-culture supernatant was seen to slightly increase the permeability of the tHBEC monolayer compared to control however the changes were not statistically significant (P > 0.05, n= 10). The increase in the tHBEC monolayer permeability then slowly reached a plateau after 5 hours.
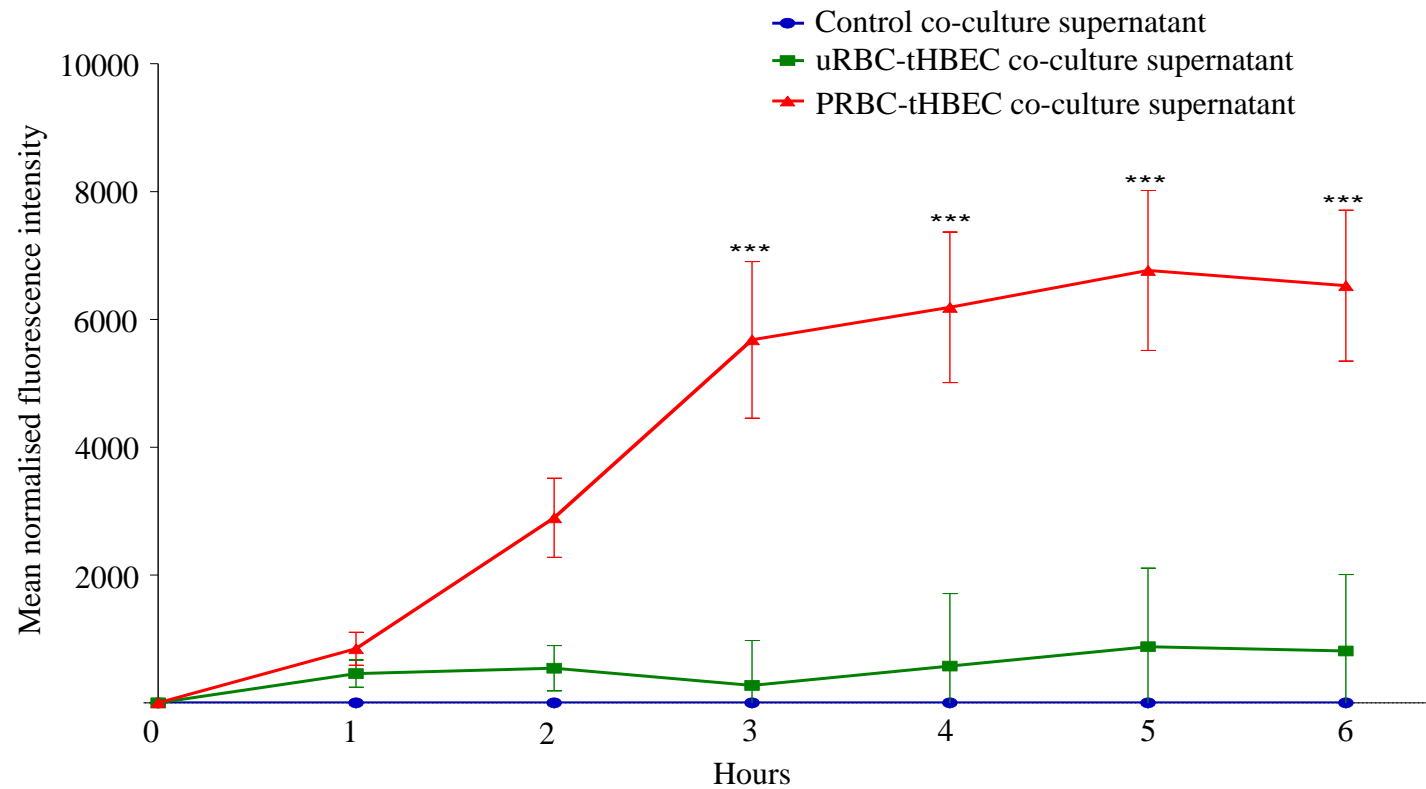
Figure 5-6: Effect of co-culture on tHBEC permeability of 40 kDa FITC-dextran.

The line graph shows the changes in the tHBEC permeability when treated with co-culture supernatant. 40 kDa FITC-dextran was used and the changes was monitored for over 6 hours (n = 10, Error bars is ±1 SEM, *** is P ≤ 0.001).

The changes in tHBEC monolayer permeability in response to the co-culture supernatant were also assayed using different sizes of FITC-dextran, 10 kDa and 70 kDa (Figure 5-7 and Figure 5-8).

When using 10 kDa FITC-dextran, the treatment with PRBC-tHBEC co-culture supernatant were caused leakage within one hour but became saturated after that. The treatment using uRBC-tHBEC co-culture supernatant also showed the same kinetics, but at a lower magnitude.

When using 70 kDa FITC-dextran (Figure 5-8) shows that it is less sensitive than 10 kDa and 40 kDa FITC-dextran. The leakage caused by PRBC-tHBEC co-culture supernatant could only be seen after 6 hours of treatment.

Since the 10 kDa FITC-dextran easily reached saturation state as early as two hours after the treatment, and the changes in the tHBEC permeability upon the same treatment could not be seen when 70 kDa FITC-dextran was used, all subsequent experiments were performed using the 40 kDa FITC-dextran.
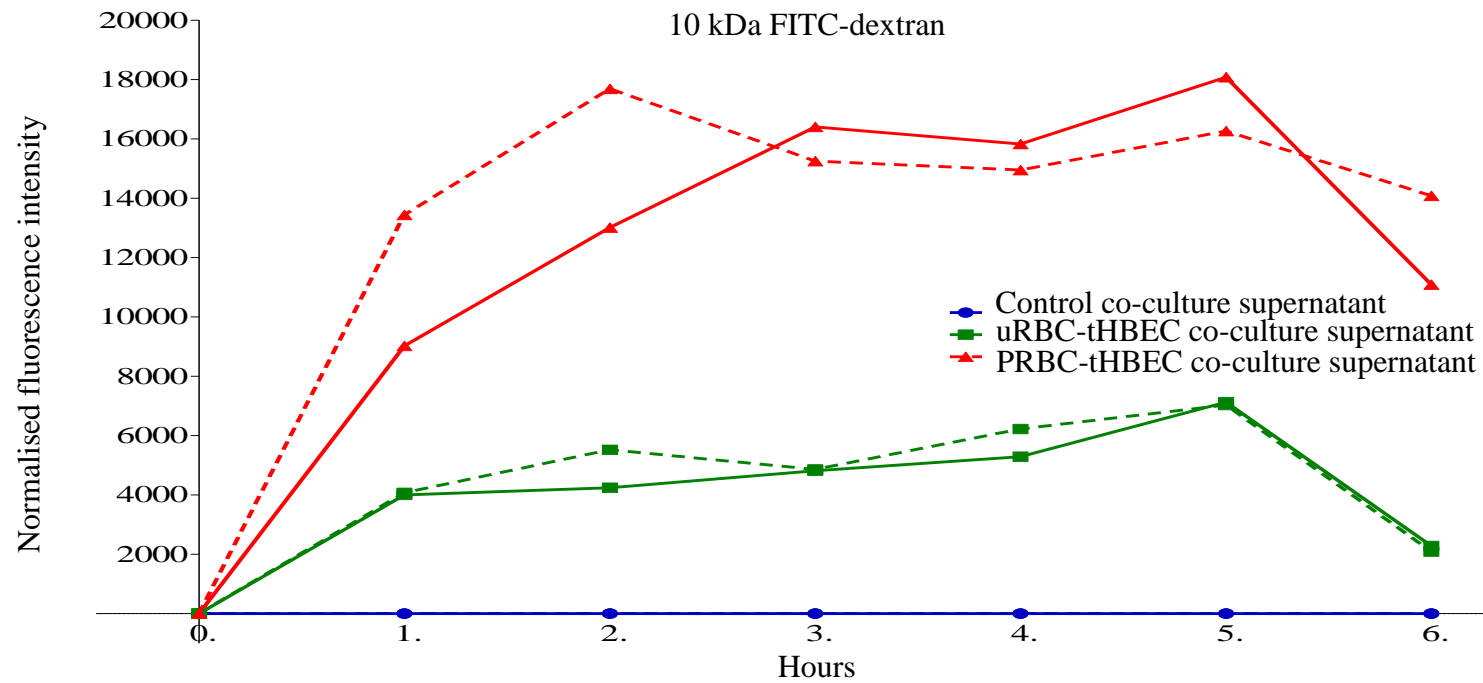
Figure 5-7: Effect of co-culture on tHBEC permeability of 10 kDa FITC-dextran

The changes in the permeability of tHBEC monolayer treated with co-culture supernatant, detected using 10 kDa FITC-dextran over the 6 hours.

Continuous and dashed line indicates the data are from two separate experiments.
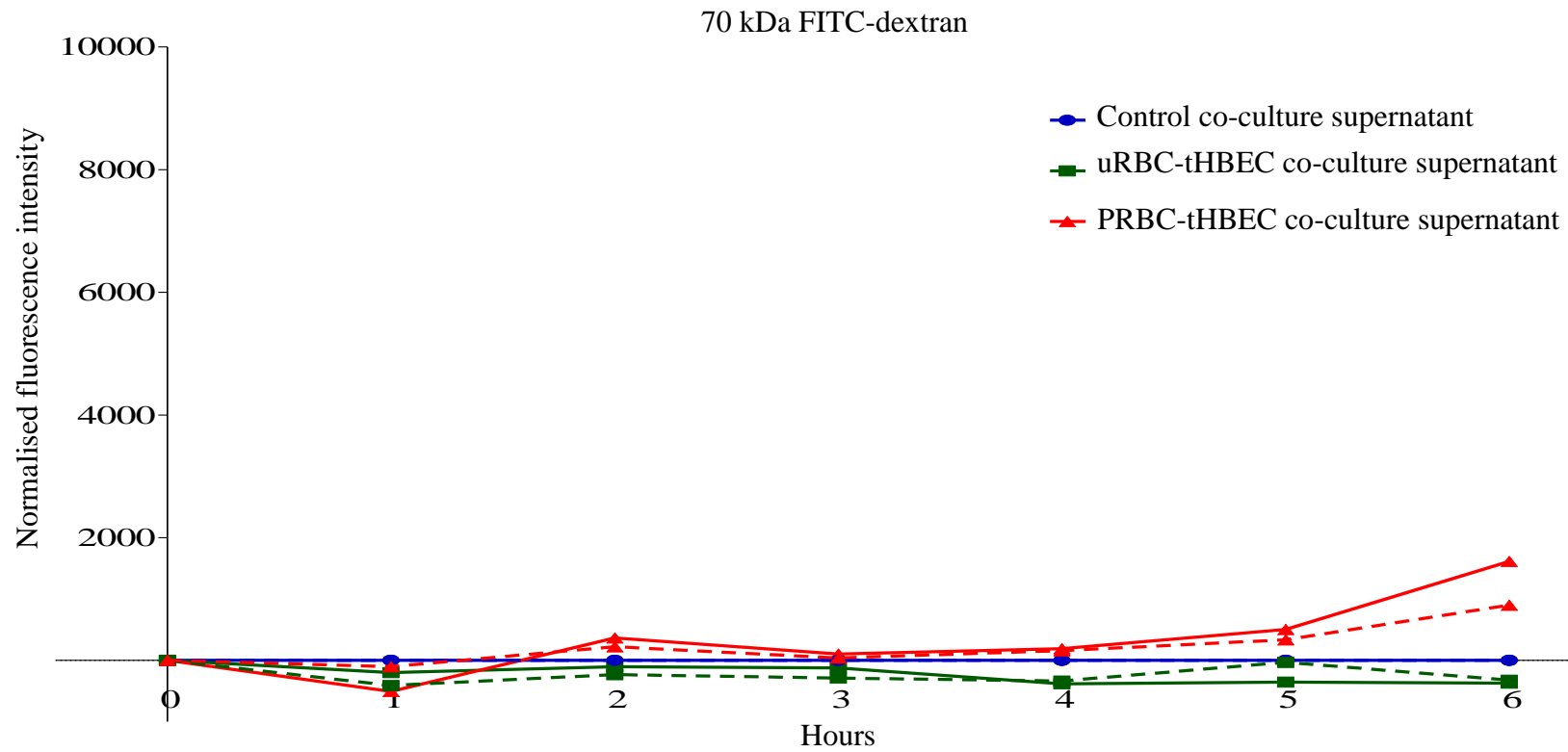
Figure 5-8: Effect of co-culture on tHBEC permeability of 70 kDa FITC-dextran

The changes in tHBEC monolayer permeability monitored using 70 kDa FITC-dextran for over 6 hours. Continuous and dashed line indicates

the data are from two separate experiments.

5.3.3 The reduction in the tHBEC monolayer permeabily caused by co-culture supernatant can be inhibited by protease inhibitor.

In the absence of protease inhibitors, PRBC-tHBEC co-culture supernatant was found to steadily increase the 40 kDa FITC-dextran that was statistically significant after two hours of treatment and reached a maximum after five hours (figure 5-6). In the same experiment, uRBC-tHBEC co-culture supernatant only produced a slight negligible change in the tHBEC monolayer permeability compared to control co-culture supernatant. As in the ECIS experiments, potential inhibitory effect of GM6001 was also investigated in the FITC-dextran permeability assay.

In this assay, PRBC-tHBEC co-culture supernatant consistently increased the tHBEC monolayer permeability over time compared to control co-culture supernatant, and this was statistically significant compared to uRBC-tHBEC co-culture supernatant ($P \leq 0.01$ at 3 hour and $P \leq 0.001$ after that) (continuous line in figure 5-9). As before, uRBC-tHBEC co-culture supernatant with DMSO caused slight leakage to the tHBEC monolayer compared to control co-culture supernatant, although this was not statistically significant ($P > 0.05$, 2 way ANOVA).

For clarity, the effect of PRBC-tHBEC co-culture supernatant in the absence and presence of GM6001 is also shown in figure 5-10, derived from data in figure 5-9. Interestingly, the increase in the tHBEC monolayer permeability caused by PRBC-tHBEC co-culture supernatant was significantly reduced at 4 to 6 hours ($P \leq 0.05$) when GM6001 was present. The maximum reduction was at 6 hour with up to 2-fold reduction in permeability compared to the DMSO control of the same supernatant. The uRBC-tHBEC

co-culture supernatant in the presence of GM6001 produced a small reduction in the permeability of monolayer, compared to the DMSO control of the same supernatant, but this was not statistically significant (P > 0.05).
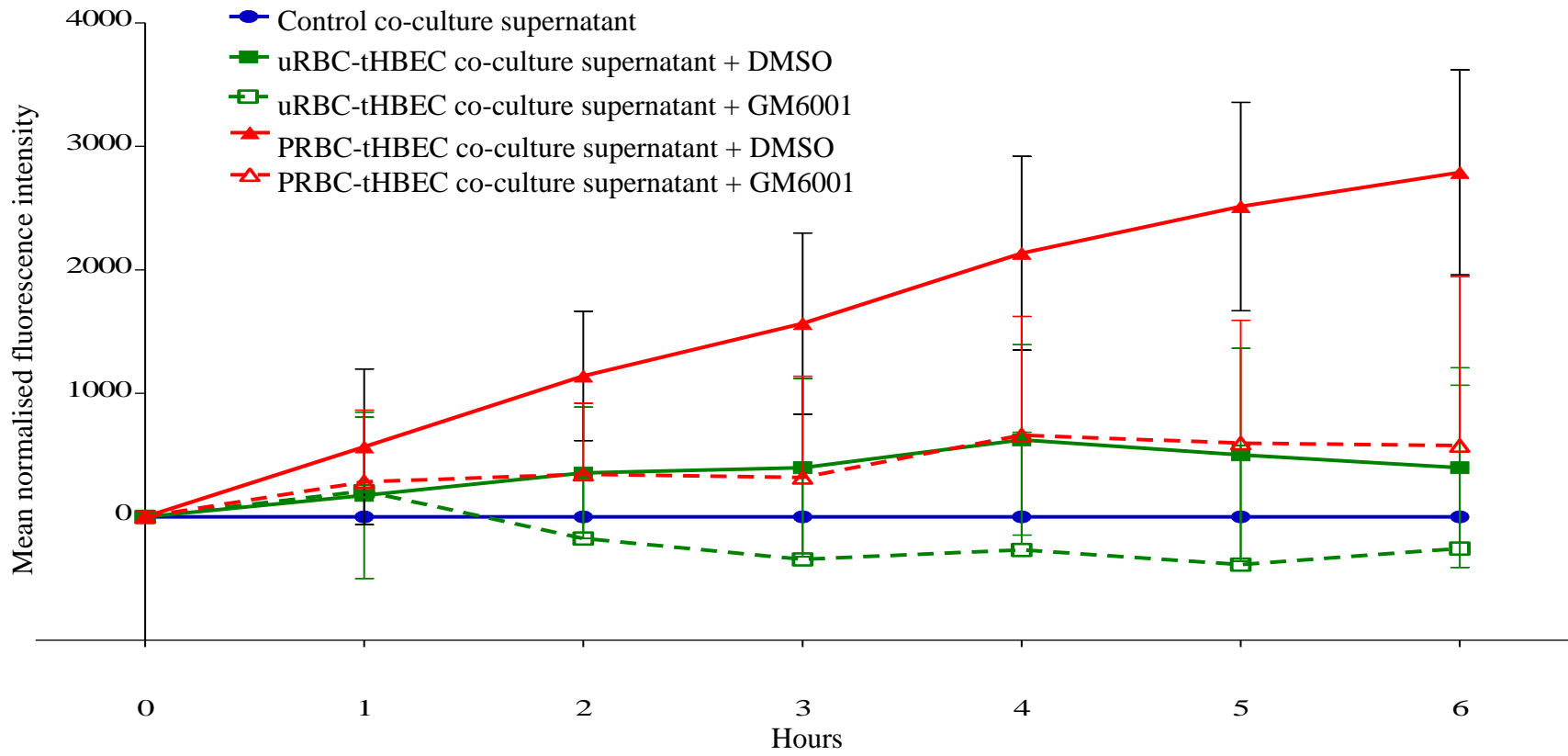
Figure 5-9: The alterations in the tHBEC monolayer permeability by co-culture supernatant with the addition of DMSO, as control of GM6001.
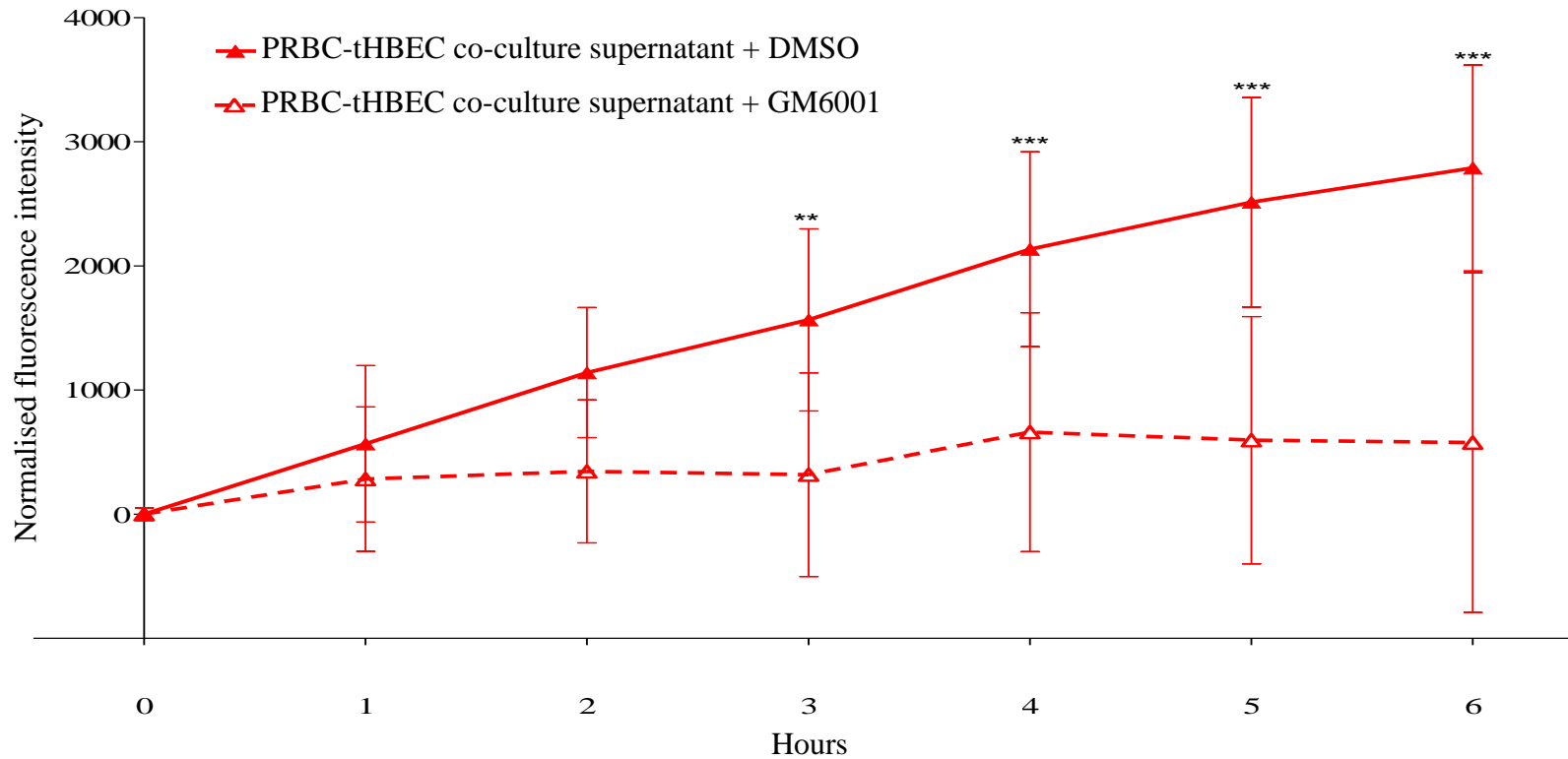
Figure 5-10: Permeability of tHBEC caused by PRBC-tHBEC co-culture supernatant.

The comparison of the reduction of tHBEC monolayer permeability by PRBC-tHBEC co-culture supernatant in the absence and presence of

GM6001. The data was extracted from figure 5-9 for clarity (n = 10, ** is P < 0.01 and *** for P < 0.001).

The PRBC-tHBEC co-culture supernatant with dH_2O control increased the permeability of tHBEC monolayer to FITC-dextran within one hour and gradually increased to reach a maximum permeability after 6 hours (Figure 5-11). uRBC-tHBEC co-culture supernatant did not cause significant changes in tHBEC monolayer permeability compared to control co-culture supernatant with dH_2O treatment.

Similar to the GM6001, the addition of rhTIMP-3 also showed a similar inhibitory effect on the increased tHBEC permeability caused by PRBC-tHBEC co-culture supernatant (dashed line in figure 5-12). The inhibitory effect by rhTIMP-3 was high highly significant ($P \leq 0.001$, n= 10) after 3 hours compared to the tHBEC treated with PRBC-tHBEC co-culture supernatant with dH_2O control. The addition of rhTIMP-3 however, did not cause any changes to the permeability of tHBEC monolayer treated with uRBC-tHBEC co-culture supernatant compared to control co-culture supernatant treatment.
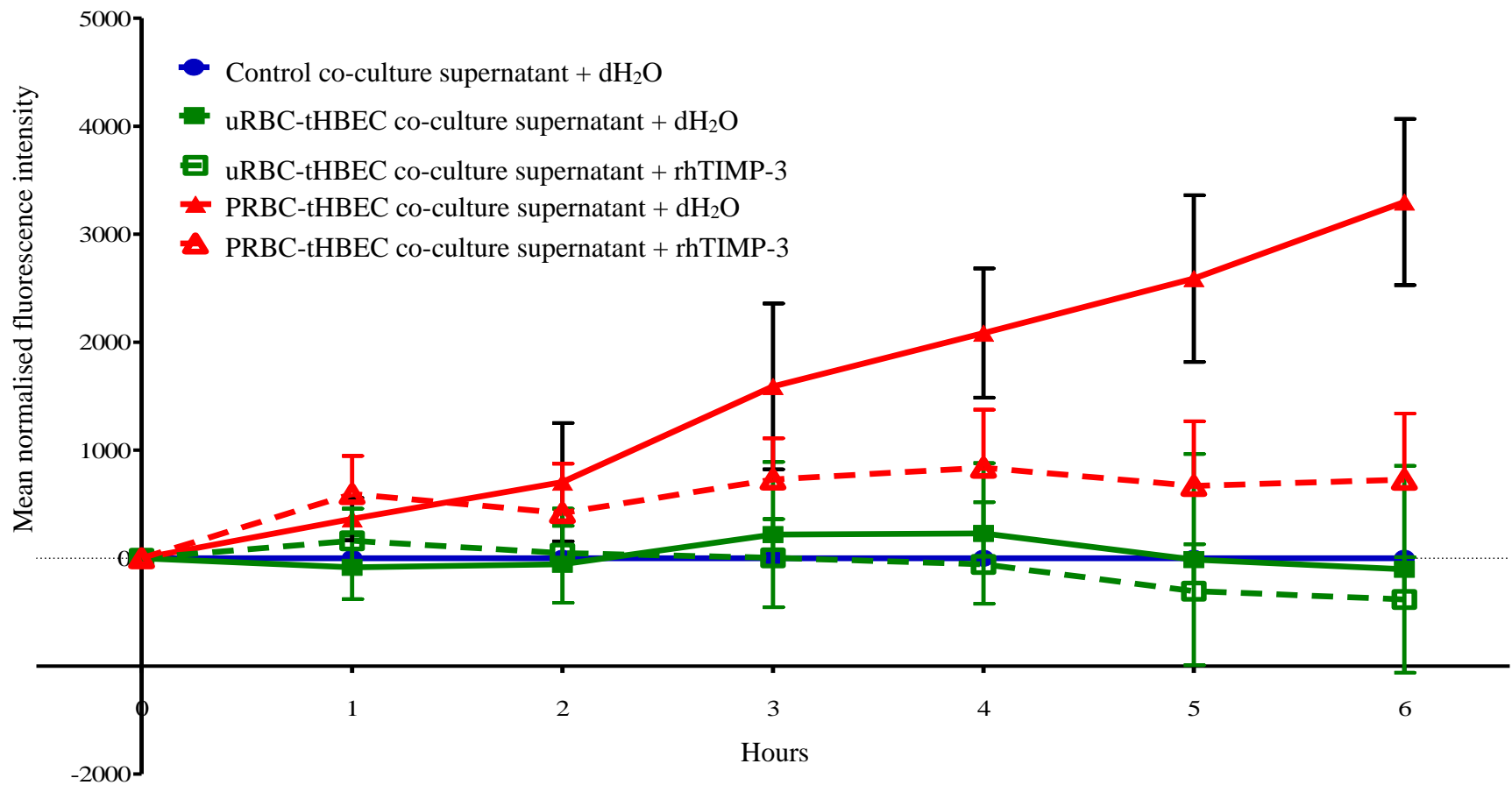
Figure 5-11: The alterations in the tHBEC monolayer permeability by co-culture supernatant in the absence and presence of rhTIMP-3. The graph was the mean normalised fluorescence intensity from 10 separate experiment, using supernatant from 10 separate co-culture experiments.
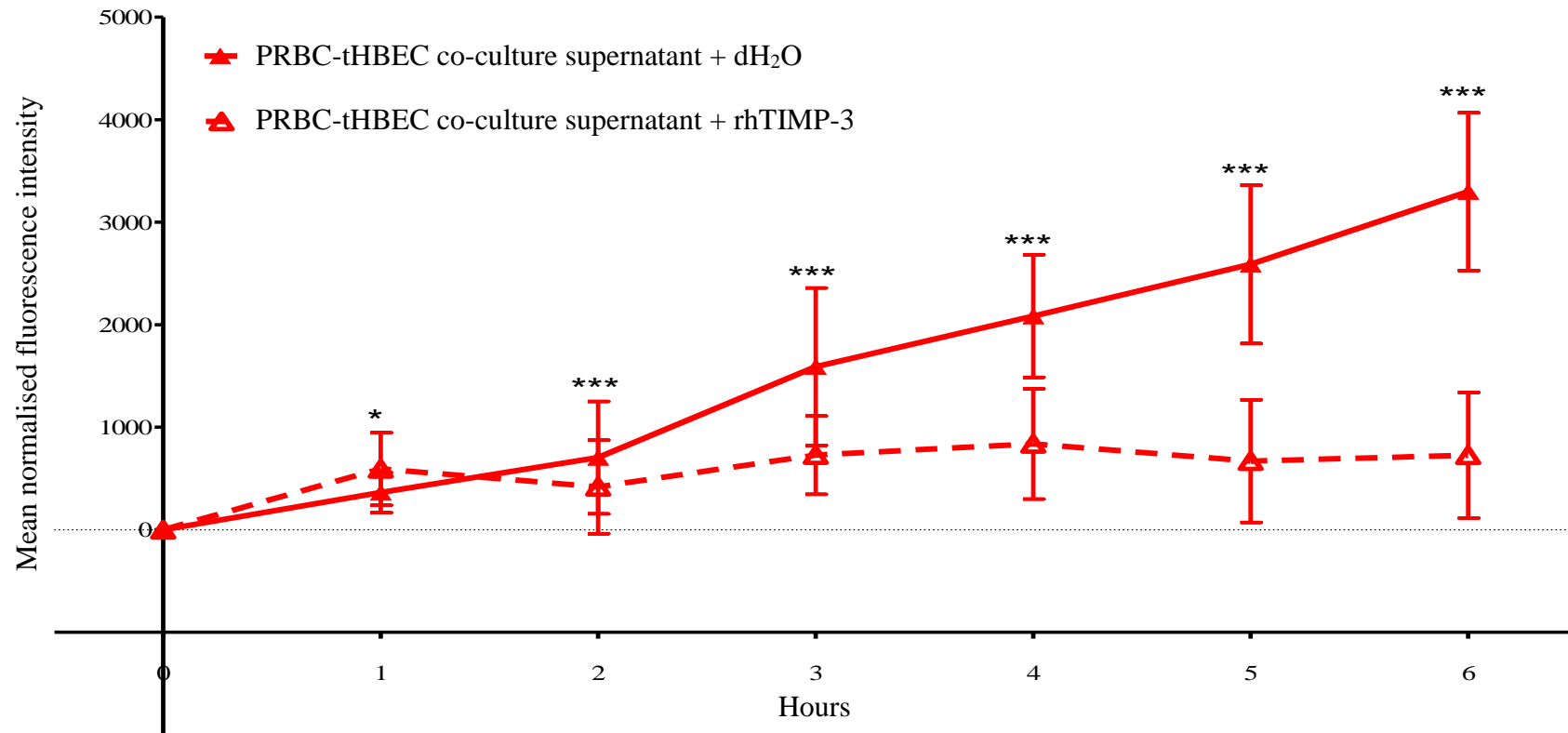
Figure 5-12: Permeability of tHBEC caused by PRBC-tHBEC co-culture supernatant in the absence and presence of TIMP-3.

The line chart summarised the changes in the tHBEC monolayer permeability treated with PRBC-tHBEC co-culture supernatant, in the presence and absence of rhTIMP-3. The difference between treatments was tested using one-way ANOVA, * is $P \leq 0.05$ and *** for $P \leq 0.001$.

5.4 Discussion

In chapter 4, it was demonstrated that the tHBEC monolayer used has comparable electrical resistance to other brain endothelial cells monolayer as *in-vitro* model of BBB. In this chapter, by using a different methodology, the tHBEC monolayer electrical resistance was measured, to determine time required to achieve maximal electrical resistance in the cell culture insert set up. It was important to establish this prior to starting the permeability assay. This is because the translucent properties of the PET membrane used in the culture insert made it impossible to observe the cells under the light microscopy and determine when a confluent monolayer was achieved. Maximal electrical resistance is necessary at the start of the experiment to allow reliable assessment of changes in permeability of the tHBEC monolayer using the FITC-dextran permeability assay. The TEER of tHBEC cultured in the cell culture insert is also directly comparable to the system used by Callahan et al. (2004). The permeability of tHBEC monolayer using 40 kDa-FITC dextran on day 2, 3, 4 and 5 was also investigated. Both methodologies show that in the cell culture insert, the tHBEC form a highly restricted barrier within 4 to 5 days of culture, and the tHBEC monolayer restricted the movement of 40 kDa-FITC-dextran. This result also reflects the association between the TEER and tHBEC monolayer permeability, where the higher the TEER, the more restricted is the tHBEC permeability (Figure 5-13).
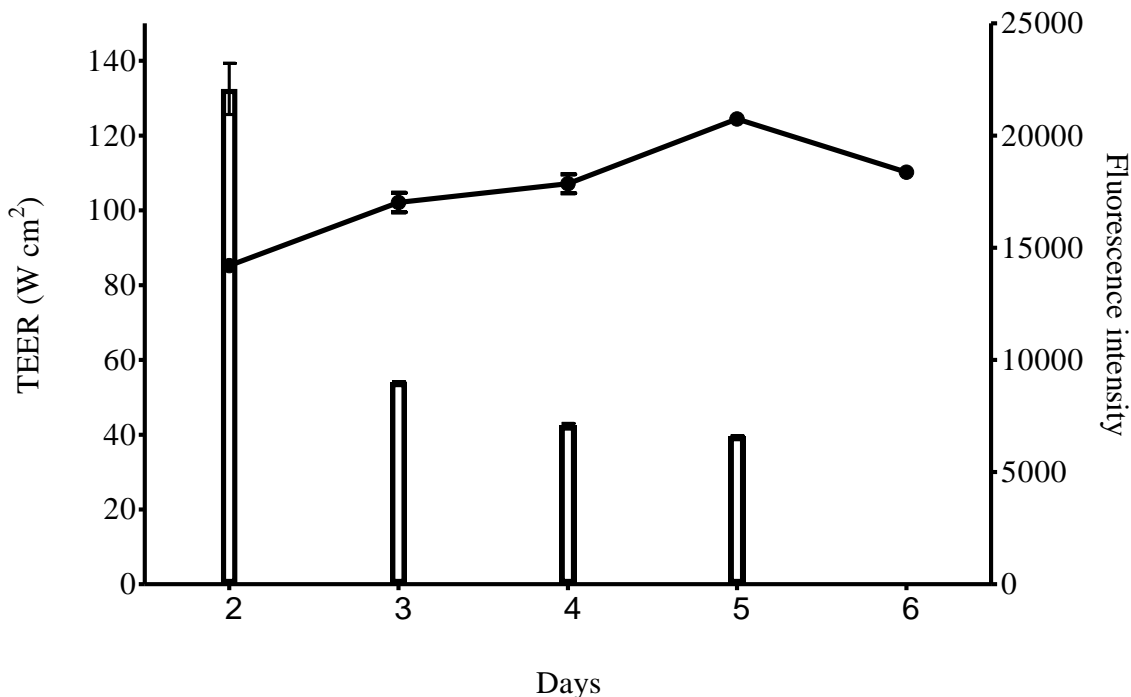
Figure 5-13: The association between tHBEC monolayer TEER (EVOM) (line) and tHBEC permeability to 40 kDa FITC-dextran (bar).

The measurement of endothelial cells permeability using FITC-dextran at continuous multi time-point is technically difficult to do. The first attempt to measure the changes in FITC-dextran migration from luminal to basolateral chamber at high time resolution, by sampling every 15 minutes was not successful. The increase in the sampling interval to every 30 minutes was also unsuccessful. At these sampling intervals, the migration of FITC-dextran is not stable and increases the noise of the background with huge variation between sampling. This might be due to the effect of frequent movement of the cell culture insert set up out of the CO_2 incubator for sampling. This can increase the disturbances to the cell culture due to fluctuations in (1) pH caused by the lack of CO_2 supply, (2) temperature for endothelial cell growth, and (3) hydrostatic pressure when lifting the culture insert out of the well for sampling. Further optimisation found that stable migration of FITC-dextran with

low background noise could be achieved by reducing the sampling time interval to once every hour. This optimised method was used in all permeability experiments in this chapter.

These studies and the ECIS studies (chapter 4) demonstrate that the tHBEC monolayer integrity and restricted permeability can be reduced by the soluble factors produced by tHBEC in response to the interaction with PRBC, but not with uRBC. This might suggest that the infiltration of serum fibrinogen across the non-sequestered vessel as seen in the post mortem studies (Brown et al., 2000, Brown et al., 2001, Dorovini-Zis et al., 2011) was due to the damage in the BBB endothelial cells induced by the soluble factors derived from the endothelial cells in vessels following PRBC sequestration.

Further investigation using inhibitors for the protease candidates which were shown to be upregulated in the PRBC-tHBEC co-culture supernatant (chapter 3) was done using GM6001 and rhTIMP-3. The addition of GM6001 inhibits the reduction in tHBEC monolayer integrity and permeability caused by PRBC-tHBEC co-culture supernatant. The inhibition effects of GM6001 in both ECIS and FITC-dextran permeability assay have different kinetic. In the FITC-dextran permeability assay, the inhibition could be seen within the first hour of treatment, however delayed to 3 hours in ECIS experiment. This might be due to the TEER spikes, which increase the background noise of the TEER measurement.

Interestingly, the addition of rhTIMP-3 was found to inhibit further reduction in the restricted barrier permeability caused by PRBC-tHBEC co-culture supernatant, which cannot be seen in ECIS experiments. The inability of ECIS experiment to show this inhibition effect may be due to the sensitivity of the method to the addition of water, the

diluent for rhTIMP-3. As the ECIS utilise electrochemical properties of a fluid, the addition of water may interfere these properties.

Loss in the ability of PRBC-tHBEC co-culture supernatant to reduce the tHBEC monolayer integrity and restricted permeability in the presence of GM6001 and rhTIMP-3 indicates that the damaging effect may be due to the proteases that are sensitive to GM6001 and rhTIMP-3. GM6001 is a potent inhibitor for the majority of MMP, especially the gelatinases family matrix metalloproteases. TIMP-3 is an endogenous regulator for MMP and was also found to inhibit ADAMTS group of proteases, especially ADAMTS-1 (Hashimoto et al., 2001).

In conclusion, the PRBC-tHBEC co-culture supernatant was not only able to induce the loss in the tHBEC monolayer integrity (chapter 4), but also increase the permeability to the 40 kDa FITC-dextran. The increase in permeability waspartially inhibited by GM6001 and rhTIMP-3 and could provide a clue to a potential inhibitor that can be used as adjunct therapy in cerebral malaria patient management.

CHAPTER SIX: ALTERATION IN HUMAN BRAIN ENDOTHELIAL INTERCELLULAR JUNCTION PROTEINS IN RESPONSE TO CO-CULTURE SUPERNATANTS.

Chapter 6: The alteration in tHBEC intercellular junction in response to co-culture supernatants.

6.1 Introduction

Majority of patients who died due to CM showed loss of ZO-1, occludin, claudin-5 and vinculin in the part of the brain with sequestered PRBC (Dorovini-Zis et al., 2011). Although the breakdown of BBB and loss of these junction proteins has been widely studied, the molecular mechanisms involved are poorly understood.

Previous chapters have demonstrated the induction or upregulation of inflammatory mediators in PRBC-tHBEC co-culture supernatants (chapter 3). Subsequent studies showed that soluble elements in these co-culture supernatants could disrupt the integrity of the BBB, demonstrated by (1) reduction in electrical resistance (chapter 4) and (2) increase in permeability of monolayer to FITC-dextran (chapter 5). Additionally, these effects could be partially inhibited using GM6001 and rhTIMP-3. This chapter will explore the hypothesis that changes in intercellular junction proteins are mediated by soluble factors in the PRBC-tHBEC co-culture supernatant.

6.2 Material and methods

6.2.1 Cell based-ELISA for tHBEC ZO-1, Claudin-5, Occludin and Vinculin.

Cell based-ELISA was used to measure the level of intercellular junction proteins of tHBEC. First, the cells were seeded into a 96 well culture plate as before. The cells were maintained as table 6-1.

Table 6-1: The summary of tHBEC maintenance for tHBEC intercellular junction cell based-ELISA.

Culturing day	1	3	4
Morning	Seeding cells		Change medium and add co-culture supernatant
Afternoon	Change the growth medium after 2 hours	Change to Q$_{5\% \text{ FBS}}$-medium	

On day 4, the medium was changed with fresh Q$_{5\% \text{ FBS}}$-medium. The co-culture supernatant was added at a ratio of 1:10 in Q$_{5\% \text{ FBS}}$-medium. The set up was incubated for either five hours or 20 hours in a cell culture incubator. Following incubation, the cells were washed once with 100 µl sterile PBS. After that, the cells were fixed in 4% paraformaldehyde prepared in PBS at room temperature for 20 minutes. The cells were then blocked with blocking solution (5% serum from species that the secondary antibody was raised) in 0.3% Triton X-100/PBS) for 30 minutes to reduce the background from the non-specific binding of antibody. Next, the blocking solution was removed by rapid flipping the plate and 50 µl of primary antibody prepared in blocker solution was added into each well and incubated for

overnight at 4°C. After that, the cells were washed three times with 150 µl PBS in each well and blocked as before. Then, 50 µl of HRP-conjugated secondary antibody diluted in blocking solution was added into each well and incubated in the dark for two hours at room temperature. The antibodies used in this assay are summarised in table 6-2. The cells were then washed as previous, before proceeding to colour development (see section 2.2.5.1).

Table 6-2: The summary of the blocking serum, primary andtibody and secondary antibody used in tHBEC intercellular junction cell based-ELISA.

Primary antibody		Secondary antibody		Blocking serum
Name	Dilution	Name	Dilution	
Goat anti-human ZO-1	1:200	Rabbit anti-Goat	1:1000	Rabbit
Mouse anti-human vinculin	1:400	Goat anti-Mouse	1:3000	Goat
Rabbit anti-human claudin-5	1:200	Goat anti-Rabbit	1:1000	Goat
Rabbit anti-human occludin	1:200	Goat anti-Rabbit	1:1000	Goat

6.2.2 Cell based-ELISA for ICAM-1

In order to determine whether tHBEC were activated by inflammatory mediators released by endothelial cells in response to sequestration, ICAM-1 was detected and measured using cell based-ELISA. tHBEC in 96 well plate were treated with the co-culture supernatants for 20 hours as described in section 6.2.1. Following the 20 hours of treatment, the medium was

removed by aspiration and the plate were subjected to cell-based ELISA protocol as in section 2.2.5.1.

6.2.3 Measurement of tHBEC viability.

In order to determine whether BBB disruption was a reflection of cell death caused by soluble factors in the co-culture supernatants, a viability assay was performed. The tHBEC were grown to confluence in a 96 well plate and treated with co-culture supernatants for 20 hours as described in section 6.2.1. Following the 20-hour incubation, 100 µl of the medium were replaced with 20 µl of reagents and incubated for another 2 hour, as per manufacturer instruction. The change in the colour of the active reagent, MTS (3-(4,5-dimethylthiazol-2-yl)-5-(3-carboxymethoxyphenyl)-2-(4-sulfophenyl)-2H-tetrazolium) to the soluble formazan was measured at 490 nm using the MultiScan+ plate reader.

6.3 Results.

6.3.1 Modulation of tHBEC intercellular junction proteins in response to co-culture supernatants.

Changes in the expression of occludin, claudin-5, ZO-1 and vinculin in response to the co-culture supernatants was measured at two different time points following exposure, 5 hours (figure 6-1) and 20 hours (figure 6-2). The treatment with PRBC-tHBEC co-culture supernatant for five hours caused a slight reduction of tHBEC occludin, but this was not statistically significant compared to control co-culture supernatant ($P > 0.05$) and uRBC-tHBEC co-culture supernatant ($P > 0.05$) (figure 6-1A). Both claudin-5 and ZO-1 expression were significantly reduced following treatment with PRBC-tHBEC co-culture supernatant for 5 hours, compared to control co-culture supernatant or uRBC-tHBEC co-culture supernatant (figure 6-1B and 6-1C). In contrast, vinculin expression was significantly increased in response to PRBC-tHBEC co-culture supernatant for five hours compared to the treatment with control co-culture supernatant or uRBC-tHBEC co-culture supernatant (figure 6-1D). It is important to note that whilst the changes in claudin-5, ZO-1 and Vinculin were significant, the changes were small in magnitude.

The modulation in the level of tHBEC monolayer junction proteins (claudin-5, ZO-1 and vinculin) in response to the 20 hours incubation with co-culture supernatant were on the whole opposite to that observed at 5 hours, in response to PRBC-tHBEC co-culture supernatants. Contrary to the data from 5 hours treatment with PRBC-tHBEC co-culture supernatant, incubation with the same co-culture supernatants for 20 hours caused slight increase to the expression of claudin-5 and ZO-1, but statistically significant compared to the treatment with uRBC-tHBEC co-culture supernatant (figure 6-2 B and 6-2C). Unlike the other intercellular junction proteins analysed, the expression of occludin was significantly

reduced following 20 hours treatment with PRBC-tHBEC co-culture supernatant compared to the treatment with control co-culture supernatant (figure 6-2A). The reduction was more pronounced than at the 5-hour time point. Vinculin expression was markedly reduced following 20 hours treatment with PRBC-tHBEC co-culture supernatant compared to the treatment with control co-culture supernatant of uRBC-tHBEC co-culture supernatant (figure 6-2D). This was contrary to the effect of the same treatment at 5-hour time point.

In conclusion, the changes in the expression of intercellular junction proteins occludin, claudin-5, ZO-1 and vinculin following treatment of tHBEC with PRBC-tHBEC co-culture supernatant was variable and dependent on the treatment period, i.e., acute short term *vs* chronic response. The effects of PRBC-tHBEC co-culture supernatant on the expression of these junction proteins are summarised in table 6-3.

Table 6-3: The differential regulation profile of tHBEC junction protein in response to the PRBC-tHBEC co-culture supernatant compared to control co-culture supernatant.

Junctional proteins	Time point			
	5 hours	Significance to control	20 hours	Significance to control
ZO-1	↓	***	↑	***
Occludin	↓	NS	↓	***
Claudin-5	↓	***	↑	***
Vinculin	↑	***	↓	***
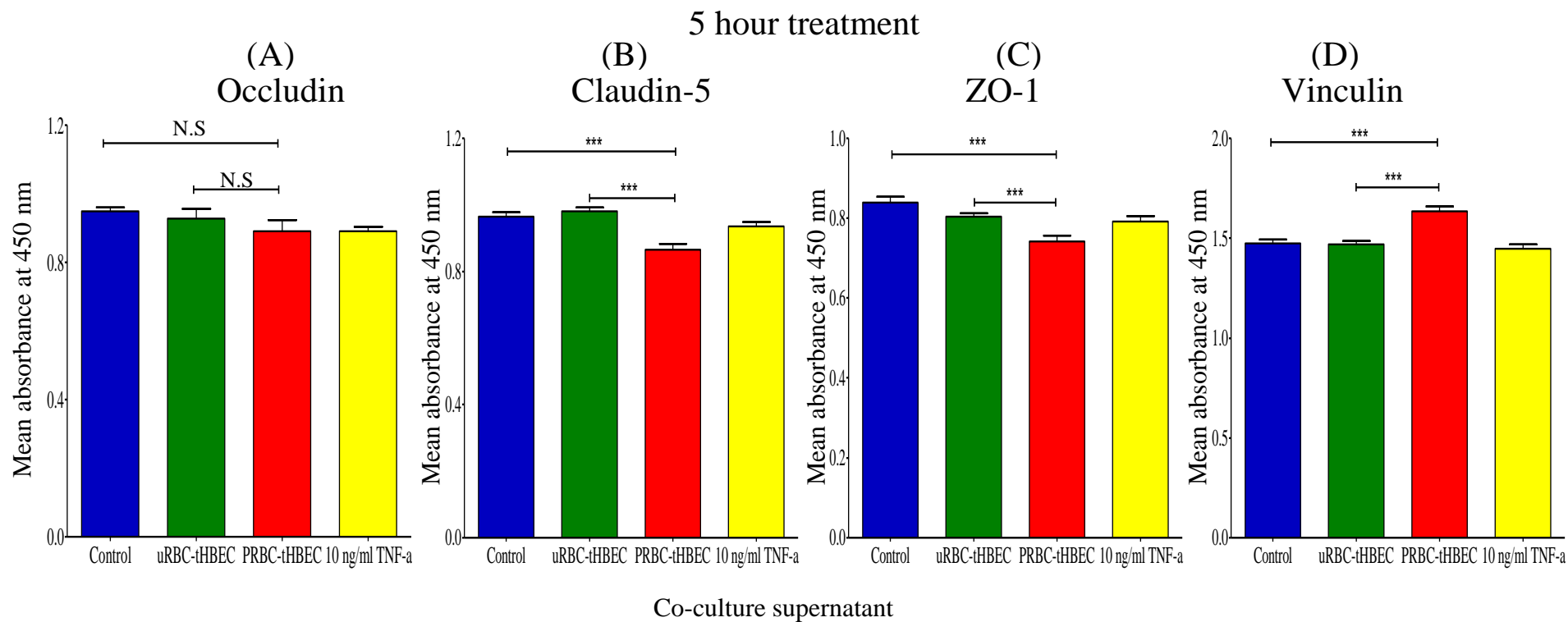
Figure 6-1: The modulation in the tHBEC junction proteins following five hours of treatments.

The mean absorbance from cell-based ELISA for (A) occludin, (B) claudin-5, (C) ZO-1 and (D) vinculin after five hours treatment with

supernatants from 10 separate co-culture experiments (n = 10, *** is $P \leq 0.001$).
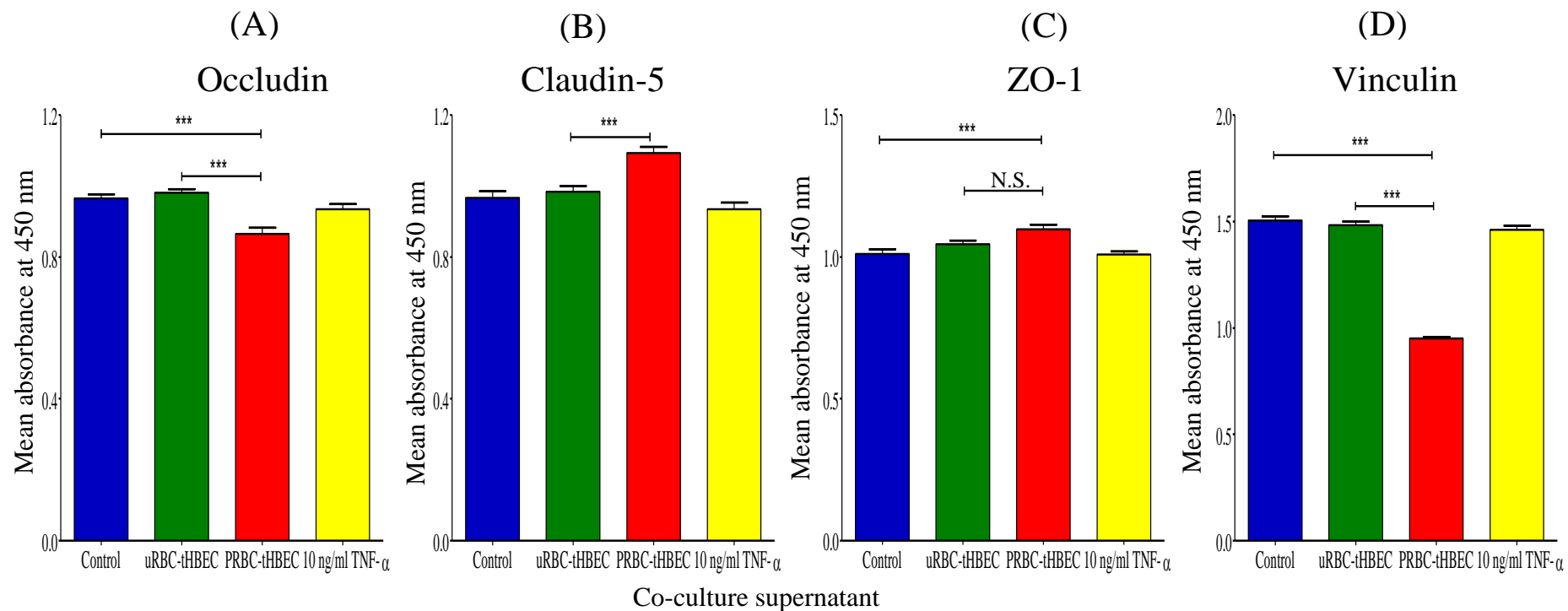
Figure 6-2: The modulation in the tHBEC junction proteins following twenty hours of treatments.

The mean absorbance from cell-based ELISA for (A) occludin, (B) claudin-5, (C) ZO-1 and (D) vinculin after twenty hours treatment with

supernatants from 10 separate co-culture experiments (n = 10, ** is P ≤ 0.01 and *** is P ≤ 0.001).

6.3.2 Activation of tHBEC in response to PRBC-tHBEC co-culture supernatant.

Interestingly, ICAM-1 expression was significantly increased in the tHBEC cultured with PRBC-tHBEC co-culture supernatant compared to either uRBC-tHBEC co-culture supernatant ($P \leq 0.001$), or control co-culture supernatant ($P \leq 0.001$) (figure 6-3). This was a consistent observation in ten separate co-culture experiments. This suggests that the PRBC-tHBEC co-culture supernatant contains soluble factors that can activate the fresh tHBEC monolayer.
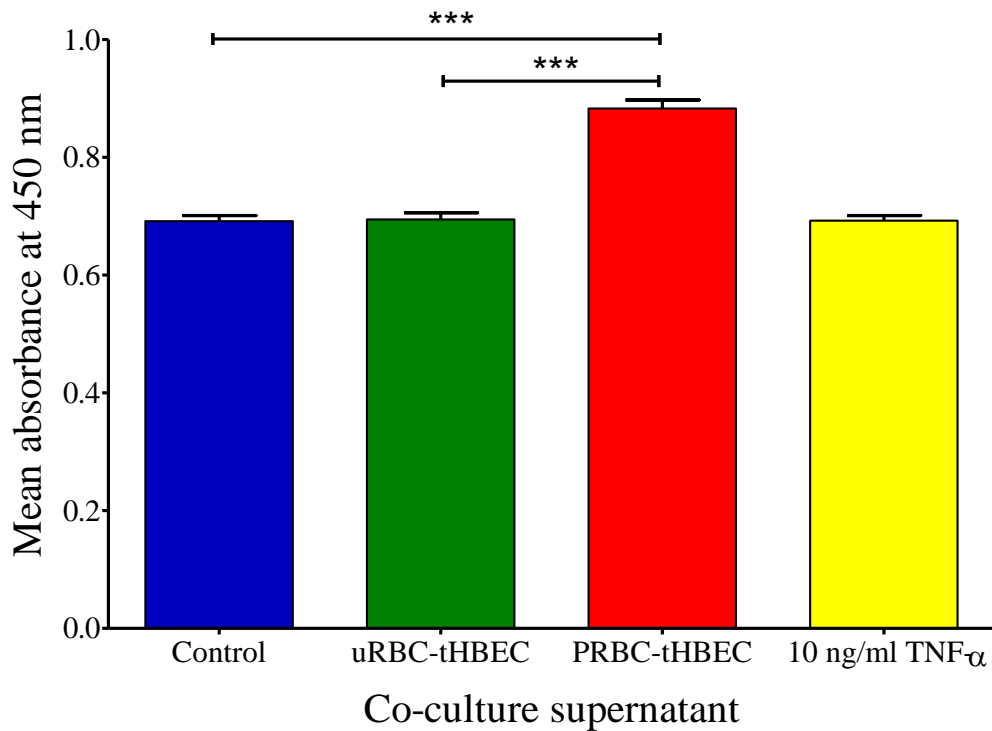
Figure 6-3: tHBEC ICAM-1 in response to co-culture supernatant.

The graph showing means absorbance from cell based-ELISA for ICAM-1 using co-culture supernatant from 10 separate experiments. The experiment was done in duplicate.

*** is $P \leq 0.001$ compared to control and uRBC-tHBEC co-culture supernatant.

6.3.3　The effect of co-culture supernatant on the tHBEC viability

There was no change in viability of tHBEC following 20 hours incubation with 1:10 dilution of co-culture supernatant in $Q_{5\% FBS}$-medium, as measured using the MTS viability assay (Figure 6-4). Statistical analysis using 1 way ANOVA showed no significant different between the treatments (P> 0.05, n = 15). This suggests that the reduction in the tHBEC electrical resistance (chapter 4) and increase in the tHBEC permeability to FITC-dextran (chapter 5) is not due to any toxic effect of the co-culture supernatants.
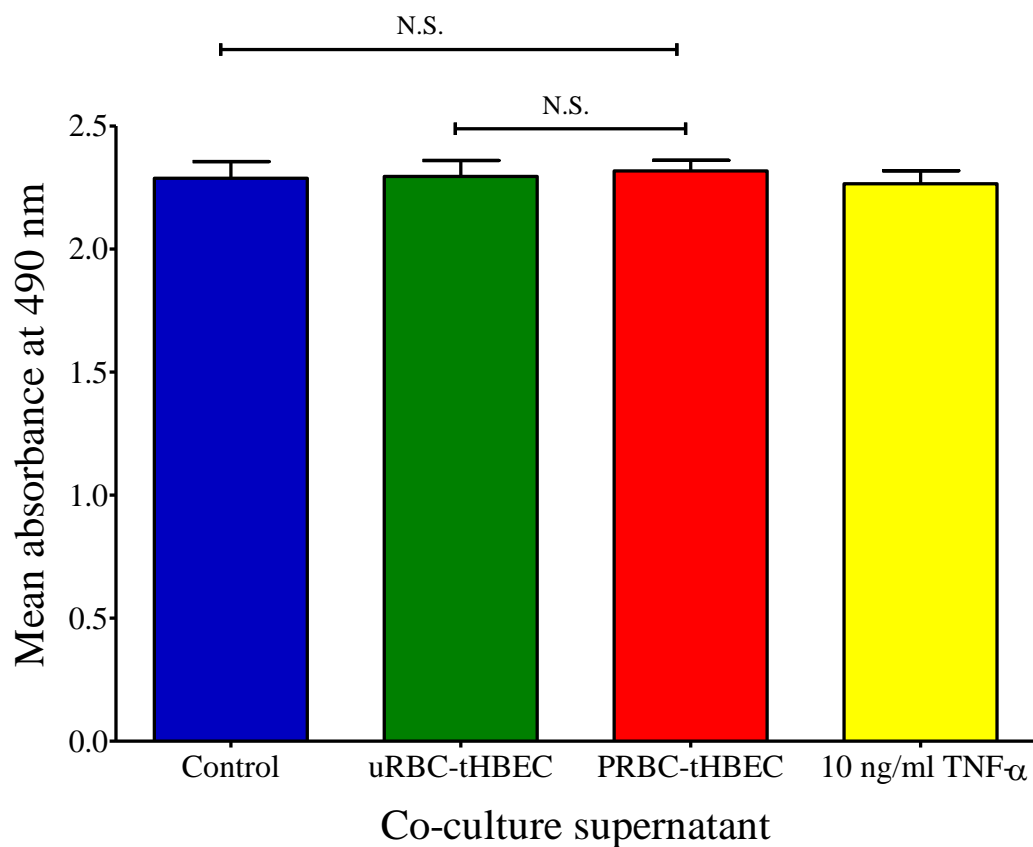
Figure 6-4:tHBEC viability in response to co-culture supernatant.

The graph shows the average absorbance of viability assay using co-culture supernatant from five separate experiment. Each supernatant was tested in duplicate. The differences between treatments were statistically analysed using 1 way-ANOVA, with Turkey's post-hoc test.

6.4 Discussion

The PRBC-tHBEC co-culture supernatant was shown to cause reduction in the integrity (chapter 4) and increase in the permeability (chapter 5) of the tHBEC monolayer. These effects were hypothesized to occur as a result to the loss of tHBEC monolayer intercellular junction proteins in response to the soluble factors in the PRBC-tHBEC co-culture supernatant, as loss in the TJP are the characteristic of the post mortem brain tissue of CM (reviewed in chapter 1). In this chapter, the effects of the PRBC-tHBEC co-culture supernatant on the tHBEC monolayer intercellular junction proteins were investigated.

There are variable changes in the intercellular junction proteins expression in response to PRBC-tHBEC co-culture supernatant. Changes in the expression of vinculin were the most notable, following either short term (5 hour) or long-term exposure (20 hour) to PRBC-tHBEC co-culture supernatant. Treatment with PRBC-tHBEC co-culture supernatant for 5 hours decrease the expression of TJP (occludin, claudin-5 and ZO-1) but increase the expression of AJP vinculin. The expression of vinculin however, markedly decreased following 20 hours treatment with PRBC-tHBEC co-culture supernatant. This may suggest the involvement of vinculin in an acute survival response initially when tHBEC are exposed to the soluble factors in PRBC-tHBEC co-culture supernatant to maintain the BBB integrity but being damaged after prolonged exposure to the PRBC-tHBEC co-culture supernatant.

Increase in the expression of claudin-5 and ZO-1 following 20 hours treatment with PRBC-tHBEC co-culture may represent the recovery of tHBEC. Similar observation was seen in the immunohistochemical analysis of the post mortem brain section from CM patients where the loss in BBB endothelial cell TJP cannot always be seen in the sequestered

vessel, suggesting the damage to the BBB are reversible (Brown et al., 1999). Additionally, the recovery of these TJP may also explain the partial recovery seen in the previous ECIS studies where the TEER increases after 20 hours of treatments with PRBC-tHBEC co-culture supernatant (data not shown).

In conclusion, the PRBC-tHBEC co-culture supernatant is able to activate the endothelial cells to increase the expression of ICAM-1 and lead to the variable changes in the expression of tHBEC intercellular junction proteins. The cell based ELISA assay provides limited information about alteration to intercellular junction proteins. This technique only quantifies the total amount of target intercellular junction proteins. Since the observed changes in intercellular junction proteins in this experiment are relatively small, it would be desirable to extend the study to determine the localisation of the intercellular junction proteins in adjacent cells of the tHBEC monolayer, using immunofluorescence microscopy. Previous studies in our laboratory by using immunofluorescence assay (data not shown), showed that direct exposure of HUVEC to PRBC caused redistribution of vinculin away from the intercellular junction suggesting that multiple mechanism are involved in TJP regulation.

CHAPTER SEVEN: GENERAL DISCUSSION.

Chapter 7: General discussion

Previous studies in our laboratory using HUVEC have demonstrated that endothelial cells can be activated by PRBC. The current study, firstly, investigates the effect of PRBC on brain endothelial cells, and secondly, elucidates the mechanisms secondary to the initial sequestration. It is well established that the endothelium is activated in brain microvessels in CM (reviewed in introduction) and has the capability of producing a plethora of inflammatory mediators. Our aim was to investigate whether specific inflammation mediators are expressed by tHBEC on activation by PRBC, which could contribute directly or indirectly to BBB disruption. This is the first study looking at what is released by brain endothelial cells in response to PRBC sequestration and its potential role in mediating BBB damage.

The initial studies explored whether the prolonged exposure to PRBC can activate tHBEC to upregulate the expression of inflammatory mediators that were reported increased *in vivo* cases of CM. As shown in chapter 3 the activation of tHBEC by PRBC was found to upregulate the expression of ICAM-1 and increase the secretion of MCP-1 and IL-8. These molecules are denoted as endothelial cell activation markers and although they show non-specific activation, they have all been demonstrated either in post mortem CM tissue or in serum or CSF of CM patients (discussed in chapter 3). Interestingly, besides their significant role in inflammatory responses, both MCP-1 and IL-8 can have an effect on vascular permeability. High concentration of MCP-1 and IL-8 have been demonstrated to increase the brain endothelial cells monolayer permeability by down regulating expression of tight junction proteins including occludin, claudin-5 and ZO-1 (Stamatovic et al., 2003a, Yu et al., 2013).

Additionally, the same activation also increased the level of soluble ICAM-1 (sICAM-1) (data not shown, courtesy of Attish Patel (Medical School project student)). These finding are in line with most of the cerebral malaria studies where the upregulation of ICAM-1 is not only seen in the post mortem brain section of CM patients (Brown et al., 1999, Dorovini-Zis et al., 2011), but also in the serum (Conroy et al., 2010) and CSF (Brown et al., 2000). This might suggest that upon infection with malaria the PRBC activates the endothelial cells to upregulate both surface ICAM-1 and sICAM-1. It is believed that ICAM-1 is capable of in amplifying sequestration due to its pro-adhesive properties (Chakravorty et al., 2008). Interestingly, *in vitro,* the level of ICAM-1 was also found to be slightly upregulated by tHBEC after co-cultured with PRBC-tHBEC co-culture supernatants (Chapter 6). This shows that co-culture supernatant may contain soluble factors that can indirectly activate the tHBEC.

Besides the upregulation of inflammatory mediators mentioned above, the activation of tHBEC by PRBC also upregulates the release of the proteases namely ADAMTS-4, ADAMTS-1, MMP-2 and MMP-9 into the supernatant (chapter 3). These proteases may have a potential involvement in BBB damage in CM by either degradation of intercellular junction proteins (TJP and AJP) or degradation of extracellular matrix (ECM) proteins. For instance, the intercellular junction proteins occludin, claudin-5 and ZO-1 were shown to be substrates for MMP-2 and MMP-9 (Feng et al., 2011, Qiu et al., 2011, Liu et al., 2012). Feng et al. (2011) demonstrated that the upregulation of the secretion of MMP-2 and MMP-9 by leukaemic cells could mediate the degradation of occludin, claudin-5 and ZO-1 on brain endothelial cells, thus disrupting the BBB. This BBB damage was inhibited by the MMP inhibitor GM6001, protecting mice against CNS leukaemia. In the case of CM, the

upregulation of MMP-2 and MMP-9 has been demonstrated in multiple studies including the post-mortem examination on serum and CSF from CM patients. The upregulation of these MMP also consistently seen in mouse model of CM, although it is well acknowledged that leukocyte extravasation which is common in mouse CM are absent in human CM (Van den Steen et al., 2006, van der Heyde et al., 2006).

ADAMTS-1 and ADAMTS-4 are interesting proteases, but to date they have not been linked to CM. ADAMTS-1 does not only show proteolytic activity, but also demonstrates anti-angiogenic activity. This has been demonstrated in a study using chick chorioallantoic membrane assays where vascularisation was inhibited with the addition of ADAMTS-1 (Vázquez et al., 1999). The study also found that the anti-angiogenic property of ADAMTS-1 is more potent than either endostatin or thrombospondin-1 (TSP-1). Interestingly, both ADAMTS-1 and ADAMTS-4 has the capability of binding to CD36 on endothelial cells through TSP-1 domain (Iruela-Arispe et al., 1999). Although CD36 is not expressed by BBB endothelial cells, CD36 was present colocalised with sequestered PRBC in CM post-mortem tissue. Thus, both ADAMTS-1 and ADAMTS-4 could potentially be localised at the BBB endothelial cells, where damage to BBB could occur. This interaction may support the local accumulation of the ADAMTS-1 and ADAMTS-4 proteases on the BBB. The damage could be mediated by a combination their proteolytic digestion of ECM proteins or maintaining the damage by inhibiting any possibility of vascular repair due to their anti-angiogenic effect. The involvement of these proteases in several CNS associated diseases was discussed in chapter 1.

Once it became clear that tHBEC express increased levels of these candidate proteins in response to PRBC, we wanted to assess whether these molecules could contribute to BBB

disruption, focusing mainly on the proteases mentioned above. The transendothelial electrical resistance (integrity) of tHBEC monolayer was decreased by the PRBC-tHBEC co-culture supernatants (chapter 4). Permeability studies demonstrated that the reduction in electrical resistance translates to increased permeability of the tHBEC monolayer allowing the passage of 40 kDa FITC-dextran (chapter 5). Interestingly, this effect was partially inhibited by the addition of GM6001. The increase in the tHBEC monolayer permeability to FITC-dextran caused by PRBC-tHBEC co-culture supernatant was partially inhibited by the addition of rhTIMP-3, the internal regulator for MMP and ADAMTS-4. These studies demonstrate that prolonged exposure of tHBEC to PRBC produces several soluble factors that can induce the reduction in integrity and increase in the permeability of tHBEC monolayer, and these soluble factors are potentially proteases that are sensitive to the inhibitors GM6001 and rhTIMP-3.

These data suggest that the integrity of the endothelial cell monolayer is compromised as a secondary response to the interaction between PRBC and endothelial cell. This may enhance the BBB damage caused directly by PRBC. Tripathi et al. (2007) demonstrated that the integrity of human brain microvascular endothelial cell monolayer is decreased when the monolayer is exposed directly to trophozoite stage *Plasmodium falciparum* at a high parasitaemia. This supports the observation of perivascular leakage of fibrinogen in vessels containing sequestered PRBC (chapter 1). However, it is important to note that this is also seen in vessels that are devoid of sequestered parasites. Thus, the impairment of the BBB structure might also be reversible, which could explain the transient neurological manifestation among CM patients with a high percentage of recovery (Adams et al., 2002). It is, however, important to note that the permeability assay in this thesis was

done within 6 hours of the treatment, which may only represent the acute damage caused by PRBC-tHBEC co-culture supernatant.

Since the loss in the BBB integrity appears to have a positive association with the loss of intercellular junction proteins as demonstrated in majority of CM post-mortem studies, we also investigated the effect of the PRBC-tHBEC co-culture supernatant on the expression of the tHBEC junctional proteins namely occludin, claudin-5, ZO-1 and vinculin (chapter 6). Our data showed differential regulation of these intercellular junction proteins following 5 hours and 20 hours treatment with PRBC-tHBEC co-culture supernatant (discussed in chapter 6). This suggests that these junctional proteins react differently towards soluble factors in the PRBC-tHBEC co-culture supernatant.

Cumulative data from chapters 4 and chapter 5 has provide evidence to support the potential involvement of proteases in causing damage to tHBEC monolayer, in particular, the candidate proteases found upregulated in the PRBC-tHBEC co-culture supernatant (chapter 3). However, the mechanism for the damage is unclear. With more emphasis on the candidate proteases, it is generally acknowledged that these proteases can interact with many different substrates. Many of the identified substrates for these proteases were found to exist in the BBB.

Besides the degradation of the tight junction proteins of the BBB, these proteases may also cause damage to the BBB by degrading the ECM proteins, such as neurocan, versican and aggrecan as discussed in chapter 1. Although there is no direct evidence for the breakdown of the brain ECM in the post-mortem study of CM, it is widely known that the ECM forms the basal layer between the BBB endothelium and astrocytes-end-feet. Thus,

any degradation of these ECM may alter the integrity of BBB as seen in the remodelling process in the brain (Rauch, 2004).Various studies have demonstrated the ability of MMP-2, MMP-9, ADAMTS-1 and ADAMTS-4 to degrade some of these major brain ECM proteins. For instance, MMP-2 and MMP-9 can degrade neurocan and collagen which forms a support between brain link proteins to the hyaluronan, a support molecule during brain development (Rauch, 2004). ADAMTS-1 and ADAMTS-4 are capable of proteolytically cleaving versican, aggrecan and brevican (Rauch, 2004), which are also ECM proteins essential to support the structure of the brain. The increase in the proteolytic activity of ADAMTS-4 had a positive association with the glioma cells infiltrative activity which was inhibited by TIMP-1 and TIMP-2 (Matthews et al., 2000).

Although our data suggest the potential involvement of ADAMTS-4, ADAMTS-1, MMP-2 and MMP-9 by the inhibition effect of GM6001 and rhTIMP-3, it is desirable to specifically inhibit these proteases individually by means of SiRNA in future studies (the use of SiRNA to block the expression of ADAMTS-4 by endothelial cells is currently being optimised in our lab). Since these proteases are also regulated internally by physiological inhibitors such TIMP-1, TIMP-2 and TIMP-3, the balance between these inhibitors and the candidate proteases in should also be considered. It is important to remember that only partial inhibition of BBB damage was seen when GM6001 and rhTIMP-3 were used in the treatment, suggesting the potential involvement of other soluble factors such as MCP-1 and IL-8 as mentioned earlier. Thus, blocking the function of these cytokines in future studies may also provide some evidence on the potential role of these cytokines in mediating BBB damage in CM.

The insight to the involvement of these proteases in the BBB damage mechanism in CM may provide some clues for the future development in CM therapeutics. However, some of the proteases that were upregulated in the PRBC-tHBEC co-culture supernatant in this study are not suitable for drug targetting. For example, MMP-2 and MMP-9 are both involved in physiological processes in human such as angiogenesis. The prolonged treatment with a MMP inhibitor such as Marimastat may also cause adverse effects to the body (Coussens et al., 2002). In addition, the inhibition of MMP-9 may not be the best target as there was no protection against CM when the MMP-9 knockout mice were infected with *Plasmodium berghei* ANKA, therefore suggesting that the role of MMP-9 is not essential in causing BBB damage (Van den Steen et al., 2006). Thus, the ADAMTS family of proteases might be the best target candidate especially due to its narrow spectrum of substrates with high specificity compared to MMP (Tortorella et al., 2009).

In conclusion, this thesis has demonstrated that the breakdown of the BBB might be initiated by many factors, which was explained in the three models of cerebral malaria pathogenesis (chapter 1). The primary factors for the alteration in BBB structure and function is the sequestration of PRBC in the brain microvasculature. This interaction initiates subsequent signalling, including an increase in the release of ADAMTS-1, ADAMTS-4, MMP-2, MMP-9, IL-8 and MCP-1. All of these soluble factors can potentially compromise the normal function of the BBB. The potential mechanism of damage investigated in this thesis is summarised in figure 7-1.
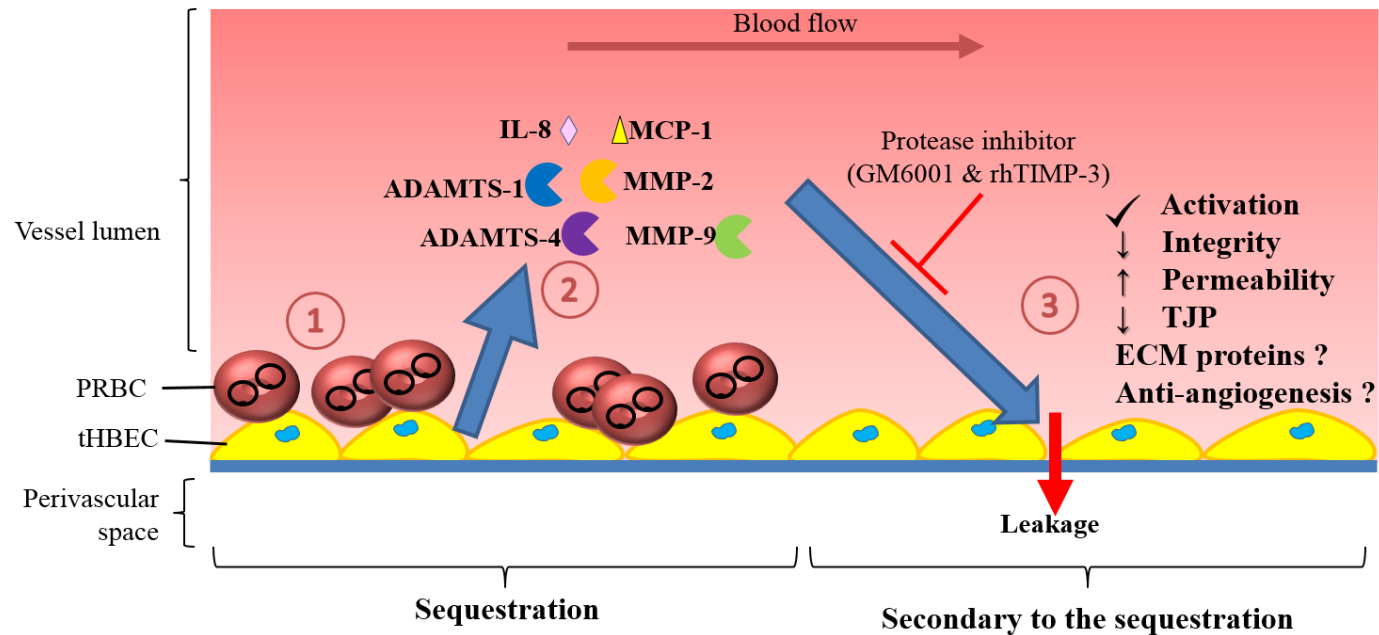
Figure 7-1: The potential involvement of MMPs and ADAMTS family members in causing BBB damage as the secondary to the sequestration.

Firstly, the interaction with PRBC activates the brain microvascular endothelial cells to release the inflammatory mediators (MCP-1 and IL-8) and proteases (ADAMTS-4, ADAMTS-1, MMP-2 and MMP-9) into luminal space of BBB. These soluble factors subsequently induce the activation, reduction of integrity, and increase of permeability of endothelial cells monolayer at vicinity. This event may lead to the breakdown of BBB. Our data demonstrates that the leakages could be inhibited by the addition of GM6001 and rhTIMP-3., suggesting the potential involvement of upregulated proteases in PRBC-tHBEC co-culture supernatant.

7.1 Future Studies

The effects of the co-culture supernatant on the brain microvascular endothelial cell monolayer integrity, permeability and intercellular junction proteins was successfully examined in this thesis. Yet, many questions remain unanswered. This thesis uses a simple model of BBB, looking at the tHBEC component of the BBB only. However, it is important to address all the cellular components of the BBB i.e. (i) endothelial cells, (ii) astrocytes and (iii) pericytes. Thus, this study must be developed using a more appropriate model that closely represents the BBB.

7.1.1 Which candidate proteases have significant role in causing BBB damage in CM?

To validate the roles of MMP-2, MMP-9, ADAMTS-1 and ADAMTS-4 either alone or in combination, it would be desirable to perform some inhibitory studies using siRNA. This is a more specific approach than the chemical inhibitors used in these studies. Most chemical inhibitors of proteases available have more than one substrate making it impossible to delineate the role of each individual protease expressed in response to PRBC, in this project.

7.1.2 Are the proteases released luminally or abluminally? Are astrocytes underlying the brain endothelial cells affected by these proteases?

To answer these question, systematic comparison of the soluble factors in the apical (luminal space) and basolateral (perivascular space) chambers of hanging cell culture insert (or transwell) is needed. Additionally, currently it is not known whether the released proteases can induce activation of astrocytes. This is very important, as the activation of astrocyte or astrogliois one of the major markers of inflammation in the brain that could lead to the brain damage. This also probably causes the long term neurological impairment in surviving CM

patients. To answer this, a three dimensional culture system is desirable (Naik and Cucullo, 2012).

Finally, this *in-vitro* characterisation of the potential involvement of proteases in the BBB damage needs to be further validated with a systemic model (animal), or supported with clinical evidence to get a better understanding of the mechanisms involved. This characterisation is also important in providing future direction for alternative adjunct therapies for cerebral malaria.

Narrated Abu Hurairah (رضي الله عنه) that the Prophet Muhammad (ﷺ) said:

مَا أَنْزَلَ اللَّهُ دَاءً إِلاَّ أَنْزَلَ لَهُ شِفَاءً

"There is no disease that Allah has sent down except that He also has sent down its

treatment."

[Sahih al-Bukhari 5678; Book 76, Hadith 1]

Appendices

8.1 Appendix A: The tHBEC identification
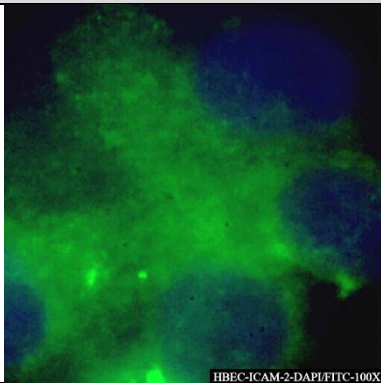
Image	Description
	Immunofluorescence of ICAM-1 (Stained with FITC conjugated antibody) on tHBEC. The nucleus was stained blue with DAPI. Image taken under x 100 objective magnification.
	Immunofluorescence of vWF (Stained with FITC conjugated antibody) on tHBEC. vWF found in the granule form, inside the cytoplasm. The nucleus was stained blue with DAPI. Image taken under x 100 objective magnification.
	Immunofluorescence of vinculin (Stained with FITC conjugated antibody) on tHBEC. The nucleus was stained blue with DAPI. Image taken under x 100 objective magnification.
	Dil-Ac-LDL uptake by tHBEC. Image taken using rhodamine filter, at x40 objective magnification.
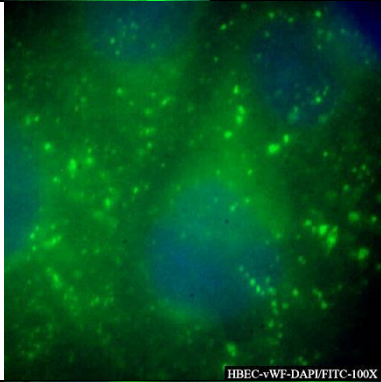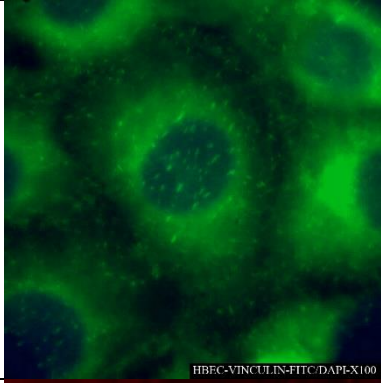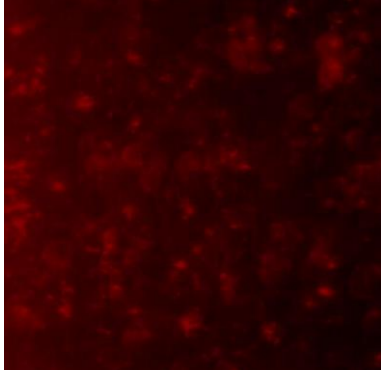
8.2 Appendix B: Appearance of PRBC

The microscopy appearance of the uRBC (A1-A3) and PRBC (B1-B3) before and after plasmogel enrichment and, after the co-culture experiments.

	Before plasmogel enrichment	After plasmogel enrichment	After co-culture experiment
A. uRBC	1	2	3
B. PRBC	1	2	3
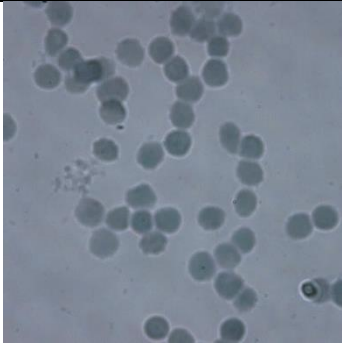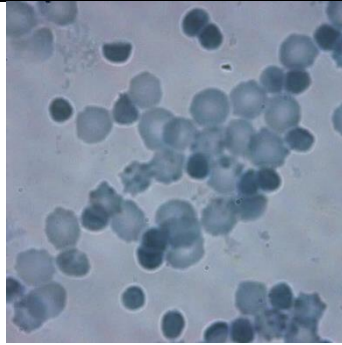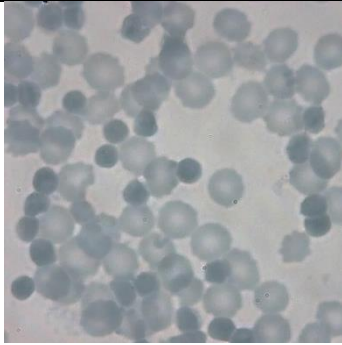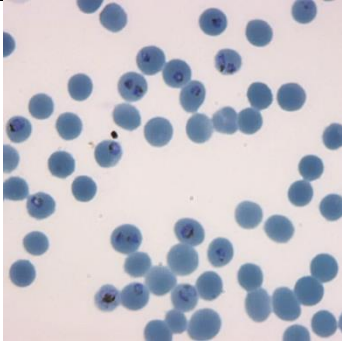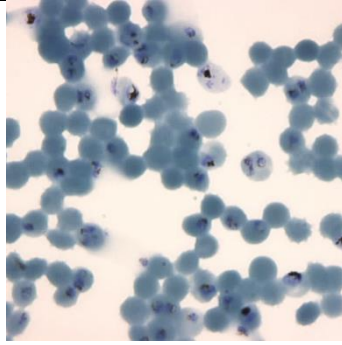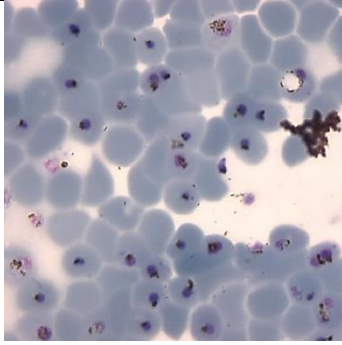
Note: All images were taken using inverted compound microscope at 100 X objective magnification. The images showed are representation from various co-culture experiments.

References

ABBOTT, N. J., RÖNNBÄCK, L. & HANSSON, E. 2006. Astrocyte–endothelial interactions at the blood–brain barrier. *Nature Reviews Neuroscience,* 7**,** 41-53.

ABE, K. & TAKEICHI, M. 2008. EPLIN mediates linkage of the cadherin–catenin complex to F-actin and stabilizes the circumferential actin belt. *Proceedings of the National Academy of Sciences,* 105**,** 13-19.

ADAMS, S., BROWN, H. & TURNER, G. 2002. Breaking down the blood-brain barrier: signaling a path to cerebral malaria? *Trends Parasitol,* 18**,** 360-6.

ALÓN, R., HAMMER, D. A. & SPRINGER, T. A. 1995. Lifetime of the P-selectin-carbohydrate bond and its response to tensile force in hydrodynamic flow. *Nature,* 374**,** 539-542.

ANDRÁS, I. E., PU, H., TIAN, J., DELI, M. A., NATH, A., HENNIG, B. & TOBOREK, M. 2005. Signaling mechanisms of HIV-1 Tat-induced alterations of claudin-5 expression in brain endothelial cells. *Journal of Cerebral Blood Flow & Metabolism,* 25**,** 1159-1170.

ANGST, B. D., MARCOZZI, C. & MAGEE, A. I. 2001. The cadherin superfamily: diversity in form and function. *Journal of Cell Science,* 114**,** 629-641.

ARMAH, H. B., WILSON, N. O., SARFO, B. Y., POWELL, M. D., BOND, V. C., ANDERSON, W., ADJEI, A. A., GYASI, R. K., TETTEY, Y. & WIREDU, E. K. 2007. Cerebrospinal fluid and serum biomarkers of cerebral malaria mortality in Ghanaian children. *Malaria journal,* 6**,** 147.

BALLABH, P., BRAUN, A. & NEDERGAARD, M. 2004. The blood–brain barrier: an overview: structure, regulation, and clinical implications. *Neurobiology of disease,* 16**,** 1-13.

BAMFORTH, S. D., KNIESEL, U., WOLBURG, H., ENGELHARDT, B. & RISAU, W. 1999. A dominant mutant of occludin disrupts tight junction structure and function. *Journal of Cell Science,* 112**,** 1879-1888.

BARAMOVA, E. N., BAJOU, K., REMACLE, A., L'HOIR, C., KRELL, H. W., WEIDLE, U. H., NOEL, A. & FOIDART, J. M. 1997. Involvement of PA/plasmin system in the processing of pro-MMP-9 and in the second step of pro-MMP-2 activation. *FEBS Letters,* 405**,** 157-162.

BARNWELL, J., ASCH, A., NACHMAN, R., YAMAYA, M., AIKAWA, M. & INGRAVALLO, P. 1989. A human 88-kD membrane glycoprotein (CD36) functions in vitro as a receptor for a cytoadherence ligand on Plasmodium falciparum-infected erythrocytes. *Journal of Clinical Investigation,* 84**,** 765.

BARUCH, D. I., PASLOSKE, B. L., SINGH, H. B., BI, X., MA, X. C., FELDMAN, M., TARASCHI, T. F. & HOWARD, R. J. 1995. Cloning the P. falciparum gene encoding PfEMP1, a malarial variant antigen and adherence receptor on the surface of parasitized human erythrocytes. *Cell,* 82**,** 77-87.

BAZZONI, G. & DEJANA, E. 2004. Endothelial Cell-to-Cell Junctions: Molecular Organization and Role in Vascular Homeostasis. *Physiological Reviews,* 84**,** 869-901.

BEESON, J. G. & BROWN, G. V. 2004. Plasmodium falciparum–Infected Erythrocytes Demonstrate Dual Specificity for Adhesion to Hyaluronic Acid and Chondroitin Sulfate A and Have Distinct Adhesive Properties. *Journal of Infectious Diseases,* 189**,** 169-179.

BERENDT, A., SIMMONS, D., TANSEY, J., NEWBOLD, C. & MARSH, K. 1989. Intercellular adhesion molecule-1 is an endothelial cell adhesion receptor for Plasmodium falciparum. *Nature,* 341**,** 57-59.

BISWAS, A. K., HAFIZ, A., BANERJEE, B., KIM, K. S., DATTA, K. & CHITNIS, C. E. 2007. Plasmodium falciparum uses gC1qR/HABP1/p32 as a receptor to bind to vascular endothelium and for platelet-mediated clumping. *PLoS pathogens,* 3**,** e130.

BOIVIN, M. J., BANGIRANA, P., BYARUGABA, J., OPOKA, R. O., IDRO, R., JUREK, A. M. & JOHN, C. C. 2007. Cognitive impairment after cerebral malaria in children: a prospective study. *Pediatrics,* 119**,** e360-e366.

BOND, M., FABUNMI, R. P., BAKER, A. H. & NEWBY, A. C. 1998. Synergistic upregulation of metalloproteinase-9 by growth factors and inflammatory cytokines: an absolute requirement for transcription factor NF-κB. *FEBS Letters,* 435**,** 29-34.

BORING, L., GOSLING, J., CLEARY, M. & CHARO, I. F. 1998. Decreased lesion formation in CCR2−/− mice reveals a role for chemokines in the initiation of atherosclerosis. *Nature,* 394**,** 894-897.

BROWN, H., CHAU, T., MAI, N., DAY, N., SINH, D., WHITE, N., HIEN, T., FARRAR, J. & TURNER, G. 2000. Blood–brain barrier function in cerebral malaria and CNS infections in Vietnam. *Neurology,* 55**,** 104-111.

BROWN, H., HIEN, T. T., DAY, N., MAI, N. T., CHUONG, L. V., CHAU, T. T., LOC, P. P., PHU, N. H., BETHELL, D., FARRAR, J., GATTER, K., WHITE, N. &

TURNER, G. 1999. Evidence of blood-brain barrier dysfunction in human cerebral malaria. *Neuropathol Appl Neurobiol,* 25**,** 331-40.

BROWN, H., ROGERSON, S., TAYLOR, T., TEMBO, M., MWENECHANYA, J., MOLYNEUX, M. & TURNER, G. 2001. Blood-brain barrier function in cerebral malaria in Malawian children. *Am J Trop Med Hyg,* 64**,** 207-13.

CALLAHAN, M. K., WILLIAMS, K. A., KIVISAKK, P., PEARCE, D., STINS, M. F. & RANSOHOFF, R. M. 2004. CXCR3 marks CD4+ memory T lymphocytes that are competent to migrate across a human brain microvascular endothelial cell layer. *J Neuroimmunol,* 153**,** 150-7.

CARLOS RODRíGUEZ-MANZANEQUE, J., WESTLING, J., THAI, S. N.-M., LUQUE, A., KNAUPER, V., MURPHY, G., SANDY, J. D. & IRUELA-ARISPE, M. L. 2002. ADAMTS1 cleaves aggrecan at multiple sites and is differentially inhibited by metalloproteinase inhibitors. *Biochemical and biophysical research communications,* 293**,** 501-508.

CDC. 2010. *The History of Malaria, an Ancient Disease* [Online]. 1600 Clifton Road, Atlanta, GA 30333, USA. Available: http://www.cdc.gov/malaria/about/history/ [Accessed 28 June 2013].

CHAITANYA, G. V., CROMER, W. E., WELLS, S. R., JENNINGS, M. H., COURAUD, P. O., ROMERO, I. A., WEKSLER, B., ERDREICH-EPSTEIN, A., MATHIS, J. M. & MINAGAR, A. 2011. Gliovascular and cytokine interactions modulate brain endothelial barrier in vitro. *J Neuroinflammation,* 8**,** 162.

CHAKRAVORTY, S., HUGHES, K. & CRAIG, A. 2008. Host response to cytoadherence in Plasmodium falciparum. *Biochemical Society Transactions,* 36**,** 221-228.

CHAKRAVORTY, S. J., CARRET, C., NASH, G. B., IVENS, A., SZESTAK, T. & CRAIG, A. G. 2007. Altered phenotype and gene transcription in endothelial cells, induced by Plasmodium falciparum-infected red blood cells: pathogenic or protective? *Int J Parasitol,* 37**,** 975-87.

CHAKRAVORTY, S. J. & CRAIG, A. 2005. The role of ICAM-1 in Plasmodium falciparum cytoadherence. *European Journal of Cell Biology,* 84**,** 15-27.

CHEN, Q., FERNANDEZ, V., SUNDSTRÖM, A., SCHLICHTHERLE, M., DATTA, S., HAGBLOM, P. & WAHLGREN, M. 1998. Developmental selection of var gene expression in Plasmodium falciparum. *Nature,* 394**,** 392-395.

CINES, D. B., POLLAK, E. S., BUCK, C. A., LOSCALZO, J., ZIMMERMAN, G. A., MCEVER, R. P., POBER, J. S., WICK, T. M., KONKLE, B. A., SCHWARTZ, B. S., BARNATHAN, E. S., MCCRAE, K. R., HUG, B. A., SCHMIDT, A.-M. &

STERN, D. M. 1998. Endothelial Cells in Physiology and in the Pathophysiology of Vascular Disorders. *Blood,* 91**,** 3527-3561.

CLARK, I., ROCKETT, K. & COWDEN, W. 1992. Possible central role of nitric oxide in conditions clinically similar to cerebral malaria. *The Lancet,* 340**,** 894-896.

CLARK, I. A. & ALLEVA, L. M. 2009. Is human malarial coma caused, or merely deepened, by sequestration? *Trends in Parasitology,* 25**,** 314-318.

CLARK, I. A. & COWDEN, W. B. 2003. The pathophysiology of falciparum malaria. *Pharmacol Ther,* 99**,** 221-60.

COHUET, A., HARRIS, C., ROBERT, V. & FONTENILLE, D. 2010. Evolutionary forces on Anopheles: what makes a malaria vector? *Trends in Parasitology,* 26**,** 130-136.

COLLIER, I. E., SAFFARIAN, S., MARMER, B. L., ELSON, E. L. & GOLDBERG, G. 2001. Substrate Recognition by Gelatinase A: The C-Terminal Domain Facilitates Surface Diffusion. *Biophysical Journal,* 81**,** 2370-2377.

COLLIER, I. E., WILHELM, S. M., EISEN, A. Z., MARMER, B. L., GRANT, G. A., SELTZER, J. L., KRONBERGER, A., HE, C. S., BAUER, E. A. & GOLDBERG, G. I. 1988. H-ras oncogene-transformed human bronchial epithelial cells (TBE-1) secrete a single metalloprotease capable of degrading basement membrane collagen. *Journal of Biological Chemistry,* 263**,** 6579-6587.

COMBES, V., ROSENKRANZ, A. R., REDARD, M., PIZZOLATO, G., LEPIDI, H., VESTWEBER, D., MAYADAS, T. N. & GRAU, G. E. 2004. Pathogenic role of P-selectin in experimental cerebral malaria: importance of the endothelial compartment. *The American journal of pathology,* 164**,** 781-786.

CONLAN, J. V., SRIPA, B., ATTWOOD, S. & NEWTON, P. N. 2011. A review of parasitic zoonoses in a changing Southeast Asia. *Vet Parasitol,* 182**,** 22-40.

CONROY, A. L., PHIRI, H., HAWKES, M., GLOVER, S., MALLEWA, M., SEYDEL, K. B., TAYLOR, T. E., MOLYNEUX, M. E. & KAIN, K. C. 2010. Endothelium-based biomarkers are associated with cerebral malaria in Malawian children: a retrospective case-control study. *PLoS One,* 5**,** e15291.

COUSSENS, L. M., FINGLETON, B. & MATRISIAN, L. M. 2002. Matrix metalloproteinase inhibitors and cancer—trials and tribulations. *Science,* 295**,** 2387-2392.

COWMAN, A. F. & CRABB, B. S. 2006. Invasion of Red Blood Cells by Malaria Parasites. *Cell,* 124**,** 755-766.

COX-SINGH, J., DAVIS, T. M. E., LEE, K.-S., SHAMSUL, S. S. G., MATUSOP, A., RATNAM, S., RAHMAN, H. A., CONWAY, D. J. & SINGH, B. 2008. Plasmodium knowlesi Malaria in Humans Is Widely Distributed and Potentially Life Threatening. *Clinical Infectious Diseases,* 46**,** 165-171.

CRABB, B. S., COOKE, B. M., REEDER, J. C., WALLER, R. F., CARUANA, S. R., DAVERN, K. M., WICKHAM, M. E., BROWN, G. V., COPPEL, R. L. & COWMAN, A. F. 1997. Targeted Gene Disruption Shows That Knobs Enable Malaria-Infected Red Cells to Cytoadhere under Physiological Shear Stress. *Cell,* 89**,** 287-296.

CROSS, A. K., HADDOCK, G., STOCK, C. J., ALLAN, S., SURR, J., BUNNING, R. A. D., BUTTLE, D. J. & WOODROOFE, M. N. 2006. ADAMTS-1 and -4 are up-regulated following transient middle cerebral artery occlusion in the rat and their expression is modulated by TNF in cultured astrocytes. *Brain Research,* 1088**,** 19-30.

CUZNER, M. L., GVERIC, D., STRAND, C., LOUGHLIN, A. J., PAEMEN, L., OPDENAKKER, G. & NEWCOMBE, J. 1996. The expression of tissue-type plasminogen activator, matrix metalloproteases and endogenous inhibitors in the central nervous system in multiple sclerosis: comparison of stages in lesion evolution. *Journal of Neuropathology & Experimental Neurology,* 55**,** 1194-1204.

DAY, N. P., HIEN, T. T., SCHOLLAARDT, T., LOC, P. P., VAN CHUONG, L., CHAU, T. T. H., MAI, N. T. H., PHU, N. H., SINH, D. X. & WHITE, N. J. 1999. The prognostic and pathophysiologic role of pro-and antiinflammatory cytokines in severe malaria. *Journal of Infectious Diseases,* 180**,** 1288-1297.

DE KONING-WARD, T. F., GILSON, P. R., BODDEY, J. A., RUG, M., SMITH, B. J., PAPENFUSS, A. T., SANDERS, P. R., LUNDIE, R. J., MAIER, A. G., COWMAN, A. F. & CRABB, B. S. 2009. A newly discovered protein export machine in malaria parasites. *Nature,* 459**,** 945-949.

DE SOUZA, J. B. & RILEY, E. M. 2002. Cerebral malaria: the contribution of studies in animal models to our understanding of immunopathogenesis. *Microbes Infect,* 4**,** 291-300.

DEHOUCK, M.-P., VIGNE, P., TORPIER, G., BREITTMAYER, J. P., CECCHELLI, R. & FRELIN, C. 1997. Endothelin-1 as a mediator of endothelial cell-pericyte interactions in bovine brain capillaries. *Journal of Cerebral Blood Flow & Metabolism,* 17**,** 464-469.

DONDORP, A. M., INCE, C., CHARUNWATTHANA, P., HANSON, J., VAN KUIJEN, A., FAIZ, M. A., RAHMAN, M. R., HASAN, M., BIN YUNUS, E., GHOSE, A., RUANGVEERAYUT, R., LIMMATHUROTSAKUL, D., MATHURA, K.,

WHITE, N. J. & DAY, N. P. 2008a. Direct in vivo assessment of microcirculatory dysfunction in severe falciparum malaria. *J Infect Dis,* 197**,** 79-84.

DONDORP, A. M., KAGER, P. A., VREEKEN, J. & WHITE, N. J. 2000. Abnormal blood flow and red blood cell deformability in severe malaria. *Parasitol Today,* 16**,** 228-32.

DONDORP, A. M., LEE, S. J., FAIZ, M. A., MISHRA, S., PRICE, R., TJITRA, E., THAN, M., HTUT, Y., MOHANTY, S., YUNUS, E. B., RAHMAN, R., NOSTEN, F., ANSTEY, N. M., DAY, N. P. J. & WHITE, N. J. 2008b. The Relationship between Age and the Manifestations of and Mortality Associated with Severe Malaria. *Clinical Infectious Diseases,* 47**,** 151-157.

DOROVINI-ZIS, K., SCHMIDT, K., HUYNH, H., FU, W., WHITTEN, R. O., MILNER, D., KAMIZA, S., MOLYNEUX, M. & TAYLOR, T. E. 2011. The Neuropathology of Fatal Cerebral Malaria in Malawian Children. *The American Journal of Pathology,* 178**,** 2146-2158.

DOUMBO, O. K., THERA, M. A., KONÉ, A. K., RAZA, A., TEMPEST, L. J., LYKE, K. E., PLOWE, C. V. & ROWE, J. A. 2009. High levels of Plasmodium falciparum rosetting in all clinical forms of severe malaria in African children. *The American journal of tropical medicine and hygiene,* 81**,** 987-993.

EGAN, T. J., COMBRINCK, J. M., EGAN, J., HEARNE, G. R., MARQUES, H. M., NTENTENI, S., SEWELL, B. T., SMITH, P. J., TAYLOR, D., VAN SCHALKWYK, D. A. & WALDEN, J. C. 2002. Fate of haem iron in the malaria parasite Plasmodium falciparum. *Biochem J,* 365**,** 343-7.

EGEBLAD, M. & WERB, Z. 2002. New functions for the matrix metalloproteinases in cancer progression. *Nature Reviews Cancer,* 2**,** 161-174.

ENGLISH, M., MUAMBI, B., MITHWANI, S. & MARSH, K. 1997a. Lactic acidosis and oxygen debt in African children with severe anaemia. *QJM,* 90**,** 563-569.

ENGLISH, M., SAUERWEIN, R., WARUIRU, C., MOSOBO, M., OBIERO, J., LOWE, B. & MARSH, K. 1997b. Acidosis in severe childhood malaria. *QJM,* 90**,** 263-270.

FENG, S., CEN, J., HUANG, Y., SHEN, H., YAO, L., WANG, Y. & CHEN, Z. 2011. Matrix Metalloproteinase-2 and -9 Secreted by Leukemic Cells Increase the Permeability of Blood-Brain Barrier by Disrupting Tight Junction Proteins. *PLoS ONE,* 6**,** e20599.

FIGTREE, M., LEE, R., BAIN, L., KENNEDY, T., MACKERTICH, S., URBAN, M., CHENG, Q. & HUDSON, B. J. 2010. Plasmodium knowlesi in human, Indonesian Borneo. *Emerging infectious diseases,* 16**,** 672-674.

FOSANG, A. J., LAST, K. & MACIEWICZ, R. 1996. Aggrecan is degraded by matrix metalloproteinases in human arthritis. Evidence that matrix metalloproteinase and aggrecanase activities can be independent. *Journal of Clinical Investigation,* 98**,** 2292.

FREVERT, U., SINNIS, P., CERAMI, C., SHREFFLER, W., TAKACS, B. & NUSSENZWEIG, V. 1993. Malaria circumsporozoite protein binds to heparan sulfate proteoglycans associated with the surface membrane of hepatocytes. *The Journal of experimental medicine,* 177**,** 1287-1298.

FRIED, M. & DUFFY, P. E. 1996. Adherence of Plasmodium falciparum to Chondroitin Sulfate A in the Human Placenta. *Science,* 272**,** 1502-1504.

FURUSE, M., FUJITA, K., HIIRAGI, T., FUJIMOTO, K. & TSUKITA, S. 1998. Claudin-1 and -2: Novel Integral Membrane Proteins Localizing at Tight Junctions with No Sequence Similarity to Occludin. *The Journal of Cell Biology,* 141**,** 1539-1550.

FURUSE, M., HIRASE, T., ITOH, M., NAGAFUCHI, A., YONEMURA, S., TSUKITA, S. & TSUKITA, S. 1993. Occludin: a novel integral membrane protein localizing at tight junctions. *The Journal of Cell Biology,* 123**,** 1777-1788.

GALLUP, J. L. & SACHS, J. D. 2001. The economic burden of malaria. *Am J Trop Med Hyg,* 64**,** 85-96.

GARCIA, F., CEBRIAN, M., DGEDGE, M., CASADEMONT, J., BEDINI, J. L., NEVES, O., FILELLA, X., CINTA CID, M., CORACHAN, M. & GRAU, J. M. 1999. Endothelial cell activation in muscle biopsy samples is related to clinical severity in human cerebral malaria. *J Infect Dis,* 179**,** 475-83.

GARNHAM, P. C. C. 1966. *Malaria Parasites and other Haemosporidia,* 5, Alfred Street, Oxford, United Kingdom, Blackwell Scientific Publications.

GAZZINELLI, R. T. & DENKERS, E. Y. 2006. Protozoan encounters with Toll-like receptor signalling pathways: implications for host parasitism. *Nat Rev Immunol,* 6**,** 895-906.

GIJBELS, K., GALARDY, R. & STEINMAN, L. 1994. Reversal of experimental autoimmune encephalomyelitis with a hydroxamate inhibitor of matrix metalloproteases. *Journal of Clinical Investigation,* 94**,** 2177.

GIJBELS, K., MASURE, S., CARTON, H. & OPDENAKKER, G. 1992. Gelatinase in the cerebrospinal fluid of patients with multiple sclerosis and other inflammatory neurological disorders. *Journal of Neuroimmunology,* 41**,** 29-34.

GOEL, V. K., LI, X., CHEN, H., LIU, S.-C., CHISHTI, A. H. & OH, S. S. 2003. Band 3 is a host receptor binding merozoite surface protein 1 during the Plasmodium

falciparum invasion of erythrocytes. *Proceedings of the National Academy of Sciences,* 100**,** 5164-5169.

GRAY, C., MCCORMICK, C., TURNER, G. & CRAIG, A. 2003. ICAM-1 can play a major role in mediating P. falciparum adhesion to endothelium under flow. *Mol Biochem Parasitol,* 128**,** 187-93.

GRIFFITHS, M. J., SHAFI, M. J., POPPER, S. J., HEMINGWAY, C. A., KORTOK, M. M., WATHEN, A., ROCKETT, K. A., MOTT, R., LEVIN, M. & NEWTON, C. R. 2005. Genomewide analysis of the host response to malaria in Kenyan children. *Journal of Infectious Diseases,* 191**,** 1599-1611.

HALDAR, K., MURPHY, S. C., MILNER JR, D. A. & TAYLOR, T. E. 2007. Malaria: mechanisms of erythrocytic infection and pathological correlates of severe disease. *Annu. Rev. Pathol. Mech. Dis.,* 2**,** 217-249.

HASHIMOTO, G., AOKI, T., NAKAMURA, H., TANZAWA, K. & OKADA, Y. 2001. Inhibition of ADAMTS4 (aggrecanase-1) by tissue inhibitors of metalloproteinases (TIMP-1, 2, 3 and 4). *FEBS letters,* 494**,** 192-195.

HASLER, T., HANDUNNETTI, S., AGUIAR, J., VAN SCHRAVENDIJK, M., GREENWOOD, B., LALLINGER, G., CEGIELSKI, P. & HOWARD, R. 1990. *In vitro rosetting, cytoadherence, and microagglutination properties of Plasmodium falciparum-infected erythrocytes from Gambian and Tanzanian patients*.

HAWKINS, B. T. & DAVIS, T. P. 2005. The Blood-Brain Barrier/Neurovascular Unit in Health and Disease. *Pharmacological Reviews,* 57**,** 173-185.

HAWKINS, B. T., LUNDEEN, T. F., NORWOOD, K. M., BROOKS, H. L. & EGLETON, R. D. 2007. Increased blood–brain barrier permeability and altered tight junctions in experimental diabetes in the rat: contribution of hyperglycaemia and matrix metalloproteinases. *Diabetologia,* 50**,** 202-211.

HEALY, D. P. & WILK, S. 1993. Localization of immunoreactive glutamyl aminopeptidase in rat brain. II. Distribution and correlation with angiotensin II. *Brain research,* 606**,** 295-303.

HEDDINI, A., PETTERSSON, F., KAI, O., SHAFI, J., OBIERO, J., CHEN, Q., BARRAGAN, A., WAHLGREN, M. & MARSH, K. 2001. Fresh isolates from children with severe Plasmodium falciparum malaria bind to multiple receptors. *Infection and immunity,* 69**,** 5849-5856.

HEWETT, P. 2009. Vascular Endothelial Cells from Human Micro- and Macro-vessels: Isolation, Characterisation and Culture. *In:* MURRAY, C. & MARTIN, S. (eds.) *Angiogenesis Protocols.* Humana Press.

HO, M. & WHITE, N. J. 1999. Molecular mechanisms of cytoadherence in malaria. *American Journal of Physiology-Cell Physiology,* 276**,** C1231-C1242.

HOLLESTELLE, M. J., DONKOR, C., MANTEY, E. A., CHAKRAVORTY, S. J., CRAIG, A., AKOTO, A. O., O'DONNELL, J., VAN MOURIK, J. A. & BUNN, J. 2006. von Willebrand factor propeptide in malaria: evidence of acute endothelial cell activation. *British Journal of Haematology,* 133**,** 562-569.

HORROCKS, P., PINCHES, R., CHRISTODOULOU, Z., KYES, S. A. & NEWBOLD, C. I. 2004. Variable var transition rates underlie antigenic variation in malaria. *Proceedings of the National Academy of Sciences of the United States of America,* 101**,** 11129-11134.

HUNT, N. H. & GRAU, G. E. 2003. Cytokines: accelerators and brakes in the pathogenesis of cerebral malaria. *Trends in Immunology,* 24**,** 491-499.

HUVENEERS, S., OLDENBURG, J., SPANJAARD, E., VAN DER KROGT, G., GRIGORIEV, I., AKHMANOVA, A., REHMANN, H. & DE ROOIJ, J. 2012. Vinculin associates with endothelial VE-cadherin junctions to control force-dependent remodeling. *The Journal of Cell Biology,* 196**,** 641-652.

HVIID, L. & JENSEN, A. T. R. 2015. Chapter Two - PfEMP1 – A Parasite Protein Family of Key Importance in Plasmodium falciparum Malaria Immunity and Pathogenesis. *In:* ROLLINSON, D. & STOTHARD, J. R. (eds.) *Advances in Parasitology.* Academic Press.

IDRO, R., JENKINS, N. E. & NEWTON, C. R. J. C. 2005. Pathogenesis, clinical features, and neurological outcome of cerebral malaria. *The Lancet Neurology,* 4**,** 827-840.

IRUELA-ARISPE, M. L., LOMBARDO, M., KRUTZSCH, H. C., LAWLER, J. & ROBERTS, D. D. 1999. Inhibition of angiogenesis by thrombospondin-1 is mediated by 2 independent regions within the type 1 repeats. *Circulation,* 100**,** 1423-1431.

ITOH, M., FURUSE, M., MORITA, K., KUBOTA, K., SAITOU, M. & TSUKITA, S. 1999. Direct Binding of Three Tight Junction-Associated Maguks, Zo-1, Zo-2, and Zo-3, with the Cooh Termini of Claudins. *The Journal of Cell Biology,* 147**,** 1351-1363.

IUVONE, T., D'ACQUISTO, F., CARNUCCIO, R. & DI ROSA, M. 1996. Nitric oxide inhibits LPS-induced tumor necrosis factor synthesis in vitro and in vivo. *Life Sciences,* 59**,** PL207-PL211.

JAIN, V., ARMAH, H. B., TONGREN, J. E., NED, R. M., WILSON, N. O., CRAWFORD, S., JOEL, P. K., SINGH, M. P., NAGPAL, A. C. & DASH, A. 2008. Plasma IP-10, apoptotic and angiogenic factors associated with fatal cerebral malaria in India. *Malaria journal,* 7**,** 83.

JAMBOU, R., LEGRAND, E., NIANG, M., KHIM, N., LIM, P., VOLNEY, B., EKALA, M. T., BOUCHIER, C., ESTERRE, P., FANDEUR, T. & MERCEREAU-PUIJALON, O. 2005. Resistance of Plasmodium falciparum field isolates to in-vitro artemether and point mutations of the SERCA-type PfATPase6. *The Lancet,* 366**,** 1960-1963.

JOHN, C. C., KUTAMBA, E., MUGARURA, K. & OPOKA, R. O. 2010. Adjunctive therapy for cerebral malaria and other severe forms of Plasmodium falciparum malaria.

JOHN HOPKINS UNIVERSITY, U. 2012. *Life cycle of the malaria parasite* [Online]. Available: http://www.core.org.cn/mirrors/jhsph/ocw.jhsph.edu/imageLibrary/index.cfm/go/il.viewImageDetails/resourceID/438DCC50-FFE9-0B64-8515BF619797AA48/index.htm [Accessed 22/07/2013 2013].

KAPPE, S. H. I., KAISER, K. & MATUSCHEWSKI, K. 2003. The Plasmodium sporozoite journey: a rite of passage. *Trends in Parasitology,* 19**,** 135-143.

KARUNAWEERA, N. D., GRAU, G. E., GAMAGE, P., CARTER, R. & MENDIS, K. N. 1992. Dynamics of fever and serum levels of tumor necrosis factor are closely associated during clinical paroxysms in Plasmodium vivax malaria. *Proc Natl Acad Sci U S A,* 89**,** 3200-3.

KASHIWAGI, M., TORTORELLA, M., NAGASE, H. & BREW, K. 2001. TIMP-3 is a potent inhibitor of aggrecanase 1 (ADAM-TS4) and aggrecanase 2 (ADAM-TS5). *Journal of Biological Chemistry,* 276**,** 12501-12504.

KNIESEL, U. & WOLBURG, H. 2000. Tight Junctions of the Blood–Brain Barrier. *Cellular and Molecular Neurobiology,* 20**,** 57-76.

KOCHAR, D., KUMAWAT, B., KOCHAR, S., HALWAI, M., MAKKAR, R., JOSHI, A. & THANVI, I. 2002. Cerebral malaria in Indian adults: a prospective study of 441 patients from Bikaner, north-west India. *The Journal of the Association of Physicians of India,* 50**,** 234-241.

KUEHN, A. & PRADEL, G. 2010. The coming-out of malaria gametocytes. *BioMed Research International,* 2010.

KUNO, K., KANADA, N., NAKASHIMA, E., FUJIKI, F., ICHIMURA, F. & MATSUSHIMA, K. 1997. Molecular cloning of a gene encoding a new type of metalloproteinase-disintegrin family protein with thrombospondin motifs as an inflammation associated gene. *Journal of Biological Chemistry,* 272**,** 556-562.

KWIATKOWSKI, D. 1989. Febrile temperatures can synchronize the growth of Plasmodium falciparum in vitro. *The Journal of Experimental Medicine,* 169**,** 357-361.

KWIATKOWSKI, D., SAMBOU, I., TWUMASI, P., GREENWOOD, B., HILL, A., MANOGUE, K., CERAMI, A., CASTRACANE, J. & BREWSTER, D. 1990. TNF concentration in fatal cerebral, non-fatal cerebral, and uncomplicated Plasmodium falciparum malaria. *The Lancet,* 336**,** 1201-1204.

KYES, S., HORROCKS, P. & NEWBOLD, C. 2001. Antigenic variation at the infected red cell surface in malaria. *Annual Reviews in Microbiology,* 55**,** 673-707.

LAUER, S. A., RATHOD, P. K., GHORI, N. & HALDAR, K. 1997. A Membrane Network for Nutrient Import in Red Cells Infected with the Malaria Parasite. *Science,* 276**,** 1122-1125.

LIEBNER, S., KNIESEL, U., KALBACHER, H. & WOLBURG, H. 2000. Correlation of tight junction morphology with the expression of tight junction proteins in blood-brain barrier endothelial cells. *European Journal of Cell Biology,* 79**,** 707-717.

LIPPOLDT, A., KNIESEL, U., LIEBNER, S., KALBACHER, H., KIRSCH, T., WOLBURG, H. & HALLER, H. 2000. Structural alterations of tight junctions are associated with loss of polarity in stroke-prone spontaneously hypertensive rat blood–brain barrier endothelial cells. *Brain research,* 885**,** 251-261.

LIU, J., JIN, X., LIU, K. J. & LIU, W. 2012. Matrix metalloproteinase-2-mediated occludin degradation and caveolin-1-mediated claudin-5 redistribution contribute to blood–brain barrier damage in early ischemic stroke stage. *The Journal of Neuroscience,* 32**,** 3044-3057.

LO, E. H., SINGHAL, A. B., TORCHILIN, V. P. & ABBOTT, N. J. 2001. Drug delivery to damaged brain. *Brain Research Reviews,* 38**,** 140-148.

LOU, J., CHOFFLON, M., JUILLARD, C., DONATI, Y., MILI, N., SIEGRIST, C.-A. & GRAU, G. E. 1997. Brain microvascular endothelial cells and leukocytes derived from patients with multiple sclerosis exhibit increased adhesion capacity. *Neuroreport,* 8**,** 629-633.

LOVEGROVE, F. E., GHARIB, S. A., PEÑA-CASTILLO, L., PATEL, S. N., RUZINSKI, J. T., HUGHES, T. R., LILES, W. C. & KAIN, K. C. 2008. Parasite burden and CD36-mediated sequestration are determinants of acute lung injury in an experimental malaria model. *PLoS pathogens,* 4**,** e1000068.

LYKE, K., BURGES, R., CISSOKO, Y., SANGARE, L., DAO, M., DIARRA, I., KONE, A., HARLEY, R., PLOWE, C. & DOUMBO, O. 2004a. Serum levels of the proinflammatory cytokines interleukin-1 beta (IL-1β), IL-6, IL-8, IL-10, tumor

necrosis factor alpha, and IL-12 (p70) in Malian children with severe Plasmodium falciparum malaria and matched uncomplicated malaria or healthy controls. *Infection and immunity, 72*, 5630-5637.

LYKE, K. E., BURGES, R., CISSOKO, Y., SANGARE, L., DAO, M., DIARRA, I., KONE, A., HARLEY, R., PLOWE, C. V., DOUMBO, O. K. & SZTEIN, M. B. 2004b. Serum levels of the proinflammatory cytokines interleukin-1 beta (IL-1beta), IL-6, IL-8, IL-10, tumor necrosis factor alpha, and IL-12(p70) in Malian children with severe Plasmodium falciparum malaria and matched uncomplicated malaria or healthy controls. *Infect Immun, 72*, 5630-7.

MACCORMICK, I. J. C., BEARE, N. A. V., TAYLOR, T. E., BARRERA, V., WHITE, V. A., HISCOTT, P., MOLYNEUX, M. E., DHILLON, B. & HARDING, S. P. 2014. *Cerebral malaria in children: using the retina to study the brain.*

MACPHERSON, G. G., WARRELL, M. J., WHITE, N. J., LOOAREESUWAN, S. & WARRELL, D. A. 1985. Human cerebral malaria. A quantitative ultrastructural analysis of parasitized erythrocyte sequestration. *Am J Pathol, 119*, 385-401.

MAIER, A. G., RUG, M., O'NEILL, M. T., BROWN, M., CHAKRAVORTY, S., SZESTAK, T., CHESSON, J., WU, Y., HUGHES, K., COPPEL, R. L., NEWBOLD, C., BEESON, J. G., CRAIG, A., CRABB, B. S. & COWMAN, A. F. 2008. Exported Proteins Required for Virulence and Rigidity of Plasmodium falciparum-Infected Human Erythrocytes. *Cell, 134*, 48-61.

MAITLAND, K., PAMBA, A., ENGLISH, M., PESHU, N., MARSH, K., NEWTON, C. & LEVIN, M. 2005. Randomized Trial of Volume Expansion with Albumin or Saline in Children with Severe Malaria: Preliminary Evidence of Albumin Benefit. *Clinical Infectious Diseases, 40*, 538-545.

MARCHAND, R. P., CULLETON, R., MAENO, Y., QUANG, N. T. & NAKAZAWA, S. 2011. Co-infections of Plasmodium knowlesi, P. falciparum, and P. vivax among Humans and Anopheles dirus Mosquitoes, Southern Vietnam. *Emerging Infectious Diseases, 17*, 1232-1239.

MARSH, K., FORSTER, D., WARUIRU, C., MWANGI, I., WINSTANLEY, M., MARSH, V., NEWTON, C., WINSTANLEY, P., WARN, P., PESHU, N., PASVOL, G. & SNOW, R. 1995. Indicators of Life-Threatening Malaria in African Children. *New England Journal of Medicine, 332*, 1399-1404.

MATTHEWS, R. T., GARY, S. C., ZERILLO, C., PRATTA, M., SOLOMON, K., ARNER, E. C. & HOCKFIELD, S. 2000. Brain-enriched hyaluronan binding (BEHAB)/brevican cleavage in a glioma cell line is mediated by a disintegrin and metalloproteinase with thrombospondin motifs (ADAMTS) family member. *Journal of Biological Chemistry, 275*, 22695-22703.

MCGREGOR, I. 1992. Malaria: edited by AJ Knell, Oxford University Press, 1991.£ 8.95 (89 pages) ISBN 0 19 854742 0. *Parasitology Today,* 8**,** 214-215.

MEDANA, I. M., MAI, N. T., DAY, N. P., HIEN, T. T., BETHELL, D., PHU, N. H., FARRAR, J., WHITE, N. J. & TURNER, G. D. 2001. Cellular stress and injury responses in the brains of adult Vietnamese patients with fatal Plasmodium falciparum malaria. *Neuropathol Appl Neurobiol,* 27**,** 421-33.

MEDANA, I. M. & TURNER, G. D. H. 2006. Human cerebral malaria and the blood–brain barrier. *International Journal for Parasitology,* 36**,** 555-568.

MEDINA-FLORES, R., WANG, G., BISSEL, S. J., MURPHEY-CORB, M. & WILEY, C. A. 2004. Destruction of extracellular matrix proteoglycans is pervasive in simian retroviral neuroinfection. *Neurobiology of Disease,* 16**,** 604-616.

MENASHI, S., LU, H., SORIA, C. & LEGRAND, Y. 1993. 2 Endothelial cell proteases: Physiological role and regulation. *Baillière's Clinical Haematology,* 6**,** 559-576.

MILLER, L. H., HUDSON-TAYLOR, D., GAMAIN, B. & SAUL, A. J. 2002. Definition of the minimal domain of CIDR1alpha of Plasmodium falciparum PfEMP1 for binding CD36. *Mol Biochem Parasitol,* 120**,** 321-3.

MINAGAR, A., SHAPSHAK, P., FUJIMURA, R., OWNBY, R., HEYES, M. & EISDORFER, C. 2002. The role of macrophage/microglia and astrocytes in the pathogenesis of three neurologic disorders: HIV-associated dementia, Alzheimer disease, and multiple sclerosis. *Journal of the neurological sciences,* 202**,** 13-23.

MIYAZAKI, K., HASEGAWA, M., FUNAHASHI, K. & UMEDA, M. 1993. A metalloproteinase inhibitor domain in Alzheimer amyloid protein precursor.

MORITA, K., SASAKI, H., FURUSE, M. & TSUKITA, S. 1999. Endothelial Claudin: Claudin-5/Tmvcf Constitutes Tight Junction Strands in Endothelial Cells. *The Journal of Cell Biology,* 147**,** 185-194.

MURPHY, G., COCKETT, M. I., WARD, R. & DOCHERTY, A. 1991. Matrix metalloproteinase degradation of elastin, type IV collagen and proteoglycan. A quantitative comparison of the activities of 95 kDa and 72 kDa gelatinases, stromelysins-1 and-2 and punctuated metalloproteinase (PUMP). *Biochem. J,* 277**,** 277-279.

NAG, S. 2011. Morphology and Properties of Brain Endothelial Cells. *In:* NAG, S. (ed.) *The Blood-Brain and Other Neural Barriers.* Humana Press.

NAGASE, H., VISSE, R. & MURPHY, G. 2006. Structure and function of matrix metalloproteinases and TIMPs. *Cardiovascular Research,* 69**,** 562-573.

NAGASE, H. & WOESSNER, J. F. 1999. Matrix Metalloproteinases. *Journal of Biological Chemistry,* 274**,** 21491-21494.

NAIK, P. & CUCULLO, L. 2012. In vitro blood–brain barrier models: Current and perspective technologies. *Journal of Pharmaceutical Sciences,* 101**,** 1337-1354.

NAKAJI, K., IHARA, M., TAKAHASHI, C., ITOHARA, S., NODA, M., TAKAHASHI, R. & TOMIMOTO, H. 2006. Matrix Metalloproteinase-2 Plays a Critical Role in the Pathogenesis of White Matter Lesions After Chronic Cerebral Hypoperfusion in Rodents. *Stroke,* 37**,** 2816-2823.

NEBL, T., DE VEER, M. J. & SCHOFIELD, L. 2005. Stimulation of innate immune responses by malarial glycosylphosphatidylinositol via pattern recognition receptors. *Parasitology,* 130 Suppl**,** S45-62.

NEUHAUS, J., RISAU, W. & WOLBURG, H. 1991. Induction of Blood-Brain Barrier Characteristics in Bovine Brain Endothelial Cells by Rat Astroglial Cells in Transfilter Coculturea. *Annals of the New York Academy of Sciences,* 633**,** 578-580.

NEWBOLD, C., WARN, P., BLACK, G., BERENDT, A., CRAIG, A., SNOW, B., MSOBO, M., PESHU, N. & MARSH, K. 1997. Receptor-specific adhesion and clinical disease in Plasmodium falciparum. *The American journal of tropical medicine and hygiene,* 57**,** 389-398.

NEWTON, C. R. J. C. & KRISHNA, S. 1998. Severe Falciparum Malaria in Children: Current Understanding of Pathophysiology and Supportive Treatment. *Pharmacology & Therapeutics,* 79**,** 1-53.

NGUANSANGIAM, S., DAY, N. P. J., HIEN, T. T., MAI, N. T. H., CHAISRI, U., RIGANTI, M., DONDORP, A. M., LEE, S. J., PHU, N. H., TURNER, G. D. H., WHITE, N. J., FERGUSON, D. J. P. & PONGPONRATN, E. 2007. A quantitative ultrastructural study of renal pathology in fatal Plasmodium falciparum malaria. *Tropical Medicine & International Health,* 12**,** 1037-1050.

NITTA, T., HATA, M., GOTOH, S., SEO, Y., SASAKI, H., HASHIMOTO, N., FURUSE, M. & TSUKITA, S. 2003. Size-selective loosening of the blood-brain barrier in claudin-5–deficient mice. *The Journal of Cell Biology,* 161**,** 653-660.

NWANE, P., ETANG, J., CHOUASMALL YI, U. M., TOTO, J. C., MIMPFOUNDI, R. & SIMARD, F. 2011. Kdr-based insecticide resistance in *Anopheles gambiae* s.s populations in Cameroon: spread of the L1014F and L1014S mutations. *BMC Res Notes,* 4**,** 463.

O'MEARA, W. P., BEJON, P., MWANGI, T. W., OKIRO, E. A., PESHU, N., SNOW, R. W., NEWTON, C. R. J. C. & MARSH, K. 2008. Effect of a fall in malaria

transmission on morbidity and mortality in Kilifi, Kenya. *The Lancet,* 372**,** 1555-1562.

OAKLEY, M. S., GERALD, N., MCCUTCHAN, T. F., ARAVIND, L. & KUMAR, S. 2011. Clinical and molecular aspects of malaria fever. *Trends in Parasitology,* 27**,** 442-449.

OCKENHOUSE, C. F., BETAGERI, R., SPRINGER, T. A. & STAUNTON, D. E. 1992a. Plasmodium falciparum-infected erythrocytes bind ICAM-1 at a site distinct from LFA-1, Mac-1, and human rhinovirus. *Cell,* 68**,** 63-69.

OCKENHOUSE, C. F., HO, M., TANDON, N. N., VAN SEVENTER, G. A., SHAW, S., WHITE, N. J., JAMIESON, G. A., CHULAY, J. D. & WEBSTER, H. K. 1991. Molecular basis of sequestration in severe and uncomplicated Plasmodium falciparum malaria: differential adhesion of infected erythrocytes to CD36 and ICAM-1. *J Infect Dis,* 164**,** 163-9.

OCKENHOUSE, C. F., TEGOSHI, T., MAENO, Y., BENJAMIN, C., HO, M., KAN, K. E., THWAY, Y., WIN, K., AIKAWA, M. & LOBB, R. R. 1992b. Human vascular endothelial cell adhesion receptors for Plasmodium falciparum-infected erythrocytes: roles for endothelial leukocyte adhesion molecule 1 and vascular cell adhesion molecule 1. *The Journal of Experimental Medicine,* 176**,** 1183-1189.

OGATA, Y., ENGHILD, J. J. & NAGASE, H. 1992. Matrix metalloproteinase 3 (stromelysin) activates the precursor for the human matrix metalloproteinase 9. *Journal of Biological Chemistry,* 267**,** 3581-3584.

PAPADOPOULOS, M. C., SAADOUN, S., WOODROW, C. J., DAVIES, D. C., COSTA-MARTINS, P., MOSS, R. F., KRISHNA, S. & BELL, B. A. 2001. Occludin expression in microvessels of neoplastic and non-neoplastic human brain. *Neuropathology and Applied Neurobiology,* 27**,** 384-395.

PATNAIK, J. K., DAS, B. S., MISHRA, S. K., MOHANTY, S., SATPATHY, S. K. & MOHANTY, D. 1994. Vascular clogging, mononuclear cell margination, and enhanced vascular permeability in the pathogenesis of human cerebral malaria. *The American journal of tropical medicine and hygiene,* 51**,** 642-647.

Malaria: affects animal as well as humans, 2009. Radio broadcast. Directed by PERKINS, S. Australia.

PHYO, A. P., NKHOMA, S., STEPNIEWSKA, K., ASHLEY, E. A., NAIR, S., MCGREADY, R., LER MOO, C., AL-SAAI, S., DONDORP, A. M., LWIN, K. M., SINGHASIVANON, P., DAY, N. P. J., WHITE, N. J., ANDERSON, T. J. C. & NOSTEN, F. 2012. Emergence of artemisinin-resistant malaria on the western border of Thailand: a longitudinal study. *The Lancet,* 379**,** 1960-1966.

POLIMENI, M. & PRATO, M. 2014. Host matrix metalloproteinases in cerebral malaria: new kids on the block against blood-brain barrier integrity? *Fluids and Barriers of the CNS,* 11**,** 1.

PONGPONRATN, E., RIGANTI, M., PUNPOOWONG, B. & AIKAWA, M. 1991. Microvascular sequestration of parasitized erythrocytes in human falciparum malaria: a pathological study. *The American journal of tropical medicine and hygiene,* 44**,** 168-175.

PONSFORD, M. J., MEDANA, I. M., PRAPANSILP, P., HIEN, T. T., LEE, S. J., DONDORP, A. M., ESIRI, M. M., DAY, N. P. J., WHITE, N. J. & TURNER, G. D. H. 2011. Sequestration and Microvascular Congestion Are Associated With Coma in Human Cerebral Malaria. *Journal of Infectious Diseases*.

PORTER, S., CLARK, I., KEVORKIAN, L. & EDWARDS, D. 2005. The ADAMTS metalloproteinases. *Biochem. J,* 386**,** 15-27.

POUVELLE, B., MATARAZZO, V., JURZYNSKI, C., NEMETH, J., RAMHARTER, M., ROUGON, G. & GYSIN, J. 2007. Neural Cell Adhesion Molecule, a New Cytoadhesion Receptor for Plasmodium falciparum-Infected Erythrocytes Capable of Aggregation. *Infection and Immunity,* 75**,** 3516-3522.

PRUDÊNCIO, M., RODRIGUEZ, A. & MOTA, M. M. 2006. The silent path to thousands of merozoites: the Plasmodium liver stage. *Nature Reviews Microbiology,* 4**,** 849-856.

PU, H., HAYASHI, K., ANDRAS, I. E., EUM, S., HENNIG, B. & TOBOREK, M. 2007. Limited role of COX-2 in HIV Tat-induced alterations of tight junction protein expression and disruption of the blood–brain barrier. *Brain Research,* 1184**,** 333-344.

QIN, H., SUN, Y. & BENVENISTE, E. N. 1999. The Transcription Factors Sp1, Sp3, and AP-2 Are Required for Constitutive Matrix Metalloproteinase-2 Gene Expression in Astroglioma Cells. *Journal of Biological Chemistry,* 274**,** 29130-29137.

QIU, L.-B., ZHOU, Y., WANG, Q., YANG, L.-L., LIU, H.-Q., XU, S.-L., QI, Y.-H., DING, G.-R. & GUO, G.-Z. 2011. Synthetic gelatinases inhibitor attenuates electromagnetic pulse-induced blood–brain barrier disruption by inhibiting gelatinases-mediated ZO-1 degradation in rats. *Toxicology,* 285**,** 31-38.

RAUCH, U. 2004. Extracellular matrix components associated with remodeling processes in brain. *Cellular and Molecular Life Sciences CMLS,* 61**,** 2031-2045.

REIFF, S. B. & STRIEPEN, B. 2009. Malaria: The gatekeeper revealed. *Nature,* 459**,** 918-919.

RÉNIA, L., HOWLAND, S. W., CLASER, C., GRUNER, A. C., SUWANARUSK, R., TEO, T.-H., RUSSELL, B. & NG, L. F. 2012. Cerebral malaria: mysteries at the blood-brain barrier. *Virulence,* 3**,** 193-201.

REYBURN, H., MBATIA, R., DRAKELEY, C. & ET AL. 2005. Association of transmission intensity and age with clinical manifestations and case fatality of severe plasmodium falciparum malaria. *JAMA,* 293**,** 1461-1470.

ROBERTS, D. D., SHERWOOD, J. A., SPITALNIK, S. L., PANTON, L. J., HOWARD, R. J., DIXIT, V. M., FRAZIER, W. A., MILLER, L. H. & GINSBURG, V. 1985. Thrombospondin binds falciparum malaria parasitized erythrocytes and may mediate cytoadherence. *Nature,* 318**,** 64-66.

ROBSON, K., FREVERT, U., RECKMANN, I., COWAN, G., BEIER, J., SCRAGG, I., TAKEHARA, K., BISHOP, D., PRADEL, G. & SINDEN, R. 1995. Thrombospondin-related adhesive protein (TRAP) of Plasmodium falciparum: expression during sporozoite ontogeny and binding to human hepatocytes. *The EMBO journal,* 14**,** 3883.

RODRÍGUEZ FERNÁNDEZ, J., GEIGER, B., SALOMON, D. & BEN-ZE'EV, A. 1993. Suppression of vinculin expression by antisense transfection confers changes in cell morphology, motility, and anchorage-dependent growth of 3T3 cells. *The Journal of Cell Biology,* 122**,** 1285-1294.

ROGERSON, S. J. & CARTER, R. 2008. Severe vivax malaria: newly recognised or rediscovered. *PLoS Med,* 5**,** e136.

ROLLINS, B., YOSHIMURA, T., LEONARD, E. & POBER, J. 1990. Cytokine-activated human endothelial cells synthesize and secrete a monocyte chemoattractant, MCP-1/JE. *The American journal of pathology,* 136**,** 1229.

ROSENBERG, G. A. & YANG, Y. 2007. Vasogenic edema due to tight junction disruption by matrix metalloproteinases in cerebral ischemia. *Neurosurgical Focus,* 22**,** 1-9.

ROWE, A., OBEIRO, J., NEWBOLD, C. I. & MARSH, K. 1995. Plasmodium falciparum rosetting is associated with malaria severity in Kenya. *Infect Immun,* 63**,** 2323-6.

ROWE, J. A., CLAESSENS, A., CORRIGAN, R. A. & ARMAN, M. 2009. Adhesion of Plasmodium falciparum-infected erythrocytes to human cells: molecular mechanisms and therapeutic implications. *Expert Rev Mol Med,* 11**,** e16.

SAITOU, M., FURUSE, M., SASAKI, H., SCHULZKE, J.-D., FROMM, M., TAKANO, H., NODA, T. & TSUKITA, S. 2000. Complex Phenotype of Mice Lacking Occludin, a Component of Tight Junction Strands. *Molecular Biology of the Cell,* 11**,** 4131-4142.

SCHERF, A., HERNANDEZ-RIVAS, R., BUFFET, P., BOTTIUS, E., BENATAR, C., POUVELLE, B., GYSIN, J. & LANZER, M. 1998. Antigenic variation in malaria: in situ switching, relaxed and mutually exclusive transcription of var genes during intra-erythrocytic development in Plasmodium falciparum. *The EMBO Journal,* 17**,** 5418-5426.

SERGHIDES, L., SMITH, T. G., PATEL, S. N. & KAIN, K. C. 2003. CD36 and malaria: friends or foes? *Trends in parasitology,* 19**,** 461-469.

SERIROM, S., RAHARJO, W. H., CHOTIVANICH, K., LOAREESUWAN, S., KUBES, P. & HO, M. 2003. Anti-Adhesive Effect of Nitric Oxide on Plasmodium falciparum Cytoadherence under Flow. *The American Journal of Pathology,* 162**,** 1651-1660.

SEYDEL, K. B., MILNER, D. A., KAMIZA, S. B., MOLYNEUX, M. E. & TAYLOR, T. E. 2006. The distribution and intensity of parasite sequestration in comatose Malawian children. *Journal of Infectious Diseases,* 194**,** 208-215.

SIANO, J. P., GRADY, K. K., MILLET, P. & WICK, T. M. 1998. Short report: Plasmodium falciparum: cytoadherence to alpha (v) beta3 on human microvascular endothelial cells. *The American journal of tropical medicine and hygiene,* 59**,** 77-79.

SILAMUT, K., PHU, N. H., WHITTY, C., TURNER, G. D., LOUWRIER, K., MAI, N. T., SIMPSON, J. A., HIEN, T. T. & WHITE, N. J. 1999. A quantitative analysis of the microvascular sequestration of malaria parasites in the human brain. *The American journal of pathology,* 155**,** 395-410.

SILVIE, O., FRANETICH, J.-F., CHARRIN, S., MUELLER, M. S., SIAU, A., BODESCOT, M., RUBINSTEIN, E., HANNOUN, L., CHAROENVIT, Y., KOCKEN, C. H., THOMAS, A. W., VAN GEMERT, G.-J., SAUERWEIN, R. W., BLACKMAN, M. J., ANDERS, R. F., PLUSCHKE, G. & MAZIER, D. 2004. A Role for Apical Membrane Antigen 1 during Invasion of Hepatocytes by Plasmodium falciparum Sporozoites. *Journal of Biological Chemistry,* 279**,** 9490-9496.

SIMMONS, D., MAKGOBA, M. W. & SEED, B. 1988. ICAM, an adhesion ligand of LFA-1, is homologous to the neural cell adhesion molecule NCAM. *Nature,* 331**,** 624-627.

SINGH, B., SUNG, L. K., MATUSOP, A., RADHAKRISHNAN, A., SHAMSUL, S. S. G., COX-SINGH, J., THOMAS, A. & CONWAY, D. J. 2004. A large focus of naturally acquired Plasmodium knowlesi infections in human beings. *The Lancet,* 363**,** 1017-1024.

SPRINGMAN, E. B., ANGLETON, E. L., BIRKEDAL-HANSEN, H. & VAN WART, H. E. 1990. Multiple modes of activation of latent human fibroblast collagenase: evidence for the role of a Cys73 active-site zinc complex in latency and a "cysteine

switch" mechanism for activation. *Proceedings of the National Academy of Sciences,* 87**,** 364-368.

STAMATOVIC, S. M., KEEP, R. F. & ANDJELKOVIC, A. V. 2008. Brain endothelial cell-cell junctions: how to "open" the blood brain barrier. *Current neuropharmacology,* 6**,** 179.

STAMATOVIC, S. M., KEEP, R. F., KUNKEL, S. L. & ANDJELKOVIC, A. V. 2003a. Potential role of MCP-1 in endothelial cell tight junction `opening': signaling via Rho and Rho kinase. *Journal of Cell Science,* 116**,** 4615-4628.

STAMATOVIC, S. M., KEEP, R. F., KUNKEL, S. L. & ANDJELKOVIC, A. V. 2003b. Potential role of MCP-1 in endothelial cell tight junctionopening': signaling via Rho and Rho kinase. *Journal of cell science,* 116**,** 4615-4628.

STERNLICHT, M. D. & WERB, Z. 2001. How matrix metalloproteinases regulate cell behavior. *Annual review of cell and developmental biology,* 17**,** 463.

STINS, M. F., GILLES, F. & KIM, K. S. 1997. Selective expression of adhesion molecules on human brain microvascular endothelial cells. *J Neuroimmunol,* 76**,** 81-90.

SUSOMBOON, P., MANEERAT, Y., DEKUMYOY, P., KALAMBAHETI, T., IWAGAMI, M., KOMAKI-YASUDA, K., KAWAZU, S., TANGPUKDEE, N., LOOAREESUWAN, S. & KANO, S. 2006. Down-regulation of tight junction mRNAs in human endothelial cells co-cultured with Plasmodium falciparum-infected erythrocytes. *Parasitol Int,* 55**,** 107-12.

SUWANARUSK, R., COOKE, B. M., DONDORP, A. M., SILAMUT, K., SATTABONGKOT, J., WHITE, N. J. & UDOMSANGPETCH, R. 2004. The Deformability of Red Blood Cells Parasitized by Plasmodium falciparum and P. vivax. *Journal of Infectious Diseases,* 189**,** 190-194.

SZMITKO, P. E., WANG, C.-H., WEISEL, R. D., DE ALMEIDA, J. R., ANDERSON, T. J. & VERMA, S. 2003. New markers of inflammation and endothelial cell activation part I. *Circulation,* 108**,** 1917-1923.

TAUCHI, R., IMAGAMA, S., NATORI, T., OHGOMORI, T., MURAMOTO, A., SHINJO, R., MATSUYAMA, Y., ISHIGURO, N. & KADOMATSU, K. 2012. The endogenous proteoglycan-degrading enzyme ADAMTS-4 promotes functional recovery after spinal cord injury. *J Neuroinflammation,* 9**,** 53.

TAYLOR, T. E., BORGSTEIN, A. & MOLYNEUX, M. E. 1993. Acid-base status in paediatric Plasmodium falciparum malaria. *QJM,* 86**,** 99-109.

TAYLOR, T. E., FU, W. J., CARR, R. A., WHITTEN, R. O., MUELLER, J. S., FOSIKO, N. G., LEWALLEN, S., LIOMBA, N. G. & MOLYNEUX, M. E. 2004.

Differentiating the pathologies of cerebral malaria by postmortem parasite counts. *Nat Med,* 10**,** 143-5.

TILLEY, L., DIXON, M. W. A. & KIRK, K. 2011. The Plasmodium falciparum-infected red blood cell. *The International Journal of Biochemistry & Cell Biology,* 43**,** 839-842.

TORTORELLA, M., BURN, T., PRATTA, M., ABBASZADE, I., HOLLIS, J., LIU, R., ROSENFELD, S., COPELAND, R., DECICCO, C. & WYNN, R. 1999. Purification and cloning of aggrecanase-1: a member of the ADAMTS family of proteins. *Science,* 284**,** 1664-1666.

TORTORELLA, M. D., MALFAIT, F., BARVE, R. A., SHIEH, H.-S. & MALFAIT, A.-M. 2009. A review of the ADAMTS family, pharmaceutical targets of the future. *Current pharmaceutical design,* 15**,** 2359-2374.

TRAGER, W. & JENSEN, J. B. 1976. Human malaria parasites in continuous culture. *Science,* 193**,** 673-675.

TREERATANAPIBOON, L., PSATHAKI, K., WEGENER, J., LOOAREESUWAN, S., GALLA, H. J. & UDOMSANGPETCH, R. 2005. In vitro study of malaria parasite induced disruption of blood-brain barrier. *Biochem Biophys Res Commun,* 335**,** 810-8.

TREUTIGER, C. J., HEDDINI, A., FERNANDEZ, V., MULLER, W. A. & WAHLGREN, M. 1997. PECAM-1/CDS31, an endothelial receptor for binding Plasmodium falciparum-infected erythrocytes. *Nature medicine,* 3**,** 1405-1408.

TRIGLIA, T., HEALER, J., CARUANA, S. R., HODDER, A. N., ANDERS, R. F., CRABB, B. S. & COWMAN, A. F. 2000. Apical membrane antigen 1 plays a central role in erythrocyte invasion by Plasmodium species. *Molecular Microbiology,* 38**,** 706-718.

TRIPATHI, A. K., SULLIVAN, D. J. & STINS, M. F. 2006. Plasmodium falciparum-Infected Erythrocytes Increase Intercellular Adhesion Molecule 1 Expression on Brain Endothelium through NF-κB. *Infection and Immunity,* 74**,** 3262-3270.

TRIPATHI, A. K., SULLIVAN, D. J. & STINS, M. F. 2007. Plasmodium falciparum—Infected Erythrocytes Decrease the Integrity of Human Blood-Brain Barrier Endothelial Cell Monolayers. *Journal of Infectious Diseases,* 195**,** 942-950.

TURNER, G. D., MORRISON, H., JONES, M., DAVIS, T. M., LOOAREESUWAN, S., BULEY, I. D., GATTER, K. C., NEWBOLD, C. I., PUKRITAYAKAMEE, S. & NAGACHINTA, B. 1994. An immunohistochemical study of the pathology of fatal malaria: evidence for widespread endothelial activation and a potential role for intercellular adhesion molecule-1 in cerebral sequestration. *The American journal of pathology,* 145**,** 1057.

UDOMSANGPETCH, R., REINHARDT, P. H., SCHOLLAARDT, T., ELLIOTT, J. F., KUBES, P. & HO, M. 1997. Promiscuity of clinical Plasmodium falciparum isolates for multiple adhesion molecules under flow conditions. *The Journal of Immunology,* 158**,** 4358-64.

VAN DE STOLPE, A. & VAN DER SAAG, P. 1996. Intercellular adhesion molecule-1. *Journal of Molecular Medicine,* 74**,** 13-33.

VAN DEN STEEN, P. E., DUBOIS, B., NELISSEN, I., RUDD, P. M., DWEK, R. A. & OPDENAKKER, G. 2002. Biochemistry and Molecular Biology of Gelatinase B or Matrix Metalloproteinase-9 (MMP-9). *Critical Reviews in Biochemistry and Molecular Biology,* 37**,** 375-536.

VAN DEN STEEN, P. E., VAN AELST, I., STARCKX, S., MASKOS, K., OPDENAKKER, G. & PAGENSTECHER, A. 2006. Matrix metalloproteinases, tissue inhibitors of MMPs and TACE in experimental cerebral malaria. *Lab Invest,* 86**,** 873-88.

VAN DER HEYDE, H. C., NOLAN, J., COMBES, V., GRAMAGLIA, I. & GRAU, G. E. 2006. A unified hypothesis for the genesis of cerebral malaria: sequestration, inflammation and hemostasis leading to microcirculatory dysfunction. *Trends Parasitol,* 22**,** 503-8.

VAN WART, H. E. & BIRKEDAL-HANSEN, H. 1990. The cysteine switch: a principle of regulation of metalloproteinase activity with potential applicability to the entire matrix metalloproteinase gene family. *Proceedings of the National Academy of Sciences,* 87**,** 5578-5582.

VÁZQUEZ, F., HASTINGS, G., ORTEGA, M.-A., LANE, T. F., OIKEMUS, S., LOMBARDO, M. & IRUELA-ARISPE, M. L. 1999. METH-1, a human ortholog of ADAMTS-1, and METH-2 are members of a new family of proteins with angio-inhibitory activity. *Journal of Biological Chemistry,* 274**,** 23349-23357.

VERMA, S., KUMAR, M., GURJAV, U., LUM, S. & NERURKAR, V. R. 2010a. Reversal of West Nile virus-induced blood-brain barrier disruption and tight junction proteins degradation by matrix metalloproteinases inhibitor. *Virology,* 397**,** 130-138.

VERMA, S., KUMAR, M., GURJAV, U., LUM, S. & NERURKAR, V. R. 2010b. Reversal of West Nile virus-induced blood-brain barrier disruption and tight junction proteins degradation by matrix metalloproteinases inhibitor. *Virology,* 397**,** 130-8.

VIEBIG, N. K., WULBRAND, U., FÖRSTER, R., ANDREWS, K. T., LANZER, M. & KNOLLE, P. A. 2005. Direct activation of human endothelial cells by Plasmodium falciparum-infected erythrocytes. *Infection and immunity,* 73**,** 3271-3277.

VIRGINTINO, D., ROBERTSON, D., BENAGIANO, V., ERREDE, M., BERTOSSI, M., AMBROSI, G. & RONCALI, L. 2000. Immunogold cytochemistry of the blood–brain barrier glucose transporter GLUT1 and endogenous albumin in the developing human brain. *Developmental Brain Research,* 123**,** 95-101.

WASSMER, S. C., CIANCIOLO, G. J., COMBES, V. & GRAU, G. E. 2005. Inhibition of endothelial activation: a new way to treat cerebral malaria? *PLoS medicine,* 2**,** e245.

WASSMER, S. C., COMBES, V., CANDAL, F. J., JUHAN-VAGUE, I. & GRAU, G. E. 2006. Platelets potentiate brain endothelial alterations induced by Plasmodium falciparum. *Infection and immunity,* 74**,** 645-653.

WASSMER, S. C., TAYLOR, T., MACLENNAN, C. A., KANJALA, M., MUKAKA, M., MOLYNEUX, M. E. & GRAU, G. E. 2008. Platelet-Induced Clumping of Plasmodium falciparum-Infected Erythrocytes from Malawian Patients with Cerebral Malaria—Possible Modulation In Vivo by Thrombocytopenia. *Journal of Infectious Diseases,* 197**,** 72-78.

WAYNE, G. J., DENG, S.-J., AMOUR, A., BORMAN, S., MATICO, R., CARTER, H. L. & MURPHY, G. 2007. TIMP-3 inhibition of ADAMTS-4 (Aggrecanase-1) is modulated by interactions between aggrecan and the C-terminal domain of ADAMTS-4. *Journal of Biological Chemistry,* 282**,** 20991-20998.

WEE YONG, V., FORSYTH, P. A., BELL, R., KREKOSKI, C. A. & EDWARDS, D. R. 1998. Matrix metalloproteinases and diseases of the CNS. *Trends in Neurosciences,* 21**,** 75-80.

WEKSLER, B., ROMERO, I. A. & COURAUD, P.-O. 2013. The hCMEC/D3 cell line as a model of the human blood brain barrier. *Fluids Barriers CNS,* 10**,** 16.

WEKSLER, B. B., SUBILEAU, E. A., PERRIÈRE, N., CHARNEAU, P., HOLLOWAY, K., LEVEQUE, M., TRICOIRE-LEIGNEL, H., NICOTRA, A., BOURDOULOUS, S., TUROWSKI, P., MALE, D. K., ROUX, F., GREENWOOD, J., ROMERO, I. A. & COURAUD, P. O. 2005. Blood-brain barrier-specific properties of a human adult brain endothelial cell line. *The FASEB Journal,* 19**,** 1872-1874.

WESTLING, J., GOTTSCHALL, P. E., THOMPSON, V. P., COCKBURN, A., PERIDES, G., ZIMMERMANN, D. R. & SANDY, J. D. 2004. ADAMTS4 (aggrecanase-1) cleaves human brain versican V2 at Glu405-Gln406 to generate glial hyaluronate binding protein. *Biochem J,* 377**,** 787-95.

WHO. 2013. *Malaria Fact Sheet* [Online]. Available: http://www.who.int/mediacentre/factsheets/fs094/en/index.html [Accessed June 24th 2013].

WHO 2014. World malaria report 2014. *In:* WORLD HEALTH ORGANISATION, W. (ed.). Geneva.

WOLBURG, H. 2007. The Endothelial Frontier. *Blood-Brain Barriers.* Wiley-VCH Verlag GmbH & Co. KGaA.

WORLD HEALTH ORGANISATION, W. 2012. World Malaria Report 2012.

YAMAGAMI, S., TAMURA, M., HAYASHI, M., ENDO, N., TANABE, H., KATSUURA, Y. & KOMORIYA, K. 1999. Differential production of MCP-1 and cytokine-induced neutrophil chemoattractant in the ischemic brain after transient focal ischemia in rats. *Journal of leukocyte biology,* 65**,** 744-749.

YOSHIYAMA, Y., ASAHINA, M. & HATTORI, T. 2000. Selective distribution of matrix metalloproteinase-3 (MMP-3) in Alzheimer's disease brain. *Acta Neuropathologica,* 99**,** 91-95.

YU, H., HUANG, X., MA, Y., GAO, M., WANG, O., GAO, T., SHEN, Y. & LIU, X. 2013. Interleukin-8 Regulates Endothelial Permeability by Down-regulation of Tight Junction but not Dependent on Integrins Induced Focal Adhesions. *International Journal of Biological Sciences,* 9**,** 966-979.

YUAN, S. Y. & RIGOR, R. R. 2010. Regulation of endothelial barrier function.

ZHANG, Y., HUANG, C., KIM, S., GOLKARAM, M., DIXON, M. W. A., TILLEY, L., LI, J., ZHANG, S. & SURESH, S. 2015. Multiple stiffening effects of nanoscale knobs on human red blood cells infected with Plasmodium falciparum malaria parasite. *Proceedings of the National Academy of Sciences.*